2009

The Role of Nucleotide Signaling in the Regulation of ICl,swell in Human 1321N1 Astrocytoma Cells

Ian C. Wenker
Wright State University

THE ROLE OF NUCLEOTIDE SIGNALING IN THE REGULATION OF $I_{Cl,swell}$ IN HUMAN 1321N1 ASTROCYTOMA CELLS

A thesis submitted in partial fulfillment
of the requirements for the degree of
Master of Science

By

IAN CHRISTOPHER WENKER
B.S., Xavier University, 2005

2009
Wright State University

WRIGHT STATE UNIVERSITY

SCHOOL OF GRADUATE STUDIES

January 13, 2009

I HEREBY RECOMMEND THAT THE THESIS PREPARED UNDER MY SUPERVISION BY Ian Christopher Wenker ENTITLED The Role of Nucleotide Signaling in the Regulation of $I_{Cl,swell}$ in Human 1321N1 Astrocytoma Cells BE ACCEPTED IN PARTIAL FULFILLMENT OF THE REQUIREMENTS FOR THE DEGREE OF Master of Science

James E. Olson, Ph.D.
Thesis Director

Timothy C. Cope, Ph.D.
Department Chair

Committee on
Final Examination

Christopher N. Wyatt, Ph.D.

Francisco J. Alvarez, Ph.D.

Joseph F. Thomas, Jr., Ph.D.
Dean, School of Graduate Studies

Abstract

Wenker, Ian Christopher. M.S., Department of Physiology and Biophysics, Wright State University, 2009. The Role of Nucleotide Signaling in the Regulation of $I_{Cl,swell}$ in Human 1321N1 Astrocytoma Cells

Swollen cells expel osmolytes to decrease volume in a process referred to as Regulatory Volume Decrease, or RVD. The plasma membrane current $I_{Cl,swell}$ is ubiquitously expressed in mammalian cells and contributes significantly to RVD. In a variety of cell types, activation of $I_{Cl,swell}$ is enhanced by nucleotide signaling. In this study, we used human astrocytoma cells to examine whether nucleotide signaling is necessary or sufficient for $I_{Cl,swell}$ activation. Three clones of the 1321N1 human astrocytoma cell line were used for voltage clamp recordings. One clone was transfected with P2Y1 receptors, another with P2Y2 receptors and a third was devoid of any P2Y receptors (Parental). In physiological solutions, hyposmotic exposure (HOE) caused increased membrane conductance in each cell line. HOE also depolarized the reversal potential in P2Y1 and P2Y2, but not in Parental, cell lines. In solutions containing no permeable cations, HOE activated $I_{Cl,swell}$ in morphologically round cells of each cell line and in morphologically flat P2Y1 and P2Y2 cells. However, morphologically flat Parental cells did not demonstrate HOE-induced $I_{Cl,swell}$ activity. Exogenous ATP activated a chloride current with an electrophysiological profile different from $I_{Cl,swell}$. I conclude that P2Y nucleotide signaling may play a role in gating $I_{Cl,swell}$, but is not necessary for its activation. P2Y receptor stimulation is sufficient to activate a chloride current, but whether the response is mediated by P2Y1 or P2Y2 receptors requires further investigation.

Table of Contents

List of Figures

Acknowledgments

There are many people that were either directly or indirectly involved with the work described in this thesis. Without these people not only would the completion of this thesis have been impossible, but not nearly so enjoyable. To list everyone and their impact would be superfluous, so I will mention only those that came to mind at the moment this was written.

The attainment of a graduate degree is not a common occurrence. Successful students generally display a number of virtues, one of which is a desire for knowledge. I have been fortunate enough to have had teachers throughout my life that fostered my desire for knowledge. I cannot begin to name them all but I would like to thank my first educators; my parents. The ways in which they have supported my educational endeavors is innumerable. As long as I can remember they have encouraged me to ask questions and search for answers, and for this I am truly thankful.

During my master's studies two professors in particular sparked my interest in neuroscience; Dr. Robert Putnam and Dr. Melvin Goldfinger. Dr. Putnam taught me how to apply mathematics to physiology and in so doing rekindled a fire for quantitative thought that had been dormant for quite some time. Dr. Goldfinger pointed out to me that some people spend their lives analyzing electrical traces. It is in no small part due to his class that I am starting a career doing that very thing. Thank you both for igniting my interest in neuroscience.

I would like to thank all the members of the Olson lab; Brian Tucker, Amanda Reese, Crystal Stuckey, Jim Leasure, Nancy Andrews and Dr. Guang-ze Li. Thank you all for your friendship and support. Specifically I would like to thank Brian Tucker for his comradery in the lab and Dr. Li for facilitating my entrance into the world of electrophysiology.

Finally, I cannot thank my advisor, Dr. James Olson, enough. It was a pleasure to work in his company. He was always available to me during my time in the lab and was just as interested in my education as the research I performed. My final acknowledgment must be for his help writing this thesis. The fact that this thesis is at all comprehensible is due largely to Dr. Olson's extensive editing.

Dedication

I would like to dedicate this thesis to my parents, Joe and Donna Wenker, and my siblings, Emily and Zach. I love you all very much.

I. Background and Literature Review

A. Glial Cells

Introduction

Glial cells were discovered during the mid-19th century. This was not too long after Scwhann and Schleiden theorized that all living matter was composed of cells in 1839 (Kimelberg 2004). It was Rudolf Virchow who first coined the term neuroglia, meaning "neural-cement," in 1856 (Ndubaku & de Bellard 2008). Virchow's histochemical stains illustrated clear distinctions between neurons and glia but were unable to delineate between the different subtypes of glia. Using the black chrome-silver reaction Camillo Golgi was the first to distinguish radial glia from other glia and neurons in 1895 (Kimelberg 2004). Ramon y Cajal was the first to use the term astrocyte to describe the fibrous and protoplasmic glial subset (Somjen 1988). He identified astrocytes using gold sublimate, which stained for what is known today as glial fibrillary acidic protein, GFAP. In 1920 Cajal's student del Rio Hortega was able to distinguish oligodendrondrocytes and microglia from the other two glial subsets (Somjen 1988).

Neuroglia have since been split into two broader classes of macroglia and microglia, the latter being the primary immune cell in the brain. Macroglia in the peripheral nervous system (PNS) consist of Schwann cells and satellite cells. Schwann cells' main role is that of axon myelination (Ndubaka & de Bellard 2008). Their long end feet wrap around myelinated fibers of the PNS resulting in faster signal transduction. Satellite cells line the exterior portion of the PNS and regulate the exterior chemical environment (Topilko 2007). Macroglia in the CNS consist of four distinct types; oligodendrocytes, radial glia, ependymal cells and astrocytes. Similar to Schwann cells,

oligodendrocytes have small somas and large end feet that are responsible for axon myelination (Ndubaka & de Bellard 2008). Radial glia have many roles in the CNS. In the developing brain, radial glia act as scaffolding for immature neuron migration (Kimelberg 2004). In the cerebellum and retina, radial glia are involved in synaptic plasticity and bidirectional communication with neurons, respectively. Ependymal cells create the walls of the ventricles (Meiniel 2007). Astrocytes are the most numerous cells in the CNS and perform many functions as discussed below.

Astrocyte Physiology

Astrocytes account for approximately 20-30% of brain cells in the mature CNS and are crucial for maintaining relative homeostasis (Kimelberg 2004, Hertz & Zielke 2004). In the microenvironment astrocytes mediate neurotransmitter and ionic homeostasis, synaptic formation, neuronal excitability and migration, detoxification and maintenance of the blood brain barrier (Markiewicz & Lukomska 2006). Proper astrocyte function is very important for the function of the brain as a whole. Astrocytes are known to secrete a wide variety of neurotrophic factors, such as nerve growth factor, NGF, and brain-derived neurotrophic factor BDNF (Villegas, Poletta & Carri 2003). Astrocytes regulate the extracellular space near synapses after high neuronal output by absorbing potassium (Leis, Bekar & Walz 2005, Olsen, Campbell & Sontheimer 2007) as well as neurotransmitters (Hertz & Zielke 2004).

The electrophysiology of astrocytes is quite uniform. Sontheimer and colleagues recorded electrically from astrocytes in three different regions of the rat brain; the hippocampus, cerebral cortex and spinal cord. Each cell type had very similar

electrophysiological properties (Bordey & Sontheimer 2000). All cells expressed transient K_A currents, rectifying K_{DR} currents and inward Na^+ currents in all three regions at all stages of development. Older animals also exhibited K_{IR} in all three regions. Sontheimer and colleagues also recorded from Bergmann glia in the cerebellum that appeared not to have K_{DR} or K_A currents. After employing leak subtraction, both K_{DR} and K_A currents were also found in these cells.

Originally astrocytes, as well as other glial cells, were thought to simply provide neurons with structural support, but in more recent decades it has become clear that astrocytes also are directly involved in synaptic communication. They are able to stabilize as well as modulate synaptic activity (Haydon 2000). Astrocytes express many neurotransmitter receptors that, when activated, initiate calcium signaling (Schipke & Kettenman 2002, Villegas et al. 2003). These calcium waves spread between adjacent astrocytes via gap junctions and nucleotide signaling (Inoue, Schuichi & Tsuda 2007), which can then trigger release of ATP and glutamate; the main mediators of neuron-glia cross-talk (Villegas et al. 2003). Astrocytes also have been found to communicate with microglia and capillaries (Inoue et al. 2007).

Astrocyte Pathophysiology

Astrocytes participate, along with microglia, in the general immune response of the brain by secreting pro-inflammatory cytokines Tumor Growth Factor-β1, Tumor Necrosis Factor-α, and Interleukins 1β and 6 (Dong 2001). While a controlled inflammatory response can be beneficial under many circumstances, it has been observed that in pathological states these pro-inflammatory mediators can lead to neuronal damage

and cell death. The neurotoxic effects of TNF-α (Kielen & Drew 205) and IL-1β (John, Lee & Brosnan 2003) have both been illustrated *in vitro*. The damage caused by inflammation is thought to contribute to several disease states such as Alzheimer's disease, Parkinson's disease, Huntington's disease, amyotrophic lateral sclerosis (ALS) and multiple sclerosis (MS) (Markiewicz & Lukomska 2006).

Rapid swelling of astrocytes is observed after numerous traumatic brain injuries, including stroke (Barron et al. 1988, Kimelberg et al. 2000, Mongin & Kimelberg 2005, Somjen 2004). Decreased extracellular space (ECS) is also observed after the traumatic event (Van Harreveld 1972). While other factors, such as dendritic swelling, could contribute to the decrease in ECS, it would seem that the swelling of astrocytes must play a significant role (Mongin & Kimelberg 2005). After 30 minutes of a focal ischemia astrocytes' intermediate metabolism is compromised leading to a decreased buffering capacity for extracellular potassium and glutamate (Hagberg et al. 2001). The combination of decreased ECS and astrocyte buffering capacity causes an increase of harmful substances in the ECS, including excitatory amino acids (EAA), reactive oxygen species (ROS), prostanoids and nitric oxide (NO) (Sykova & Chvatal 2000). It is not surprising to find that edema is a common cause of delayed death after stroke and other brain injury (Markiewicz & Lukomska 2006). The mechanisms of cell swelling and recovery in the brain are not fully understood. Future research will address some of these uncertainties and potentially lead to better treatment of patients with brain edema.

B. Nucleotide Signaling

Adenosine Tri-phosphate

Adenosine tri-phosphate, ATP, a purine nucleotide, plays important roles in many different areas of the life sciences. Most notably ATP is the "molecular currency" of energy transfer within a cell. Much of the study of biochemistry is concerned with its synthesis and metabolism. ATP is generated during glycolysis, photosynthesis and cellular respiration and the energy stored in the three phosphate bonds can be used for many cellular functions. Transmembrane pumps, such as the Na-K-ATPase, use the energy stored in the phosphate bonds of ATP to move molecules against their electrochemical gradient. ATP is also important biologically in aspects other than as a transducer of chemical potential energy. Cellular signaling pathways utilize ATP. In intracellular signal transduction pathways, ATP is used as a substrate by kinases that phosphorylate proteins and lipids, and adenylate cyclase that produces the second messenger molecule, cyclic AMP. More recently ATP has been found to be involved in intercellular signaling, acting in autocrine, paracrine and neurocrine mechanisms on extracellular nucleotide receptors (Burnstock 1972).

Perhaps due to the fact that ATP is such an important molecule for cell metabolism it was difficult for the scientific community to accept that it was involved in intercellular signaling. The first observation that ATP can act extracellularly occurred during experiments on cardiac tissue in 1929 (Drury & Szent-Györgyi 1929). Later it was found to act in the intestine (Gillespie 1934) and parts of the spinal cord (Buchthal, Engbaek, Sten-Knudsen & Thomasen 1947), as well as other areas. Exogenous ATP causes electrophysiological changes in certain brain regions (Galindo 1967) and acts as

an antagonist to certain anesthetics (Kuperman, Okamoto, Beyer & Volpert 1964). In 1970 Geoffrey Burnstock postulated that ATP is used for specific intercellular signaling (Burnstock 1970). He discovered nerves in the autonomic nervous system innervating the gut and bladder that utilized ATP as their neurotransmitter. Since then ATP has been described as a neurotransmitter in the autonomic, central and nociceptive nervous systems and is a cotransmitter in many other regions (see Burnstock 2007 for review).

Pericellular ATP

Early studies of ATP release usually involved bioluminescent measurements of the bathing solution of the cells subjected to mechanical stress (Schwiebert & Zsembery 2003). This technique resulted in calculated concentrations of ATP in the nanomolar range, well below the micromolar concentrations needed to stimulate most nucleotide receptors (Bours, Swennen, Virgilio, Cronstein & Danelie 2006). Using a different technique, Dubyak and colleagues discovered that ATP concentrations in the area near the cell membrane, termed the pericellular space, are several orders of magnitude higher than that of the bulk bath solution (Joseph, Buchakjian & Dubyak 2003). The technique used membrane attached protein-A luciferase to analyze ATP release in the pericellular space. Micromolar amounts of ATP were found to accumulate in the pericellular space of human astrocytoma cells (Joseph et al. 2003) and primary airway epithelial cells (Okada, Nicholas, Kreda, Lazarowski & Boucher 2006) when stimulated by Ca^{2+} mobilizing enzymes or hypotonic stress, respectively.

ATP Release during Cell Swelling

It has been shown in many cell types that ATP is released during cellular swelling (Sabirov, Dutta & Okada 2001, Wehner, Olsen, Tinel, Kinne-Saffran & Kinne 2003). When using a technique that measures ATP concentration in close proximity to the cell membrane, ATP concentrations increase to 10s of μM when cells are exposed to hyposmotic media (Dubyak & El-Moatassum 1993). This concentration of ATP is large enough to stimulate the P2Y sub-type of nucleotide receptors (Dezaki, Tsumura, Maeno, Okada 2000). The effects of ATP release on RVD were studied by exposing human intestine 407 cells to hyposmotic media and measuring cell volume over a time course of several minutes (Dezaki 2000). In control experiments the cells exhibited RVD. In separate experiments, cells were exposed to either suramin, a broad P2 receptor blocker, apyrase, an ATP-hydrolyzing enzyme, ATP or UTP, along with the hyposmotic media. Both suramin and apyrase blunted the RVD effect while the addition of micromolar amounts of ATP and UTP caused an increase in the amount of RVD. This suggests that the release of ATP during cell swelling plays a significant role in the mechanism of RVD. Similar effects of suramin and apyrase on RVD responses have been found in other cell types (Wang, Roman, Lidofsky & Fritz 1996, Roman et al. 1997, Roman, Feranchak, Salter, Wang & Fritz 1999).

The mechanism for ATP release during cell swelling has been a highly debated subject for more than a decade. Early proposed mechanisms for ATP release included the cystic fibrosis transmembrane conductance regulator, CFTR, (Schwiebert et al. 1995) and the volume-regulated anion channel, VRAC (Hisadome et al. 2002). Evidence against both CFTR and VRAC as ATP conductive pathways has been demonstrated in human

intestine 407 cells (Hazama et al. 1999) as well as mouse mammary C127 cells (Hazama et al. 2000). Although these two specific anion channels are unlikely to mediate ATP release, other evidence suggests an anion channel is likely. In recent studies (Sabirov et al. 2001, Dutta, Okada & Sabirov 2002) a maxi-conductance, volume-activated anion channel has been found to facilitate swelling induced ATP release. A similar maxi-anion channel in kidney macula densa cells conducts ATP during exposure to increased extracellular NaCl levels (Bell et al. 2003). Another proposed mechanism of release is through connexin 43 hemichannels. C6 glioma cells transfected with connexin 43 demonstrated ATP release and calcium signaling upon mechanical stimulation, while the parental cells lacking connexin 43 were unable to do so (Stout, Costantin, Naus & Charls 2002, Kang et al. 2008).

The main effect of autocrine ATP signaling appears to involve calcium signaling. In human intestine 407 cells, activation of P2Y receptors by micromolar amounts of ATP and UTP increases intracellular Ca^{2+} (Dezaki et al. 2000). Hyposmotic exposure also increases intracellular Ca^{2+} and exogenous ATP or UTP augments this response. In these cells the increase in intracellular Ca^{2+} is due to release from intracellular stores as well as from influx via Ca^{2+}-permeable cation channels (Dezaki et al. 2000, Hafting, Haug, Ellefsen & Sand 2006). These increases in intracellular Ca^{2+} activate the intermediate-conductance K^+ and IK channels in Intestine 407 cells (Wang, Morishima & Okada 2003) and large-conductance K^+, BK, channels in Vero cells (Hafting et al. 2006). Although increased extracelluar ATP was not able to activate chloride currents in Intestine 407 cells (Dezaki et al. 2000), more recent research in rat primary cultured astrocytes

indicates that perhaps ATP can activate VRACs via P2Y2 signaling (Darby, Kuzmiski, Panenka, Feighan & Macvicar 2003).

Nucleotide-converting Ecto-enzymes

Another factor in the nucleotide signaling cascade is the presence of nucleotide converting enzymes in the extracellular space. When ATP is accumulated in the pericellular space it comes into contact with many nucleotide-converting ecto-enzymes that convert ATP to ADP, AMP, adenosine, inosine and hypoxanthine. Converting ecto-enzyme families include ecto-nucleoside triphosphate diphosphohydrolase (E-NTDPase) (Zimmermann 1996), which dephosphorylates ATP and ADP, ecto-nucleotide pyrophosphatase/phosphodiesterase (E-NPP) (Stefan 2005), which can hydrolyze pyrophosphate and phosphodiester bonds in many molecules including nucleotides, and ecto-5'-nucleotidase (Zimmermann 1992), which dephosphorylates AMP to adenosine. Adenosine can then be further broken down by adenosine deaminase (ADA) and purine nucleoside phophorylase (PNP) or be transported, by active or facilitated diffusion, back into the cell (Thorn & Jarvis 1996). Most cell types express one or more of these enzymes on the extracellular side of their membrane. Thus ATP and other nucleotide concentrations are determined not only by the amount released but also by the metabolic rate of these ecto-enzymes (for review see Yegutkin 2008).

Nucleotide Receptor Subtypes

The membrane receptors whose ligands are purines and pyrimidines are commonly referred to as nucleotide receptors. There are at least three different families

of nucleotide receptors; P1 (also referred to as adenosine receptors), P2X and P2Y receptors. Nucleotide receptors have been found to be located in many regions of the body and function in an equally wide array of cellular processes.

P1 receptors are G-protein coupled receptors. There are four P1 receptor subtypes; A1, A2A, A2B and A3, which all respond to adenosine as their endogenous agonist. When A1 and A3 receptors are activated they stimulate G_s, which causes an increase in cAMP. Activation of A2A and A2B receptors stimulates G_i, which causes a decrease in cAMP (Burnstock 2007). P1 receptor activation causes decreased heart rate, coronary vasodilatation and A2B, in combination with neutrin-1, is involved with axon elongation in neurons (see Fredholm, Ijzerman, Jacobson & Klotz 2001 for review of P1 receptors).

P2X receptors are ionotropic with two transmembrane domains. There are seven cloned P2X subtypes; P2X1-7, which all respond to ATP as their endogenous agonist. P2X receptors act as cation channels and upon activation by ATP, allow the flow of sodium, potassium and in some cases calcium. This causes depolarization of the cell membrane, which in turn activates Ca^{2+} channels (Dubyak & El-Moatassum 1993). P2X1-6 are all very similar in structure while P2X7 has an elongated intracellular peptide sequence on the carboxy end. When exposed to ATP it initially functions as the other P2X receptors, however if the ATP exposure is prolonged its pore enlarges and larger molecules can flow through. It is mainly expressed in immune cells and glia, and seems to allow the release of proinflamatory cytokines (Burnstock 2008). P2X receptors have been located in neurons, glia, bone, muscle, endothelium and hematopoietic cells (Burnstock 2004, North 2002), and have functions including fast synaptic transmission

(Bardoni 1997), neurotransmitter release (Khakh & Henderson 1998) and pain signaling (Cockayne et al. 2000).

P2Y receptors are G-coupled with seven transmembrane spanning domains. There are eight P2Y receptor subtypes that have been cloned; P2Y1, P2Y2, P2Y4, P2Y6 and P2Y11 through P2Y14 (Burnstock 2007, Erb, Weaver, Seye & Weisman 2006). P2Y receptors respond to a more varied array of endogenous agonists, including ATP, ADP and even UTP. The strength of response to these agonists varies by receptor subtype, which is sometimes used to identify receptor subtype. For instance, if a cell exhibits a physiological response to ATP and UTP, but not ADP then the responsible receptor is either P2Y2 or P2Y4. G-proteins utilized by P2Y receptors are G_i, G_o, $G_{s,}$ G_q/G_{11}, $G_{\alpha i}$, G_{12} and G_i/G_o (Erb et al. 2006). Some P2Y receptor subtypes have specific G-proteins they associate with, but many can associate with multiple. The P2Y2 receptor can activate G_o, G_q/G_{11} and G_{12} (Erb et al. 2006). Stimulation of these G-proteins by recombinant P2Y receptors can either activate phospholipase C (PLC) or adenylate cyclase, causing intracellular Ca^{2+} release or changes in cAMP levels, respectively (Burnstock 2007). P2Y signaling is responsible for numerous physiological responses (Burnstock 2007). P2Y receptors are thought to play a role in the activation of ion channels, including the volume-regulated anion channel (Darby et al. 2003) and of N-type Ca^{2+} channels (Abbracchio et al. 2006). P2Y receptor expression has been shown to influence cell proliferation in a number of cell types (Bagchi et al. 2005) and is upregulated in response to tissue injury (Ahn, Camden, Schrader, Redman & Turner 2000, Schafer, Sedehizade, Welte & Reiser 2003, Tu et al. 2000). In the brain, nucleotide signaling seems to be neuroprotective. The P2Y2 receptor subtype expression has been

found to increase cell survival rates in cultured astrocytes subjected to trauma (Chorna et al. 2004).

Although specific agonists exist for many of the nucleotide receptor subtypes, the use of pharmacology to identify subtype activation is difficult. There is much overlap in the agonist profiles of many nucleotide receptors, and often specificity is very concentration dependent (Burnstock 2007). Similarly, agonists for nucleotide receptors lack specificity. In this study genetically modified cells are used to overcome this obstacle. Cells transfected with particular P2Y receptors are utilized to ensure physiological responses can be attributed to specific receptor subtypes.

C. Cell Swelling and Regulatory Volume Decrease

Cellular Swelling

The concept of cell volume regulation is so fundamental that many first learn of it in high school biology. Cells collected from a student's mouth, or perhaps a nearby pond, are studied under a microscope while tap water replaces the normal liquid environment. The cells viewed in the microscope increase in size and eventually burst. However, cells exposed to a solution of one-half tap water and one-half liquid from natural environment will initially swell, but eventually shrink back to their original size. This second outcome is reproducible in almost all animal cells (for one exception see De Smet, Oike, Droogmans, Van Driessche, & Nilius 1994).

Cells also are subject to changes in volume due to a number of physiological situations. Renal cells must respond to osmotic changes that occur during antidiuresis and diuresis (Beck 1988). Pathological situations in the brain, such as ischemia and traumatic

brain injury (TBI) often present with cellular swelling (Barron et al. 1988, Kimelberg et al. 2000, Somjen 2002). Causes for swelling can even be cell specific. For instance, astrocytes swell when exposed to millimolar levels of glutamate (Bender, Schousboe, Reichelt & Norneberg 1998, Koyama, Baba & Iwata 1991). Transepithelial transport of solutes into cells can cause cell swelling even when the extracellular environment remains isotonic (McCarty & O'Neil 1991).

Water Flux

Most biological matter is water, which flows easily through the plasma membrane of almost all mammalian cells. Thus, a cell swells because it has taken on more water. Likewise, when a cell loses water it shrinks. The relation of water flux through a semi-permeable membrane can be described by the equation:

$$Jv = Lp\ (\Delta p - \Delta \pi)$$

where Jv is the flux of water, Lp is the hydraulic conductivity of the cell's membrane, Δp is the change in hydrostatic pressure and $\Delta \pi$ is the change in osmotic pressure. While Lp, Δp and $\Delta \pi$ all affect the resulting flux in water, and hence the change in cell volume, in a physiological setting $\Delta \pi$ is the variable with the most potential to change.

Most animal cells' membranes are very permeable to water as compared to other molecules, meaning the Lp is high. This is because water is small, unlike larger organic molecules, and is uncharged, unlike impermeable ions. The Lp is increased in many membranes by the presence of aquaporins, which create pores in the cell membrane and

facilitate the movement of water (Agre, Brown & Nielson 1995, Echevarria, Windhager, Tate & Frindt 1994, Fushimi et al. 1993, Hill 1994). The expression of aquaporins also can be regulated and thus effect the ability of water to flux across a cell membrane. In the vast majority of circumstances water easily passes through biological membranes and thus any change in osmolarity will be followed by the obligatory water flux.

Hydrostatic pressure, Δp, is the physical pressure exerted by water, generally generated by gravity or some other physical force, such as hydrostatic pressure that moves plasma through the capillary walls. A cell membrane can only withstand a hydrostatic pressure gradient of 2 kPa (Guharay 1984). Thermodynamically this is equal to an osmotic gradient difference of 1 mOsm. Considering isotonic conditions are about 290 mOsm, we can calculate that a decrease in extracellular osmolarity of 1 mOsm would result in the cell swelling by only 0.35%. When an intact cytoskeleton is present, the membrane can withstand greater hydrostatic gradients (Jacobson 1983, Mills 1987). Even so, Δp is only able to play a minimal role in flux of water in or out of an animal cell.

$\Delta \pi$ is the difference in osmotic pressure between two solutions separated by a semi-permeable membrane. Each solution exerts its own osmotic pressure, and for dilute solutions π can be described by the equation:

$$\pi = i \cdot M \cdot R \cdot T$$

where i is the van't Hoff factor, M is the molarity of the solution, R is the gas constant and T is the absolute temperature. The van't Hoff factor, named after the equation's creator, is the number of osmotically effective moles of solute actually in solution per

mole of solid solute added. In a biological system both i and R are constant. While temperature can change, it will generally be the same on either side of the membrane, causing no effect to the $\Delta \pi$. Thus M, the molarity of a solution is the main determinant of a solution's osmotic pressure. As discussed above, any difference in osmotic pressure will cause water flux and thus changes in cell volume. If the extracellular solution is isotonic with respect to the intracellular solution, the $\Delta \pi$ will equal zero, there will be no flux of water and consequently cell volume will remain unchanged.

Steady-State Volume Regulation

Cell volume regulation is a dynamic process. Even when a cell is under isosmotic conditions it must still actively regulate its volume to keep from swelling. Cells contain a cache of various membrane impermeable molecules that increase the intracellular osmolarity. Without regulation, these osmolytes would cause the cell to swell. To compensate for this, most cells utilize a process that is referred to as the Double Donnan Hypothesis (Leaf 1956, MacKnight & Leaf 1988). The cell employs the Na^+/K^+ ATPase to actively pump sodium ions out of the cell and thus decrease the concentration of intracellular sodium. This decrease in sodium concentration helps to balance the relatively high concentration of organic osmolytes in the cell. It has been shown that blocking the Na^+/K^+ ATPase with ouabain causes cell swelling (Lang, Messner & Wang 1983, MacKnight & Leaf 1988). The intracellular fluid of the cell is initially isosmotic with respect to the extracellular fluid because sodium levels are kept low inside the cell, but ouabain disables the cell's mechanism for removing this sodium. As intracellular

sodium increases so does the cell's osmolarity. Thus, water will flux into the cell and it will swell.

Cell Volume Regulation

Theoretically a cell will increase in volume proportionally to the ratio in osmolarity between the extra and intracellular solutions. For example, a cell exposed to an extracellular solution whose osmolarity is half that of the intracellular solution should swell to twice its normal volume. However, cells do not behave as perfect osmometers. One convincing theory proposes that some portion of the cytosol is osmotically inactive, possibly due to many water molecules being bound to organic molecules, such as the cytoskeleton (Lucke & McCutcheon 1932). Figure 1 illustrates this using a Boyle – van't Hoff Plot. In this figure about 31.8% of the rat hepatocyte cells' intracellular fluid is osmotically inactive.

Most animal cells have the capacity to regulate their volume. Some of the first studies of cell volume regulation were performed in red blood cells. One of the more notable studies used duck red blood cells to demonstrate active cell volume regulation in anisotonic conditions (Kregenow 1977). A swollen cell actively decreases its volume by a process referred to as Regulatory Volume Decrease, or RVD. Similarly, a shrunken cell will increase its volume by a process referred to as Regulatory Volume Increase, or RVI. Available organic and inorganic osmolytes can be either expelled, in the case of RVD, or imported, in the case of RVI, to cause corresponding flux of water and thus return the cell closer to its initial volume. While RVI plays an important role in many physiological

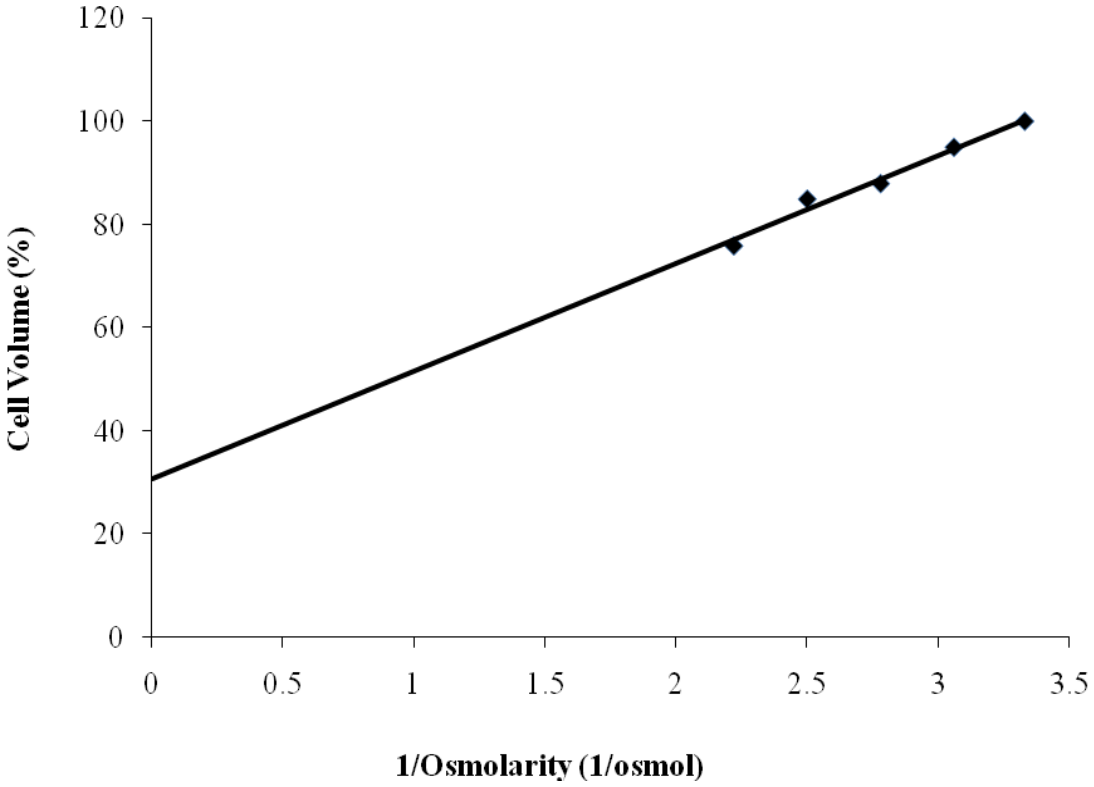

Figure 1 Boyle – van't Hoff plot of rat hepatocyte cell volumes at various extracellular osmolarities. With all volume regulatory mechanisms blocked the passive changes of rat hepatocyte volumes after 10 min exposure to hypertonicity (327, 360, 400, and 450 mOsm/l) are a linear function of the reciprocal of extracellular osmolality. The value of 3.33 is equivalent to 300 mOsm/l where cell volumes equal 100%. The intercept of the regression line with the volume axis is equivalent to the "osmotically inactive space" that amounts to 31.3% of total cell volume (adapted from Wehner and Tinel 2000).

processes, the present study focuses on the mechanisms involved in the RVD of osmotically swollen cells. (See Wehner et al. 2003 for Review)

Potassium – Chloride Cotransport

In human glioma cells it was found that 30-40% of cell RVD could be attributed to osmolytes moved by KCl cotransport (Ernest, Weaver, Van Duyn & Sontheimer 2005). KCl cotransport, via the KCC (Potassium-Chloride Cotransporter) family, in response to cell swelling has been observed in erythrocytes (Sachs & Martin 1993) as well as many other cell types (Thornhill & Laris 1984, Perry & O'Neill 1993, Shen, Chou & Ellory 2000, Orlando, Tobey, Wang, Abdulnour-Nakhoul & Orlando 2002, Lauf & Adragna 2000). At present there are four isoforms in the KCC family, KCC1 through KCC4. Research indicates that KCC1 (Mount et al. 1999, Su et al. 1999, Mercado, Song, Vazquez, Mount & Gamba 2000, Lauf et al. 2001), KCC3 (Mount et al. 1999, Race et al. 1999) and KCC4 (Mercado et al. 2000) activate during cell swelling while KCC2 does not (Payne 1997). KCCs have been shown to be stimulated in many different ways, including oxidizing agents and low Mg^{2+} (Lauf & Adragna 2000, Jennings 1999). One mechanism of activation for KCCs is dephosphorylation (Lauf and Adragna 2000, Jennings & Schultz 1991, Kaji & Tsukitani 1991). Interestingly, phosphorylation is an activator of NKCCs (sodium-potassium-chloride cotransporters) that are upregulated during RVI. This has led to the proposal of a "phosphorylation – dephosphorylation" mechanism to regulate cotransporters in response to cell volume change (Jennings & Schultz 1991, Cossins 1991, Dunham, Klimczak & Logue 1993).

Organic Osmolytes

While the inorganic ions mentioned above are capable mediators of RVD, their efflux from the cell interior also can pose problems. Changes in ion concentrations inside and outside the cell can affect the function of enzymes and proteins (Andrews, Maughan, Nosek & Godt 1991, Yancey, Clark, Hand, Bowlus & Somero 1982). In the brain, alterations of ion distribution also can affect neuronal excitability (Iwasa, Tasaki & Gibbons 1980). Uncharged organic osmolyte release does not pose such problems and are therefore considered more "compatible" to cell function. These observations have led to the "compatible osmolyte" hypothesis, which explains why certain cells use organic osmolytes, instead of ions, to achieve volume regulation. It is not surprising that cell swelling induces the exit of certain organic osmolytes in many cell types (Yancey et al. 1982, Hoffman, Lambert & Simonsen 1988, Kinne, Czekay, Grunewald, Mooren & Kinne-Saffran 1993, Burg 1995, Burg 1996, Junankar & Kirk 2000).

The amino acid taurine is a zwitterion that contributes to RVD in many cell lines, such as Ehlich Ascites tumor cells (Hoffman et al. 1988), HeLa cells (Hall, Kirk, Potts, Rae & Kirk 1996), C6 glioma cells (Jackson & Strange 1993) and astrocytes (Moran, Maar & Pasantes-Morales 1994, Olson 1999). Taurine release is passive; meaning its movement follows its electrochemical gradient (Sanchez, Pasantes-Morales, Lazaro & Cereijido 1991, Goldstein, Davis-Amara & Musch 1996, Junankar & Kirk 2000) and is inhibited by anion channel blockers (Roy & Malo 1992). This suggests that taurine is released via an ion channel and not by a transporter. Other types of organic osmolytes are also released during RVD. Studies performed in C6 glioma cells (Jackson & Strange 1993) and rat IMCD cells (Ruhfus, Bauernschmitt & Kinne 1998) demonstrate

hyposmotically induced fluxes of myo-inositol. Sorbitol also has been shown to efflux during RVD in C6 cells (Jackson & Strange 1993), rat IMCD cells (Grunewald 1989, Ruhfus et al. 1998) and Hela cells (Hall et al. 1996).

Ion Channel Mediated RVD

Under certain circumstances, such as ischemia (Askenasy & Navon 1997), a cell may encounter extracellular fluid that is significantly lower in osmolarity, and as a result, experience an influx of water. The most efficient way for a cell to perform RVD is to expel a fraction of the ions that are residing in the intracellular fluid. This will result in osmotic water efflux thus maintaining relative volume homeostasis. The fastest way for an ion to exit a cell is through a channel, as compared with cotransporter or pumps. Ions move passively through channels down their electrochemical gradient. In many cells, both chloride and potassium ions are accumulated against their electrochemical gradient thus making them optimal choices to facilitate RVD. Most mechanisms of RVD include the loss of both potassium and chloride. This coupling of ions for RVD is due in part to their opposite charges. Suppose a cell responds to a hyposmotic challenge by increasing membrane conductance for potassium, and thus causing potassium to flow out of the cell. This increase in potassium conductance also will cause the membrane to hyperpolarize, increasing the driving gradient for chloride and leading to chloride efflux. Similarly, an increase in chloride conductance will lead to an increased potassium driving force. (for reviews see Lang et al. 1998, Wehner et al. 2003).

Potassium Channels Involved in RVD

Many potassium channels have been directly or indirectly shown to become activated during cell swelling. The BK_{Ca} channel, also referred to as the Maxi-K channel,

is activated during hyposmotic conditions. BK_{Ca}'s activation during swelling has been shown in both primary and clonal kidney cultures (Dube, Parent & Suave 1990, Filipovic & Sackin 1991, Kawahara, Ogawa & Suzuki 1991, Ling, Webster & Eaton 1992, Schlatter 1993, Stoner & Morley 1995, Hirsch & Schlatter 1997, Hafting & Sand 2000). BK_{Ca} channels are activated by micromolar concentrations of intracellular Ca^{2+} and membrane depolarization (Vergara, Latorre, Marrion & Adelman 1998). They exhibit large unitary conductances in the range of 100 to 250 pS and are inhibited by tetra-ethyl-ammonium, TEA (Vergara 1998). BK_{Ca} channels are also activated in cloned kidney cells by exogenous ATP (Hafting & Sand 2000, Hafting 2006).

IK_{Ca} channels have been shown to activate under hyposmostic conditions in T lymphocytes (Khanna, Chang, Joiner, Kaczmarek & Schlichter 1999). IK_{Ca} channels are so called because they exhibit an intermediate unitary conductance that ranges from 20 to 80 pS. The currents mediated by IK_{Ca} are slightly inwardly rectified and Ca^{2+} sensitive. These experiments (Khanna et al. 1999) demonstrate hyposmotically induced intermediate potassium conductances that were inwardly rectified and Ca^{2+} sensitive. Also the conductances were inhibited by the selective IK_{Ca} channel blocker clotrimazole (Jensen, Stroback, Olesen & Chritophersen 2001 for review).

Several other potassium channels exhibit conductances triggered by hyposmotic exposure, suggesting they also play a role in RVD. Kv1.3, a voltage-activated delayed-rectifier channel, is activated during cell swelling and mediates RVD when transfected into mouse T lymphocytes (Deutsch & Chen 1993). I_{SK} channel, which is slowly activating and usually associates with K_VLQT1 to form MinK channels (Barhanin et al. 1996), is activated in Xenopus oocytes during hyposmotic exposure (Busch, Varnum,

Adelman & North 1992). More recently TASK-2 has also been shown to exhibit hyposmotically activated conductances in Ehrlich Ascites tumor cells (Niemeyer, Cid, & Sepulveda 2001).

Chloride Channels Involved in RVD

Present research suggests that in most preparations a single chloride (or anion) channel type is responsible for the majority of chloride efflux during RVD. This channel has been named VSOR, for volume-sensitive outward-rectifying chloride channel (Okada, Oiki, Hazama & Morishima 1998), VSOAC, for volume-sensitive organic osmolytes-anion channels (Jackson & Strange 1994), or VRAC, for volume-regulated anion channel (Nilius & Droogmans 2001). The current mediated by this channel has been named $I_{Cl,swell}$ (Nilius et al. 1999) and $I_{Cl,vol}$ (Hoffman & Mills 1999). VRAC is activated in response to hyposmotic exposure in almost all preparations. Although VRAC is commonly expressed functionally, its molecular identity has remained a mystery.

While the molecular nature of VRAC is unknown, the electrophysiological properties of $I_{Cl,swell}$ can distinguish it from other known cloned chloride channels. $I_{Cl,swell}$ has four basic electrophysiological characteristics. First, $I_{Cl,swell}$ is outwardly rectified, that is, conductance increases at more positive membrane potentials. The second characteristic is inactivation of currents elicited at highly positive membrane potentials. The degree of inactivation appears to vary by cell type, with the midpoint of inactivation occurring at +40 mV in T84 epithelial cells (Braun and Schulman, 1996) and +105 mV for myeloma cells (Levitan and Garber, 1995). The third characteristic is that VRAC has an Eisenmen's Sequence I of ion permeabilities (Nilius & Droogmans 2001), which

indicates that the ion flowing through the channel has a weak energy of binding to the cationic changes within the channel as compared to the energy needed to unbind the ion from water molecules (Wright & Diamond 1977). Thus, its permeability sequence is: $SCN^- > I^- > NO^{3-} > Br^- > Cl^- > HCO3^- > F^-$ > isethionate > gluconate > glycine > taurine > aspartate, glutamate. Chloride is the main osmolyte flowing through VRAC in conditions established for most electrophysiological studies, however it has been reported that cellular release of taurine (Olson & Li 1997) and aspartate (Abdullaev, Rudkauskaya, Schools, Kimelberg & Mongin 2006) also occurs via this channel. The fourth characteristic, and that for which VRAC got its name, is activation by cell swelling. The basal conductance of VRAC is very low, and it is not until swelling has occurred that it is activated (Jackson & Strange 1995).

A number of cloned chloride channels have been proposed to be the molecular source of VRAC currents. ClC-2 is a chloride channel of the ClC gene family that has been shown to activate during cell swelling (Grunder, Thiemann, Pusch & Jentz 1992) and hyperpolarization (Thiemann, Grunder, Pusch & Jentsch 1992). However, ClC-2 has an inwardly rectified current-voltage relationship and a selectivity sequence of $Cl^- > I^- >>$ Aspartate (Duan, Ye, Britton, Horowitz & Hume 2000). Another member of the ClC family, ClC-3, has many characteristics that are similar to VRAC, such as outward rectification and anion selectivity (Strange 1998, Jentsch, Friedrich & Schriever 1999, Hume, Duan, Collier, Yamazaki & Horowitz 2000). ClC-3 has a large basal conductance, which is in contrast to the very minimal, if any, basal conductance that is demonstrated by VRAC. Also, ClC-3 is inhibited by PKC, which has been found to stimulate VRAC (Okada et al. 1998, Strange 1998).

Although VRAC seems to be ubiquitously expressed, in certain preparations other chloride channels have also activated during hyposmotic exposure. BCl, sometimes called maxi Cl^-, channels are activated by hyposmotic conditions in newborn rat cardiac myocytes (Coulombe & Coraboeuf 1992), mouse neuroblastoma cells (Falke & Misler 1989) and primary cultures of rat cortical astrocytes (Jalonen 1993). SCl, or mini Cl^-, channels have also been observed in Ehlich ascites tumor cells (Christenson & Hoffmann 1992) and bovine ciliary epithelium (Zhang & Jacob 1997). The calcium activated chloride channels, CaCCs, also contribute to RVD (Jentsch 1996, Hoffmann & Mills 1999, Nilius & Droogmans 2001).

D. Summary of Background Literature

Edema is a common cause of delayed death after traumatic brain injuries and stroke (Markiewicz 2006) and astrocytes are commonly observed to swell during those situations (Barron et al. 1988, Kimelberg et al. 2000, Mongin & Kimelberg 2005, Somjen 2004). Astrocyte swelling is thought to cause a decrease in brain ECS and release EAAs and other harmful substances in these pathological situations (Sykova & Chvatal 2000). Thus research has focused on the mechanisms of RVD in astrocytes. The mysterious current $I_{Cl,swell}$ is important for RVD and is expressed in astrocytes (Darby et al. 2003, Abdullaev et al. 2006). The molecular identity of $I_{Cl,swell}$ is not known and the method of its activation is poorly understood. It would seem that exogenous ATP, acting via P2Y receptors, plays some role in $I_{Cl,swell}$ activation. In one study P2Y nucleotide receptors play a critical role in the activation of $I_{Cl,swell}$ (Darby 2003), however another study indicates P2Y receptors only modify its activity (Mongin & Kimelberg 2003). Neither

study was able to conclusively answer whether P2Y signaling is necessary or sufficient for $I_{Cl,swell}$ activation.

II. Specific Aims

Specific Aim I

The first goal of this study was to identify and characterize the hyposmotically activated current $I_{Cl,swell}$ in human 1321N1 astrocytoma cells. This was to be accomplished using voltage clamp techniques in both physiological and chloride current-isolating conditions. $I_{Cl,swell}$ was also identified pharmacologically using the drug DCPIB.

Specific Aim II

The second goal of this study was to determine if P2Y receptor expression is necessary for $I_{Cl,swell}$ activation in human 1321N1 astrocytoma cells. If P2Y receptors were found to be associated with $I_{Cl,swell}$ activation by hyposmotic exposure (HOE), a secondary goal of this aim was to determine which receptor subtype, P2Y1 or P2Y2, is responsible. This was to be accomplished using voltage clamp techniques and by examining responses to hyposmotic exposure in three subtypes of the 1321N1 cells; one with P2Y1 receptor expression, one with P2Y2 receptor expression and another lacking P2Y receptor expression. In addition, the drug PPADS was used as a broad spectrum P2Y receptor antagonist.

Specific Aim III

The final goal of this study was to determine if P2Y receptor activation was sufficient to initiate $I_{Cl,swell}$ activation in the absence of HOE. This was to be accomplished using voltage clamp techniques and by exposing the same cell subtypes mentioned above to exogenous ATP under isosmotic conditions.

III. Materials and Methods

A. **Materials**

The materials, equipment and software used during the studies performed for this thesis are listed here in alphabetical order. The reader can use this table to find the manufacturing company's name, location and, when available, the item number for each product.

Materials

Name	**Item #**	**Company**	**Location**
12 mm Coverslips	12-545-80	Fisher Scientific	Pittsburg, PA
Acrylamide	254	Amresco	Solon, OH
Alexafluor 568	A11036	Invitrogen	Carlsbad, CA
Ammonium Persulfate	A3678	Sigma-Aldrich	St. Louis, MO
β-Actin Antibody	600-401-886	Rockland	Philadelphia, PA
BCA* Solutions	B9643, C2284	Sigma-Aldrich	St. Louis, MO
$CaCl_2$	133205	J.T. Baker Chemical Co.	Phillipsburg, NJ
CsCl	C4036	Sigma-Aldrich	St. Louis, MO
CsOH	C8518	Sigma-Aldrich	St. Louis, MO
DCPIB*	1540	Tocris Biosciences	Ellisville, MO
Dextrose	1910	J.T. Baker Chemical Co.	Phillipsburg, NJ
DMEM* low glucose	D5523	Sigma-Aldrich	St. Louis, MO
ECF Western Blotting Kit	RPN5870	Amersham Biosciences	Piscataway, NJ
EGTA*	E4378	Sigma-Aldrich	St. Louis, MO
Fetal Bovine Serum	26140-079	Invitrogen	Carlsbad, CA
Geneticin (G418)	15-394N	Cambrex	East Rutherford, NJ
Glycine	G8898	Sigma-Aldrich	St. Louis, MO
Hydrochloric Acid	$A144^{SI}$-212	Fisher Scientific	Pittsburg, PA
HEPES*	H-9136	Sigma-Adrich	St. Louis, MO
Immuno-Blot PVDF Membrane	162-0174	Biorad	Hercules, CA
KCl	P-217	Fisher Scientific	Pittsburg, PA
KH_2PO_4	P-5379	Sigma-Aldrich	St. Louis, MO
KOH	5-3140	Sigma-Aldrich	St. Louis, MO
Mammalian Cell Lysis Kit	MCL-1	Sigma-Aldrich	St. Louis, MO

$MgCl_2$	MX0045-1	MCB Reagents	
Microscope slides	48312-003	VWR	West Chester, PA
Mounting Media	M01	Biomeda	Foster City, CA
Na_2ATP	A6419	Sigma-Aldrich	St. Louis, MO
Na_2HPO_4	S-0876	Sigma-Aldrich	St. Louis, MO
NaCl	S-9625	Sigma-Aldrich	St. Louis, MO
NaOH	S318-3	J.T. Baker Chemical Co.	Phillipsburg, NJ
Normal Goat Serum	64292	Invitrogen	Carlsbad, CA
P2Y1 and P2Y2 Antibodies	APR-009, APR-010	Alomone Labs	Jerusalem, Israel
Paraformaldehyde	P6148	Sigma-Aldrich	St. Louis, MO
Penicillin/Streptomycin	15070-063	Invitrogen	Carlsbad, CA
PPADS*	P-178	Sigma-Aldrich	St. Louis, MO
Precision Plus Protein Ladder	161-0374	Biorad	Hercules, CA
Protein Standards	P0914-5AMP	Sigma-Aldrich	St. Louis, MO
SDS*	S3771	Sigma-Aldrich	St. Louis, MO
StrepActin AP	161-0382	Biorad	Hercules, CA
Sucrose	S5-3	Fisher Scientific	Pittsburg, PA
TEA*	T-2265	Sigma-Aldrich	St. Louis, MO
TEMED*	761	Amresco	Solon, OH
Thin Wall Capillary Tubes	TW120F-4	World Precision Instruments inc.	Sarasota, FL
Trizma Base	T1503	Sigma-Aldrich	St. Louis, MO
Trypsin 0.25%	15050	Invitrogen	Carlsbad, CA
Tryton X100	X-100	Sigma-Aldrich	St. Louis, MO
Tween-20	P5927-100mL	Sigma-Aldrich	St. Louis, MO

* abbreviations are defined in the abbreviation section below.

Equipment and Software

Axopatch 200A amplifier	200A	Axon Instruments	Union City, CA
Clampex 8.2		Axon Instruments	Union City, CA
Clampfit 8.2		Axon Instruments	Union City, CA
Microsoft Office 2003		Microsoft	Redmond, WA
Narishige PP-83 puller	PP-83	Narishige	East Meadow, NY
Nikon Phase-contrast Microscope	TMS-F 211164	Nikon	Tokyo, Japan
Perfusion System	CF-8VS Valve Assembly	Cell Micro-Controls	Norfolk, VA
Power Supply	PowerPac Basic	Biorad	Hercules, CA
Scanning (ECF) Machine	FLA-5100	Fujifilm	Valhala, NY
Spectrometer	U-2000	Hitachi	Brisbane, CA
Vapor Pressure Osmometer	5500	Wescor	Logan, UT

B. Abbreviations

BCA = bicinchoninic acid, **DCPIB** = 4-[(2-Butyl-6,7-dichloro-2-cyclopentyl-2,3-dihydro-1-ox o-1H-inden-5-yl)oxy]butanoic acid, **DMEM** = Dulbecco's modified Eagles medium, **EGTA** = ethylene glycol tetraacetic acid, **FBS** = fetal bovine serum, **HEPES** = 4-(2-hydroxyethyl)-1-piperazineethanesulfonic acid, **PPADS** = pyridoxalphosphate-6-azophenyl-2',4'-disulphonic acid, **SDS** = sodium dodecyl sulfate, **TEA** = tetraethylammonium, **TEMED** = tetramethylethylenediamine.

C. Cell Culture

Human 1321N1 astrocytoma cells are used throughout these experiments. As originally cloned, this cell line does not express any of the P2Y subtypes (Erb 1995). Three genetic variants of the human 1321N1 astrocytoma cell line were obtained from Dr. Natalia Chorna of the University of Puerto Rico, San Juan, Puerto Rico. One cell line was stably transfected with the P2Y1 receptor subtype (P2Y1 cells), another with the P2Y2 receptor subtype (P2Y2 cells), while the third (Parental cells) retained its P2Y receptor-lacking genotype (Chorna 2004). Cells transfected with P2Y1 and P2Y2 receptors also had been simultaneously transfected with resistance to geneticin, an antibiotic similar in structure to gentamicin B1 that blocks protein synthesis in both prokaryotic and eukaryotic cells. Cells were shipped in large flasks containing Dulbecco's modified Eagle's medium. Upon arrival cells were replated in small flasks and grown to ~90% confluency. Then they were removed from the culture surface and resuspended in media containing DMEM, FBS, glycerol and DMSO before being aliquoted into 1 mL cryogenic tubes and frozen for long-term storage in liquid nitrogen.

The cells were cultured in growth medium composed of low glucose DMEM containing 5% FBS, 100 U/mL penicillin and 100 µg/mL streptomycin. Cells were maintained at 37ºC in a humidified atmosphere of 5% CO_2 and 95% air. To select for the positively transfected cells, P2Y1 and P2Y2 cells were cultured in growth media that also contained 0.5 g/L G418. Parental cells were cultured without this drug added. Every 3-4 days the growth media was replaced. Once ~90% confluency was reached, the cells were treated with 0.25% trypsin for 5 to 15 min to loosen the cells from the culture surface and the resulting cell suspension was centrifuged. The trypsin solution was removed by aspiration and the pellet of cells was resuspended in fresh growth media. A fraction of the cells then was replated. Cells for immunostaining and patch clamp experiments were grown on cleaned and sterilized 12 mm coverslips under the same conditions.

D. Electrophysiological Recordings

Recording Using PBS as the Extracellular Solution

Astrocytoma cells were plated onto 12 mm diameter glass coverslips at least one day prior to recording. Coverslips were placed on a Nikon TMC inverted phase-contrast microscope and perfused at a rate of 1-2 mL/sec (35ºC) with a phosphate buffered solution (PBS) containing (in mM): NaCl (147), KH_2PO_4 (0.5), Na_2HPO_4 (3.2), $CaCl_2$ (1), $MgCl_2$ (0.5), dextrose (5), KCl (2.7). The pH was adjusted to 7.3 using NaOH. The final osmolarity of the solution was determined to be 300 mOsm using a vapor pressure osmometer. Hyposmotic solutions were made by initially adding only 73.5 mM NaCl, and then adding NaCl until the final osmolarity was 200 mOsm. Patch pipettes pulled from thin-walled glass capillary tubes by a Narishige PP-83 puller and had a resistance of

3-9 MΩ when filled with a solution containing (in mM): KCl (135), $CaCl_2$ (0.2), $MgCl_2$ (1), EGTA (10), Na_2ATP (3), HEPES (10), and dextrose (5.5). The free calcium concentration was calculated to be 8.9 nM using Maxchelator program WEBMAXCLITE v1.15 (http://maxchelator.stanford.edu) and the pH was adjusted to 7.3 using KOH. The final osmolarity of the solution was determined to be 300 mOsm using a vapor pressure osmometer. The electrode was manipulated so that the tip lightly touched a cell's membrane. Light suction was applied via a syringe, and when the series resistance was greater than 1 gigaohm, more negative pressure was applied to break the cell membrane inside the electrode. A stable whole-cell recording was defined when the cell had a seal resistance between 100 and 500 MΩ and a capacitance between 15 and 80 pF lasting for at least five minutes before the experiment was conducted. Stable cells were held in voltage clamp mode at a holding potential (V_H) of –70 mV using an Axopatch 200A amplifier. Every 30 sec, a series of voltage pulses was applied that increased from –100 mV to +80 mV in 20 mV increments. Pulses were held for 100 msec. For some experiments, tetraethylammonium (TEA) or pyridoxalphosphate-6-azophenyl-2',4'-disulphonic acid (PPADS) was added to the PBS once a stable recording was obtained.

Recording Using CsCl in the Extracellular Solution

Experiments using CsCl solutions were performed in the same manner as those done in PBS solution. Both isosmotic and hyposmotic CsCl solutions contained (in mM): CsCl (100), HEPES (10), $CaCl_2$ (1), $MgCl_2$ (0.5), and dextrose (5). The pH was adjusted to 7.3 using CsOH. For isosmotic CsCl solution, approximately 100 mM sucrose was added until the solution had an osmolarity of 300 mOsm. Hyposmotic solutions were

made by adding sucrose until the osmolarity was 200 mOsm. Patch pipettes pulled from thin-walled glass capillary tubes by a Narishige PP-83 puller and had a resistance of 3-9 MΩ when filled with a solution containing (in mM): CsCl (100), $CaCl_2$ (1), $MgCl_2$ (1), EGTA (10), Na_2ATP (5), HEPES (10), glucose (5.5), and sucrose (100). The free calcium concentration was calculated to be 8.9 nM using Maxchelator program WEBMAXCLITE v1.15 (http://maxchelator.stanford.edu) and the pH was adjusted to 7.3 using CsOH. The final osmolarity of the solution was determined to be 300 mOsm using a vapor pressure osmometer. Cell recordings were established with the cells perfused in PBS. Stable cells exhibited seal resistances between 100 and 500 MΩ, capacitances between 15 and 80 pF and steady resting currents for at least 5 minutes. Once the recording was determined to be stable, the extracellular solution was switched to isosmotic CsCl solution and the holding voltage was changed to V_H = 0 mV. Every 30 seconds a series of voltage pulses was applied that increased from –100 mV to +80 mV in 20 mV increments. Pulses were held for 100 msec. For some experiments, DCPIB was used during recordings as a VRAC inhibitor or ATP was added to the perfusion solution.

E. Immunostaining

Solutions

Phosphate buffer was made by adding 135 mM NaCl and 2.5 mM Na_2HPO_4 to deionized distilled water (ddH_2O) and then adjusting the to a pH to of 7.4 with 1 N HCl. Paraformaldehyde fixative solution was made by adding 0.5, 1, 2, or 4% (w/v)

paraformaldehyde to the phosphate buffer. 1% Triton X-100 was made by adding 1% v/v Triton X-100 to phosphate buffer.

Procedure

Cells were grown as described above to 60-90% confluence, washed twice with phosphate buffer, fixed with 0.5% paraformaldehyde solution for 10 minutes and then permeabilized by exposure to 1% Triton X-100 for 5 minutes. Fixed cells were first incubated in 20% normal goat serum in phosphate buffer for 30 min before being incubated with primary antibody, either rabbit anti-P2Y1 or rabbit anti-P2Y2 diluted to 1:500 in phosphate buffer, for 1 hr at room temperature. The cells were then washed twice and incubated for 5 min with phosphate buffer. The secondary antibody, Alexafluor 568, was diluted to 1:200 in phosphate buffer and cells were incubated with this solution for 1 hr at room temperature. The cells again were washed twice and incubated for 5 minutes with the phosphate buffer and then washed twice and incubated with ddH2O. Coverslips were mounted on microscope slides using aqueous mounting media.

For some studies, specific binding was blocked by incubating antibodies with control antigen provided by the primary antibody's manufacturer prior to exposing the cells. Using methods provided by the manufacturer (Alomone Labs) control antigen was mixed with primary antibody at equal concentrations (w/w) and then incubated for 1 hr at room temperature. The solution then was centrifuged at 10,000 x g for 5 min and the resulting supernatant used in place of the primary antibody.

F. Western Blots

Solutions

Blocking powder, ECF substrate, secondary antibodies and tertiary antibodies were acquired as part of the ECF Western Blotting Kit. Mammalian cell lysis buffer contained 150 mM NaCl, 50 mM Tris-HCL, 1 mM EDTA, 0.1% SDS, 0.5% DOC, 1% Igepal and a cocktail of protease inhibitors supplied in the lysis kit that contained 4-(2-aminoethyl) benzenesulfonyl fluoride (AEBSF), pepstatin A, bestatin, leupeptin, aprotinin and trans-epoxysuccinyl-L-leucyl-amido(4-guanidino)-butane (E-64) Phosphate buffer solution (PBS) had a different solute composition than in the electrophysiological studies with (in mM) NaCl (147), KH_2PO_4 (1.5), Na_2HPO_4 (8), $CaCl_2$ (1), $MgCl_2$ (0.5), dextrose (5) and KCl (2.7). Loading buffer was a 50 mM Tris-HCl solution that contained 25% (v/v) glycerol, 2% (w/v) SDS, 1% (w/v) bromophenol blue and 5% (v/v) β-mecaptoethanol. Running buffer was an aqueous solution of 0.1% (w/v) SDS, 0.3% (w/v) trizma base and 1.44% (w/v) glycine. Transfer buffer was an aqueous solution of 0.05% (w/v) SDS, 0.3% (w/v) trizma base and 1.44% (w/v) glycine. Wash buffer was composed of PBS with 3% (v/v) Tween added. Blocking solution was made by adding 5% (w/v) blocking powder to wash buffer.

Cell Lysing

Cells grown in 100 mm culture dishes as described above were lysed using Mammalian Cell Lysis Kit. Adherent cells were washed twice with PBS and then incubated on ice with 100 µL of Mammalian Cell Lysis buffer for 15 minutes. Cell

debris was extracted by centrifugation at 12,000 x g for 15 minutes. The remaining cell lysate solution was pipetted into a 1.5 mL Eppendorf tube and stored at -70º C.

To determine protein concentration in this solution, the BCA method was used with a colorometric kit from Sigma-Aldrich Inc. and the samples and standards measured with a spectrophotometer. Briefly, 1 mL of BCA solution was added to each sample and standard, and heated at 40ºC for 25 minutes. The optical density of each standard at 562 nm then was measured in a spectrophotometer and a regression line was created, with typical R^2 values of > 0.96. Protein standards were made by adding 0, 5, 10, 30 and 50 µL of 1 mg BSA/ml protein to appropriate amounts of ddH_2O to bring the volume to 100 µL. Protein samples were made by adding 10 µL of cell lysate to 90 µL of ddH_2O. The samples were measured under identical conditions and protein concentrations were calculated using the regression line.

Gel Electrophoresis

Western blotting was performed to analyze the presence or absence of P2Y subtypes in each of the three cell lines. 10% SDS-polyacrylamide gels were made from the following reagents (in mL): acrylamide (3.3), ddH_2O (4.1), 1.5 M Tris buffer (2.5), 10% SDS (0.1), TEMED (0.005) and ammonium persulfate (0.05). The stacking gel was made with the same ingredients except 0.5 M Tris buffer and 0.01 mL of TEMED were used.

Loading buffer was added to an equal volume of cell lysate and boiled for 5 min prior to loading into the gel. A protein ladder was placed in separate lanes of the gel. The

Power Pac Basic power supply was set at 50 mA until the samples had run through the stacking gel and then increased to 100 mA for one to two hours.

Western Transfer and Imaging

Protein contents of the gel were transferred to a polyvinylidene difluoride (PVDF) membrane using electrophoresis. The transfer was run overnight at 90 mA. After transfer, the membrane was washed with wash buffer and incubated in 5% blocking solution for 1 hr. Primary antibodies were diluted into 5% blocking buffer and incubated for one hr. Anti-β-Actin was used at a dilution of 1:1000 and both Anti-P2Y1 and Anti-P2Y2 were used at a dilution of 1:200. After incubation with the primary antibody the membrane was washed twice for 10 min with wash buffer. FITC-conjugated secondary antibody was diluted to 1:600 with wash buffer and incubated with the membrane for one hr. StrepTactin AP-conjugate was added at a 1:5000 concentration at the same time as the secondary antibody to label the protein ladder. The alkaline-phosphatase-conjugated tertiary antibody to fluorescein was diluted to 1:1000 in wash buffer and incubated with the membrane for 30 min. The membrane then was washed using wash buffer a final time. ECF substrate was added to the membrane, which then was immediately placed into the ECF scanning machine. Fluorescence was excited at 488 nm and the emission was recorded with a digital imaging system. The resulting image was viewed and edited on Micrososoft Picture Manager.

At times, control antigens were preincubated with the P2Y antibodies to test for cross reactivity of the primary antibodies. Protocol for incubation with control antigen is described in section III.E. Immunostaining.

G. Data Analysis and Calculations

Electrophysiological raw data were recorded using Clampex 8.2 (Axon Instruments) and then transferred to Excel (Microsoft) for graphical analysis. Calculations made from these data include the reversal potential, cell conductance and current inhibition. Both reversal potential and conductance were determined by calculating the equation for a line connecting data points on either side of the voltage axis (e.g. Figure 2). The slope of this line was used as an estimate of cell slope conductance and the intercept of this line on the voltage axis was used as an estimate of the membrane reversal potential.

Calculating TEA Current Inhibition

The magnitude of current inhibition by TEA was calculated using Microsoft Excel using current-voltage plots of the data before the addition of TEA (blue) and after the application of 10 mM TEA to the bath solution (red) as shown in Figure 3. Since TEA inhibited only the outward rectifying component of the cell conductance, currents were measured at +80 mV. The total current prior to TEA treatment (I_T) and the current remaining after TEA treatment (I_D) were compared to the extrapolated-baseline current at +80 mV (I_{EB}). I_{EB} was estimated by calculating a linear regression line using the currents measured at -100 mV, -80 mV and -60 mV. The calculation of percent TEA-current inhibition is performed as follows:

$$\text{Percent TEA-current inhibition} = [(I_T - I_D)/(I_T - I_{EB})] \times 100\%$$

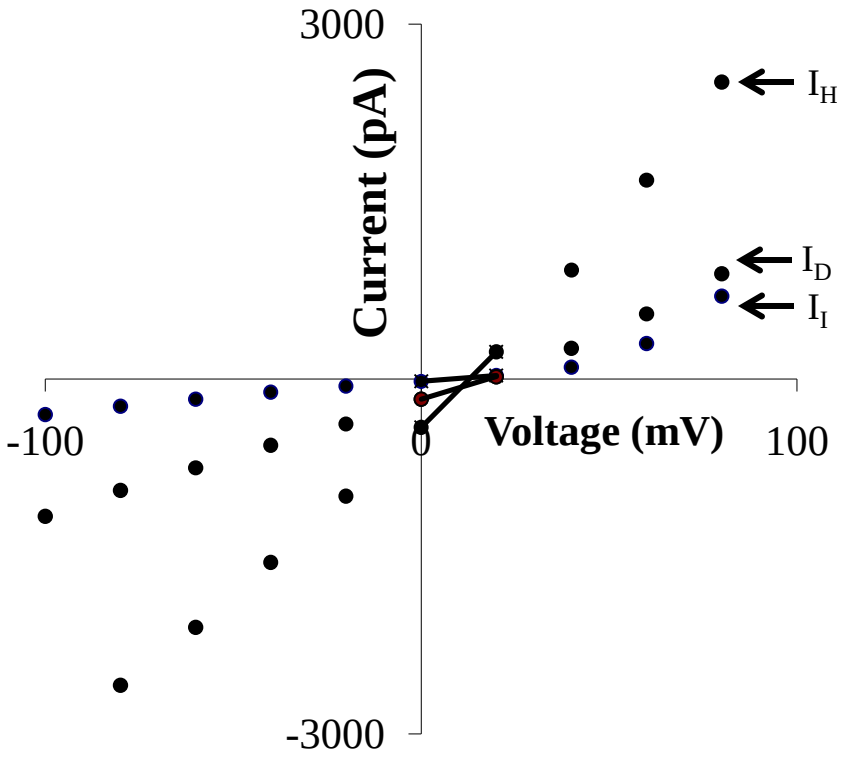

Figure 2 Example of cell reversal potential and conductance analysis. The blue data set contains currents measured from a cell in isosmotic CsCl (I_I). The pink data set contains currents from the same cell 5 min after the bath solution was changed to hyposmotic CsCl solution (I_H). The yellow data set contains the currents resulting from hyposmotic CsCl solution plus 20 μM DCPIB (I_D). Lines segments between currents on either side of the abscissa were constructed for each data set. These lines were used to estimate conductance and reversal potential.

Calculating Drug-induced Current Inhibition

Both PPADS and DCPIB were used to inhibit hyposmotically activated current. The magnitude of current inhibition by these drugs was calculated using Microsoft Excel to create a current-voltage plot of the data as shown in Figure 2. Currents elicited during isosmotic CsCl conditions (I_I), hyposmotic CsCl conditions (I_H) and hyposmotic CsCl conditions plus 20 µM DCPIB (I_D) are represented by the blue, pink and yellow data sets, respectively. The calculation of percent drug-induced current inhibition is as follows:

$$\text{Percent hyposmotic current inhibition} = [(I_H - I_D)/(I_H - I_I)] \times 100\%$$

H. Statistics

Data were analyzed by ANOVA, or Students t-test for paired or unpaired samples, as appropriate and significance indicated for $p<0.05$. All values a reported as the mean ± SEM. Clampfit 8.2 (Axon Instruments) was used for electrical recording analysis and statistical analysis.

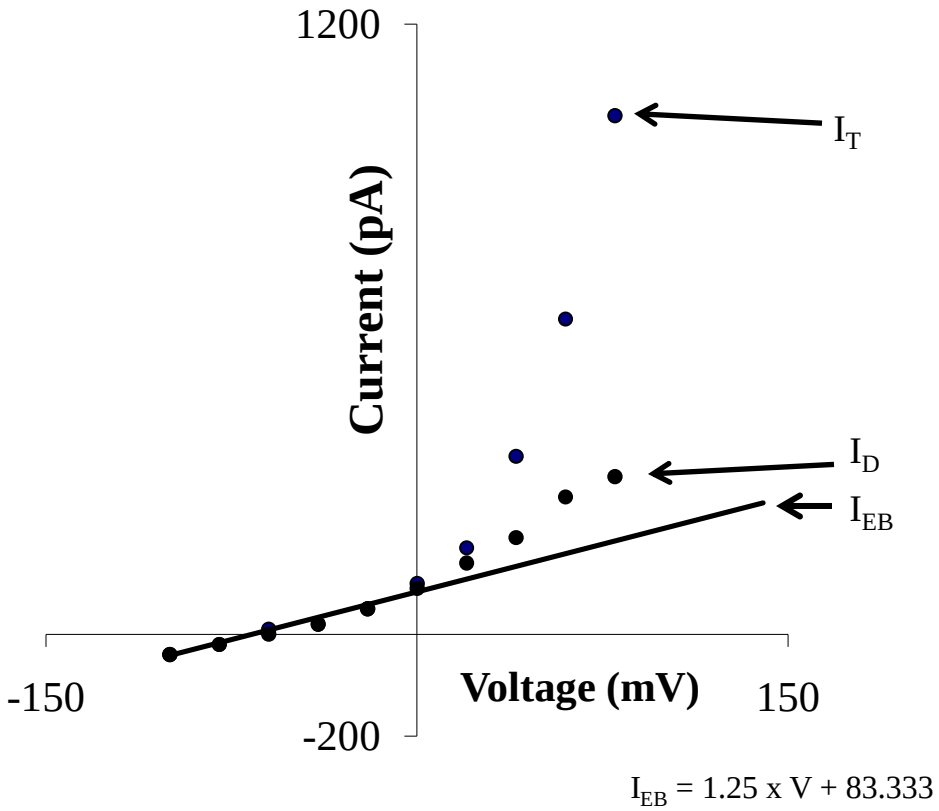

Figure 3 Example of cell membrane current analysis. The blue data set contains currents measured from a cell in isosmotic PBS without TEA. The red data set contains currents from the same cell 5 min after application of isosmotic PBS with 10 mM TEA. Data points for membrane voltages of -100 mV to -60 mV without TEA were used to create the line that represents non-rectified current for cells in isosmotic conditions. The equation for this line is displayed in the bottom right hand corner. Also on the right are indicators of the extrapolated-baseline current at +80 mV, I_{EB}, TEA-inhibited current, I_D, and total current, I_T, used in calculations as described in the text.

IV Results

A. 1321N1 Human Astrocytoma Cells Exhibit TEA Sensitivity

Whole cell voltage clamp recordings in isosmotic PBS revealed a number of basal electrophysiological attributes of 1321N1 astrocytoma cells. Under these conditions P2Y1 and P2Y2 cells had similar basal whole-cell slope conductances, measured at 0 pA and normalized to the cell capacitance of 0.1135 ± 0.0301 nS/pF and 0.1060 ± 0.0186 nS/pF, respectively. Parental cells averaged a larger basal conductance of 0.2887 ± 0.1419 nS/pF, although it was not significantly different from the receptor expressing cells ($p = 0.33$) (Figure 4A). Reversal potentials were quite negative for each cell type. P2Y1, P2Y2 and Parental cells averaged reversal potentials of -68.4 ± 3.3 mV, -68.1 ± 7.0 mV and -60.5 ± 5.6 mV (Figure 4B). All cells studied had capacitances between 10 and 60 pF.

All three cell lines exhibited TEA-sensitive outwardly rectified currents while perfused with isosmotic PBS, although in parental cells this was not statistically significant. 10 mM TEA inhibited currents measured at +80 mV by 88.3 ± 9.2% 77.9 ± 10.1%, and 28.4 ± 24.4% in P2Y1, P2Y2 and Parental cells, respectively (Figure 5A). Figure 5B shows the TEA dose-response curve in P2Y1 cells. The curve was fit using the Michaelis-Menten equation with a calculated IC_{50} of 0.37 mM and maximal inhibition of 88%.

During perfusion with 10 mM TEA whole cell normalized conductance and reversal potential were measured in each cell type. After the addition of TEA there was no significant change in slope conductance in P2Y1 ($p = 0.13$), P2Y2 ($p = 0.46$) or Parental cells ($p = 0.32$) (Figure 4A). Similarly, the reversal potential was not found to

A

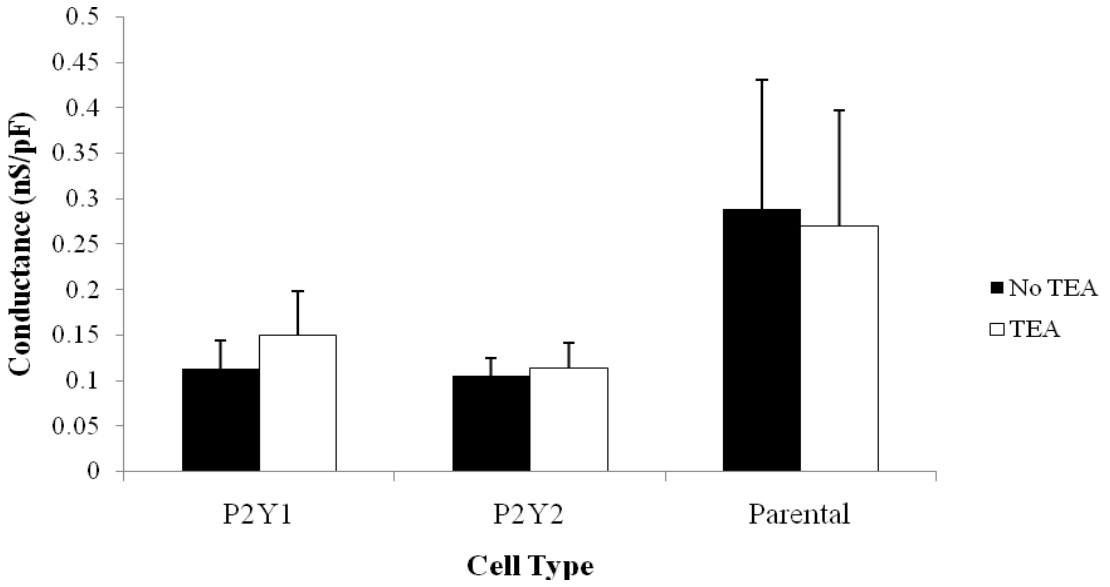

B

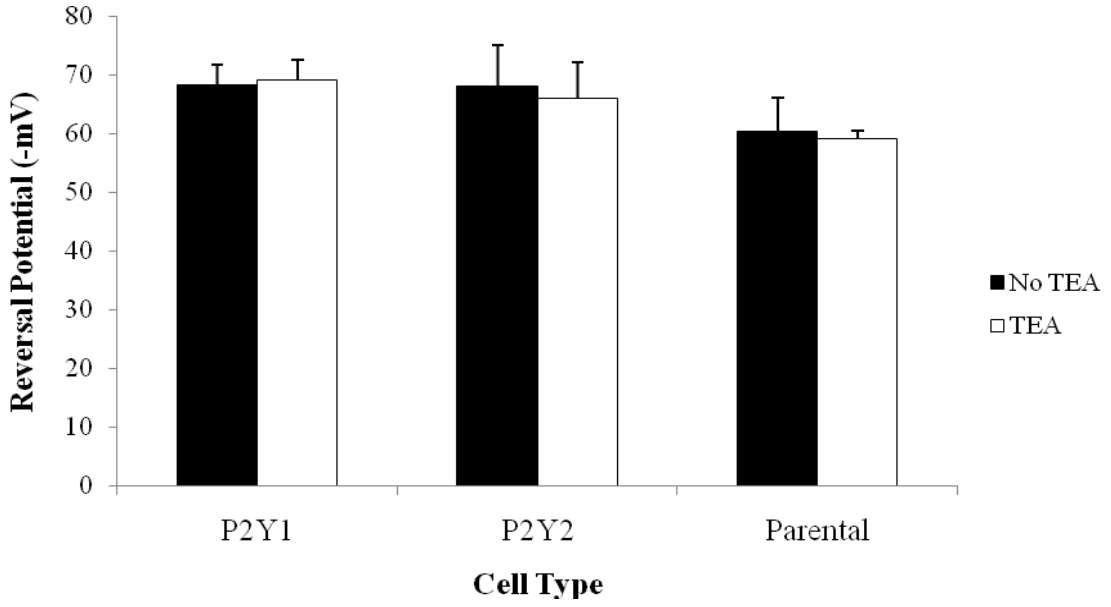

Figure 4 The effect of TEA on whole cell conductance and reversal potential in 1321N1 astrocytoma cells. A) Whole cell normalized slope conductance for P2Y1 (n=8), P2Y2 (n=7) and Parental (n=4) cells during perfusion with isosmotic PBS and isosmotic PBS plus 10 mM TEA. B) Reversal potentials for P2Y1 (n=8), P2Y2 (n=7) and Parental (n=4) cells during perfusion with isosmotic PBS and isosmotic PBS plus 10 mM TEA.

A

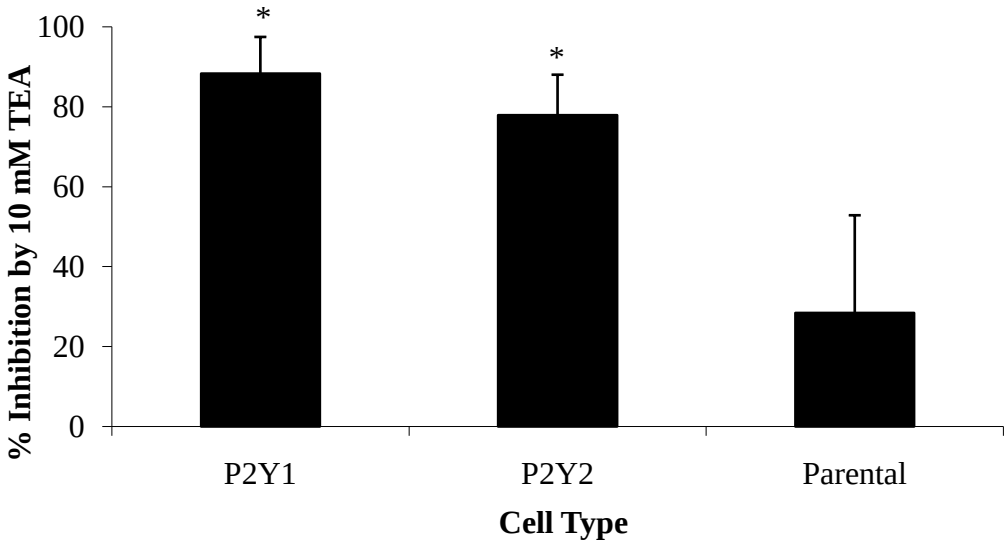

B

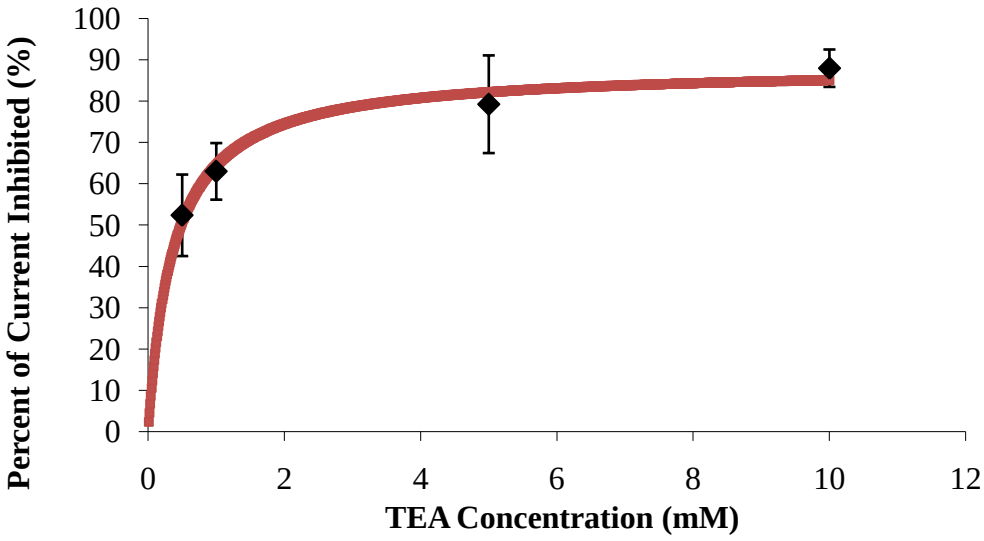

Figure 5 Effect of TEA on outwardly-rectified potassium currents in 1321N1 astrocytoma cells. A) Percent of current inhibited at +80 mV by TEA in isosmotic PBS. Measurements were taken at +80 mV in P2Y1 receptor transfected cells (n=8), P2Y2 receptor transfected cells (n=7) and Parental cells (n=4). (* indicates $p < 0.05$) B) TEA concentrations of 0.5 mM (n=3), 1 mM (n=3), 5 mM (n=4) and 10 mM (n=8) were used to inhibit outwardly rectified potassium currents in P2Y1 receptor transfected cells in isosmotic PBS. The curve was fit using first order kinetics equation calculated assuming the curve passes through the origin ($r^2 = 0.81$). The IC_{50} was determined to be 0.37 mM. Fitted curve was calculated using Clampfit 8.2.

change after application of TEA in P2Y1 ($p = 0.69$), P2Y2 ($p = 0.46$) or Parental cells ($p = 0.79$).

B. Current activated in hyposmotic PBS is PPADS-sensitive in cells expressing P2Y receptors.

The electrophysiological response to hyposmotic exposure (HOE) and subsequent addition of 100 μM PPADS, a specific nucleotide receptor blocker, was examined in each cell type by voltage clamp technique in PBS. Isosmotic and hyposmotic PBS had osmolarities of 300 mOsm and 200 mOsm, respectively, and in all conditions, 10 mM TEA was present as discussed in Materials and Methods. Raw electrophysiological data for typical P2Y1, P2Y2 and Parental cells are shown in Figures 6, 7, and 8, respectively. P2Y1 and P2Y2 cells exhibited similar electrophysiological responses to HOE. Both cell types demonstrated an increase in current amplitude within 5 to 10 min of HOE that was inhibited by 100 μM PPADS (Figures 6A and 7A). The hyposmotically activated currents in P2Y1 and P2Y2 cells were outwardly rectified (Figures 6E and 7E) and also showed time inactivation at depolarizing potentials (Figures 6C and 7C). While Parental cells also increased in current after HOE, they demonstrated no outward rectification, time inactivation or sensitivity to PPADS (Figure 8).

Cumulative data from these experiments allowed for analyses of the hyposmotically activated conductance and change in reversal potential. All cell types increased their whole-cell normalized slope conductance during HOE, measured at 0 pA, with Parental cells nearly doubling and receptor expressing cells more than doubling (Figure 9A). In contrast the reversal potentials of P2Y1 and P2Y2 cells significantly

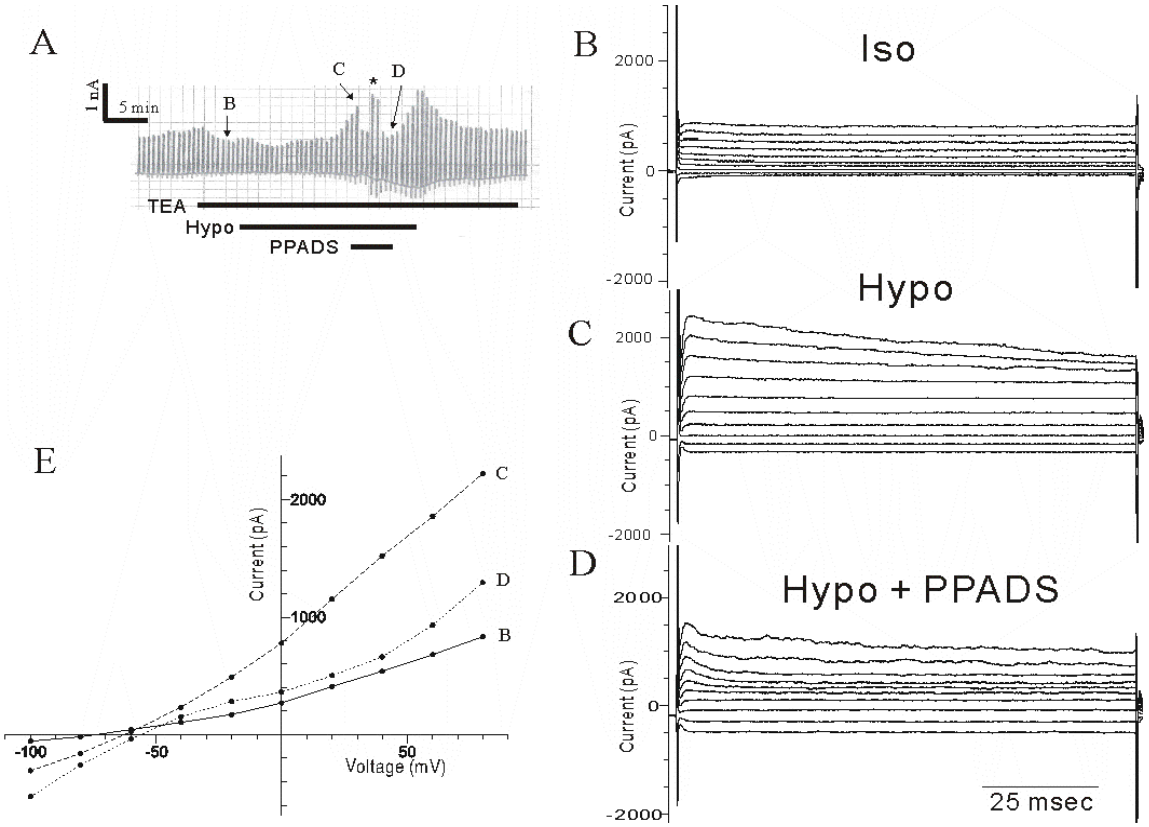

Figure 6 P2Y1 receptor transfected cells have a hyposmotically activated current that is inhibited by 100 µM PPADS in PBS. A) Illustrated is a strip chart derived from data obtained from a P2Y1 cell initially bathed in isosmotic PBS. TEA (10 mM) was added to the perfusate as indicated and the cell was subsequently exposed to hyposmotic PBS and then hyposmotic PBS plus 100 µM PPADS. Cell currents recorded while the cell was perfused with B) isosmotic PBS, C) hyposmotic PBS and D) hyposmotic PBS plus 100 µM PPADS. Location of current traces in the strip chart is similarly indicated. E) Current-voltage relationships for the three current traces in B) through D). (* indicates noise artifact.)

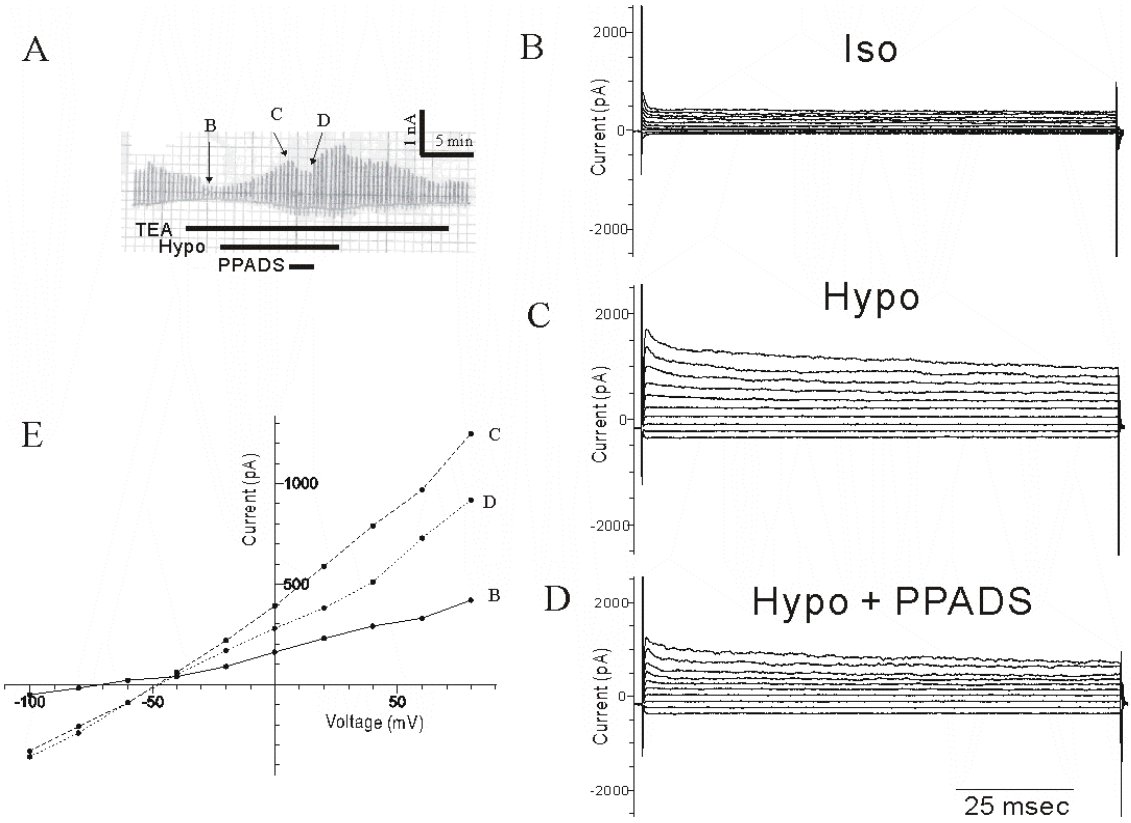

Figure 7 P2Y2 receptor transfected cells have a hyposmotically activated current that is inhibited by 100 µM PPADS in PBS. A) Illustrated is a strip chart derived from data obtained from a P2Y2 cell initially bathed in isosmotic PBS. TEA (10 mM) was added to the perfusate as indicated and the cell was subsequently exposed to hyposmotic PBS and then hyposmotic PBS plus 100 µM PPADS. Cell currents recorded while the cell was perfused with B) isosmotic PBS, C) hyposmotic PBS and D) hyposmotic PBS plus 100 µM PPADS. Location of current traces in the strip chart is similarly indicated. E) Current-voltage relationships for the three current traces in B) through D).

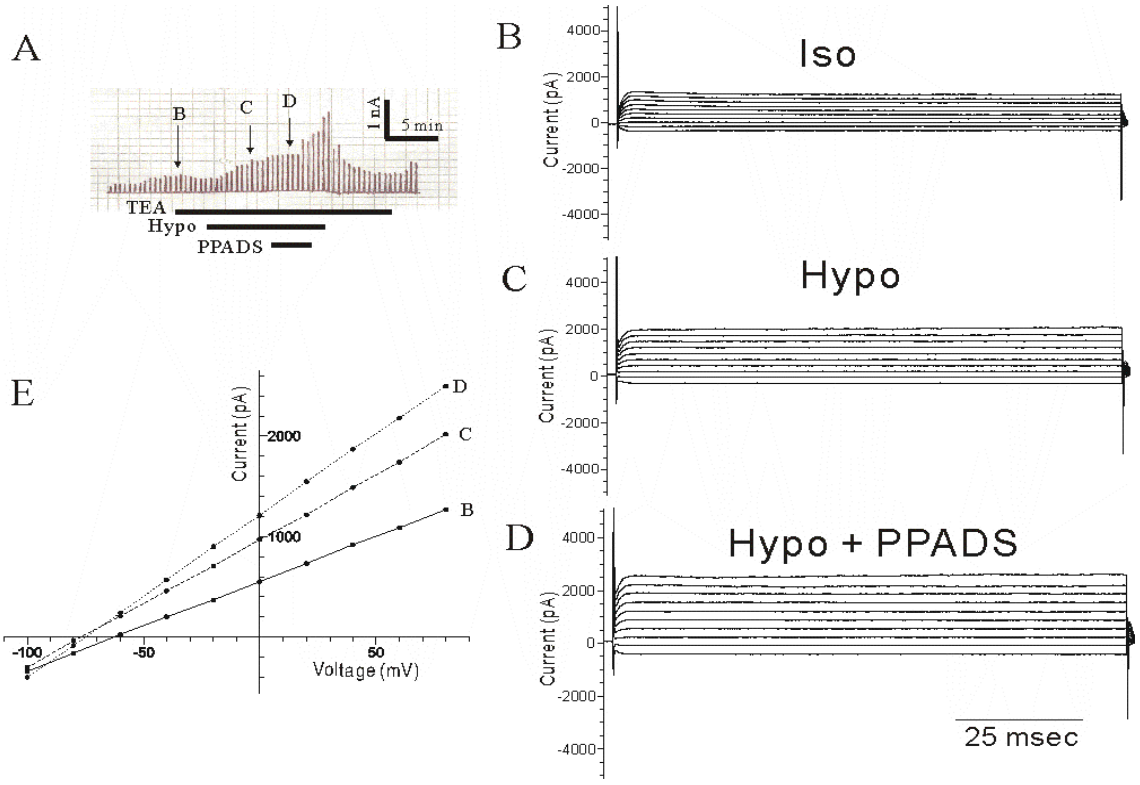

Figure 8 Parental cells have a hyposmotically activated current that is not inhibited by 100 µM PPADS in PBS. A) Illustrated is a strip chart derived from data obtained from a Parental cell initially bathed in isosmotic PBS. TEA (10 mM) was added to the perfusate as indicated and the cell was subsequently exposed to hyposmotic PBS and then hyposmotic PBS plus 100 µM PPADS. Cell currents recorded while the cell was perfused with B) isosmotic PBS, C) hyposmotic PBS and D) hyposmotic PBS plus 100 µM PPADS. Location of current traces in the strip chart is similarly indicated. E) Current-voltage relationships for the three current traces in B) through D).

A

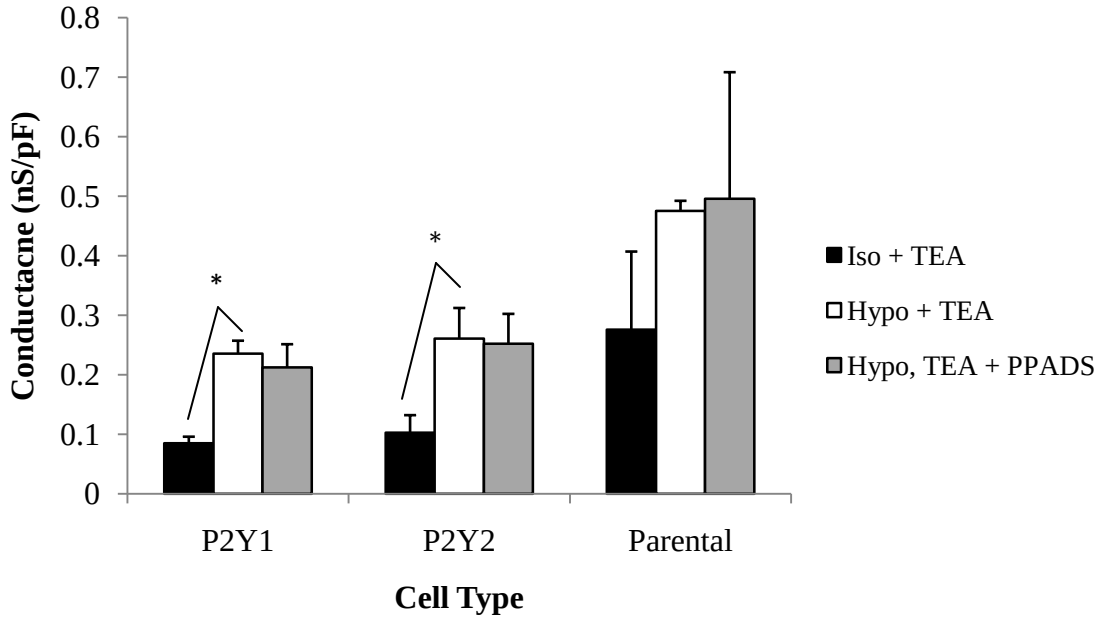

B

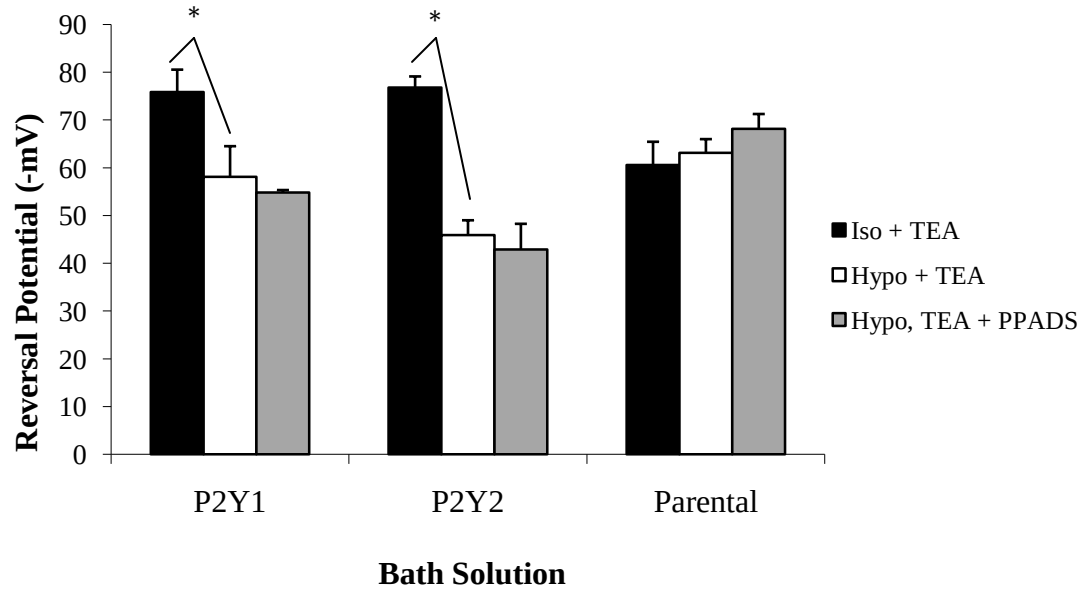

Figure 9 Effects of TEA, hyposmotic exposure and PPADS on whole cell conductance and reversal potential in 1321N1 astrocytoma cells. A) Whole cell normalized conductance for P2Y1 (n=4), P2Y2 (n=4) and Parental (n=4) cells during perfusion with isosmotic PBS plus 10 mM TEA, hyposmotic PBS plus 10 mM TEA and hyposmotic PBS plus 10 mM TEA and 100 µM PPADS. B) Reversal potentials for P2Y1 (n=4), P2Y2 (n=4) and Parental (n=4) cells during perfusion with isosmotic PBS plus 10 mM TEA, hyposmotic PBS plus 10 mM TEA and hyposmotic PBS plus 10 mM TEA with 100 µM PPADS added. (* indicates $p < 0.05$)

depolarized (p = 0.0064 and 0.0458, respectively) during HOE, while the reversal potential of Parental cells did not depolarize (Figure 9B).

The addition of 100 μM PPADS to hyposmotic medium had no significant effect on whole cell conductance or reversal potential, but did inhibit current at higher voltages in P2Y1 and P2Y2 cells (Figure 9). Whole-cell normalized slope conductance of both P2Y1 and P2Y2 cells showed no significant change (p = 0.4708 and 0.3202, respectively) after the addition of PPADS to the hyposmotic PBS. Similarly, P2Y1 and P2Y2 cells demonstrated no significant change (p = 0.3542 and 0.1446, respectively) in reversal potential in response to the drug application. However, when the current elicited by HOE was measured at +80 mV there was a significant inhibition of current in P2Y1 and P2Y2 cells of 57.3 ± 8.3% and 51.2 ± 10.1%, respectively. The extent of inhibition at higher voltages in these cell types also can be seen in the current-voltage plots in Figures 6C and 7C. The Parental cells showed no change whole-cell conductance, reversal potential or current at depolarized potential in response to PPADS (Figures 9 and 10).

In separate experiments P2Y1 and P2Y2 cells were perfused with 100 μM PPADS prior to HOE (Figures 11-13). Strip chart recordings (Figures 11A and 12A) demonstrated little increase in current amplitude during HOE. The inactivation seen in previous experiments (Figures 6 and 7) was also absent in the presence of PPADS (Figures 11C and 12C). Whole cell conductance did increase during HOE in the presence of PPADS (Figure 13A),but not significantly, and definitely not to the same extent as without PPADS. Also, in the presence of PPADS there is no significant change in reversal potential due to HOE in either receptor cell type (Figure 13B). In P2Y1 and P2Y2 cells, PPADS totally blocked (p =

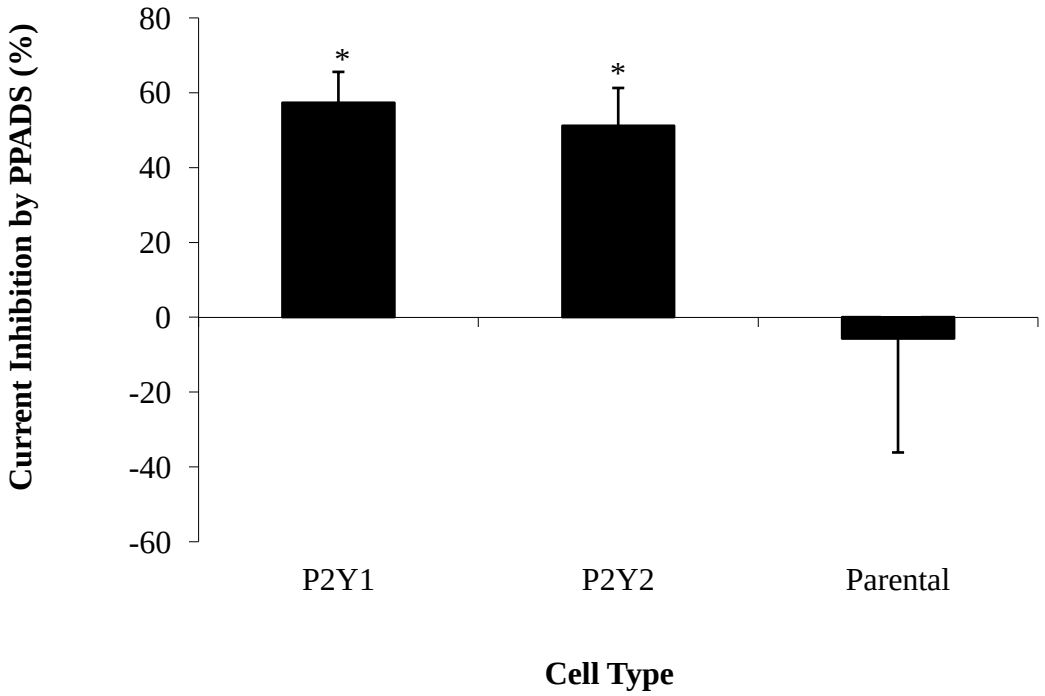

Figure 10 PPADS inhibits hyposmotic current in P2Y1 and P2Y2 receptor transfected cells but not in Parental cells in PBS. Percent inhibition of hyposmotically activated current, measured at +80 mV, by 100 μM PPADS in P2Y1 (n=4), P2Y2 (n=4) and Parental (n=4) cells. Cells were perfused in PBS solution as described in the Materials and Methods section and subjected to hyposmotic exposure for 5-10 min prior to addition of PPADS. (* indicates values significantly different from zero $p < 0.05$)

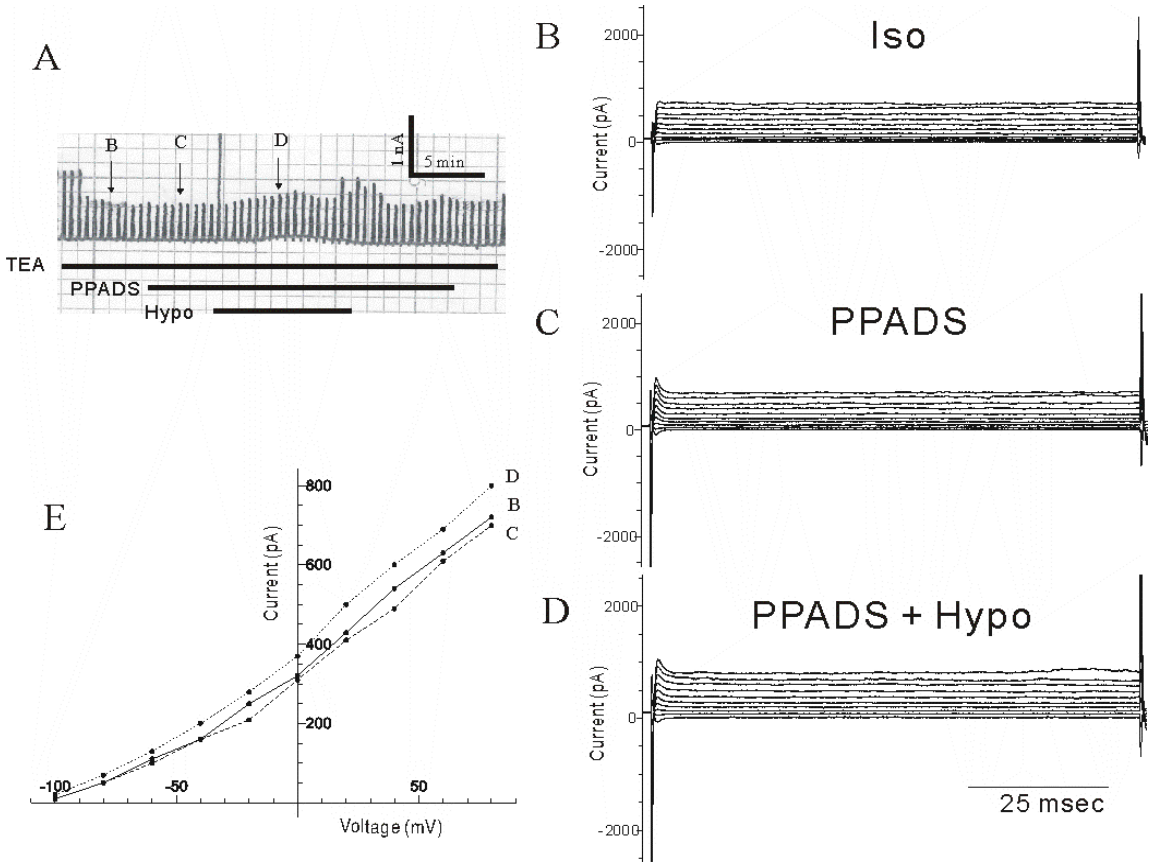

Figure 11 P2Y1 receptor transfected cells lack hyposmotically activated current when treated with 100 µM PPADS prior to hyposmotic exposure. A) Illustrated is a strip chart derived from data obtained from a P2Y1 cell initially bathed in isosmotic PBS. TEA (10 mM) was added to the perfusate as indicated and the cell was subsequently exposed to isosmotic PBS plus 100 µM PPADS and then hyposmotic PBS plus 100 µM PPADS. Cell currents recorded while the cell was perfused with B) isosmotic PBS, C) isosmotic PBS plus 100 µM PPADS and D) hyposmotic PBS plus 100 µM PPADS. Location of current traces in the strip chart is similarly indicated. E) Current-voltage relationships for the three current traces in B) through D).

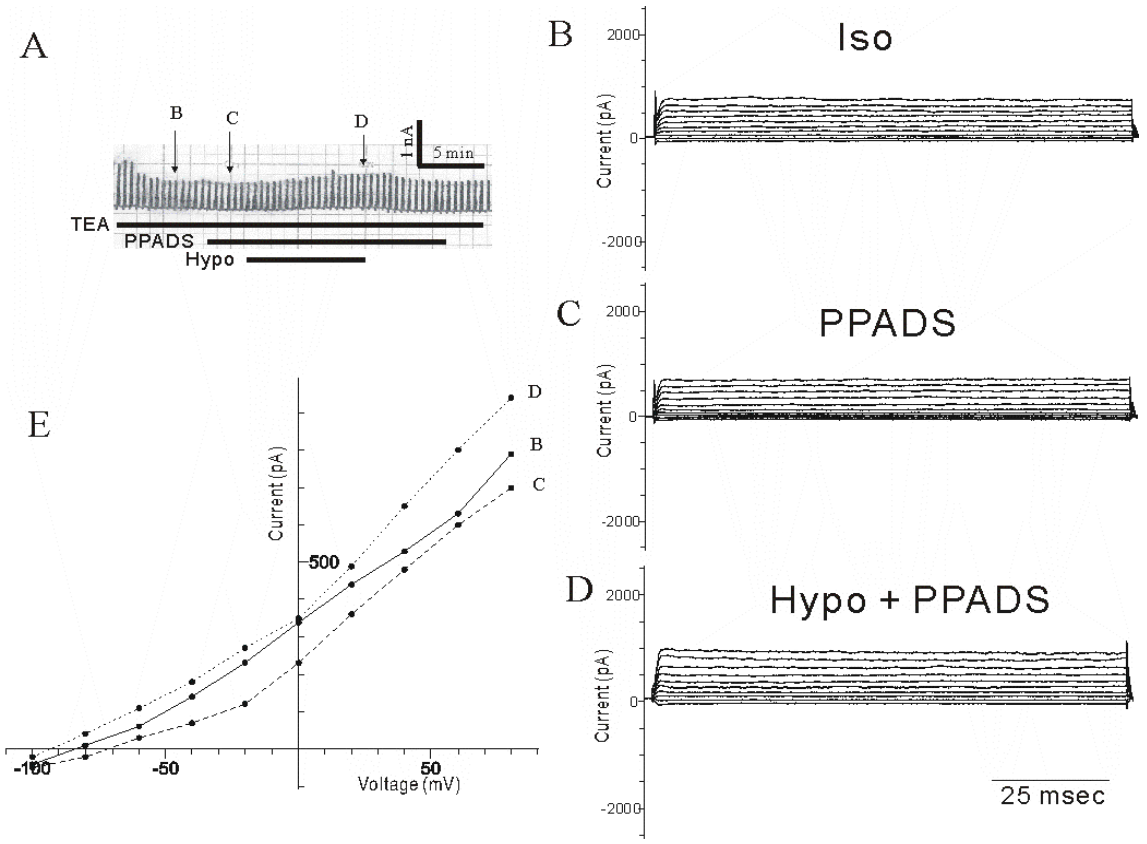

Figure 12 P2Y2 receptor transfected cells lack hyposmotically activated current when treated with 100 µM PPADS prior to hyposmotic exposure. A) Illustrated is a strip chart derived from data obtained from a P2Y2 cell initially bathed in isosmotic PBS. TEA (10 mM) was added to the perfusate as indicated and the cell was subsequently exposed to isosmotic PBS plus 100 µM PPADS and then hyposmotic PBS plus 100 µM PPADS. Cell currents recorded while the cell was perfused with B) isosmotic PBS, C) isosmotic PBS plus 100 µM PPADS and D) hyposmotic PBS plus 100 µM PPADS. Location of current traces in the strip chart is similarly indicated. E) Current-voltage relationships for the three current traces in B) through D).

A

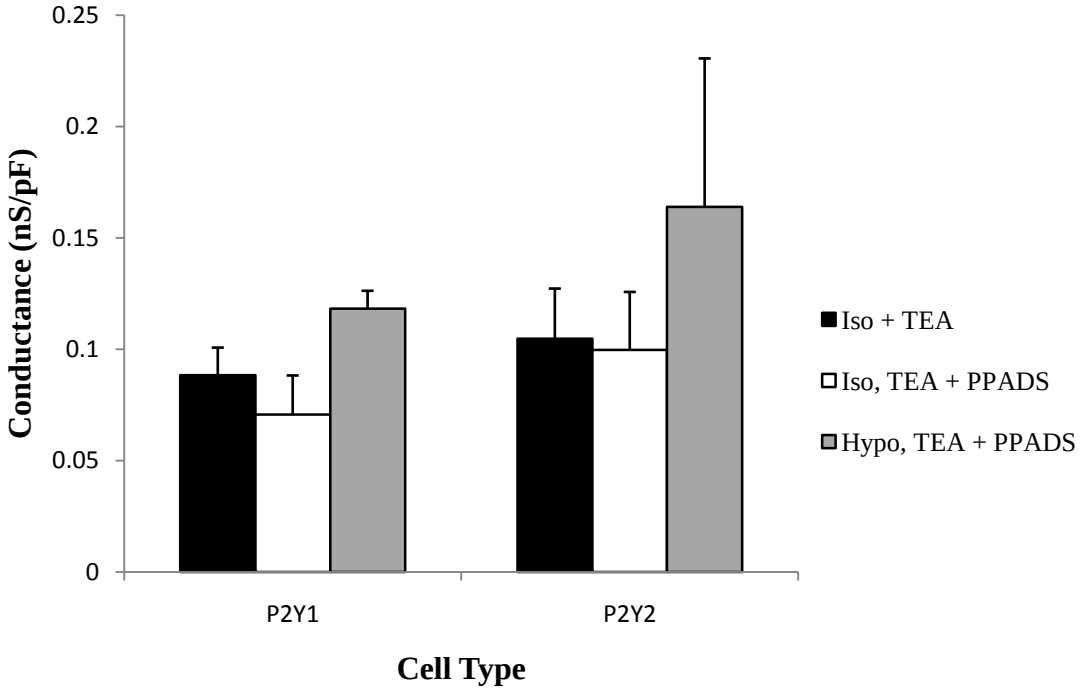
0.25
0.2
0.15
0.1
0.05
0
Conductance (nS/pF)
P2Y1
P2Y2
Cell Type
Iso + TEA
Iso, TEA + PPADS
Hypo, TEA + PPADS

B

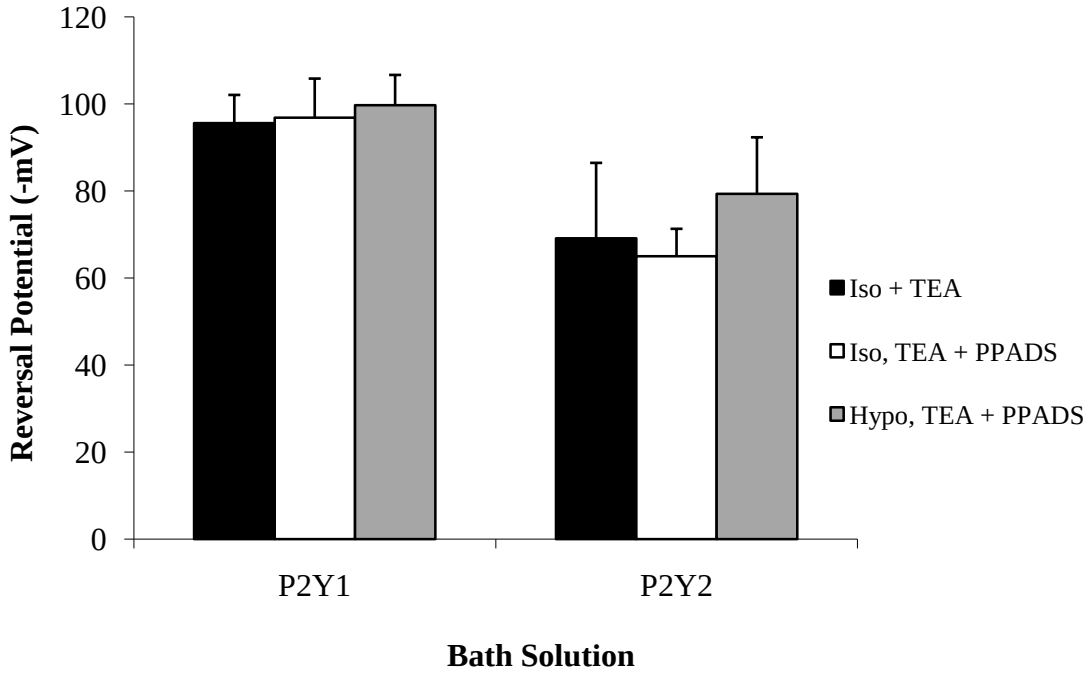
120
100
80
60
40
20
0
Reversal Potential (-mV)
P2Y1
P2Y2
Bath Solution
Iso + TEA
Iso, TEA + PPADS
Hypo, TEA + PPADS

C

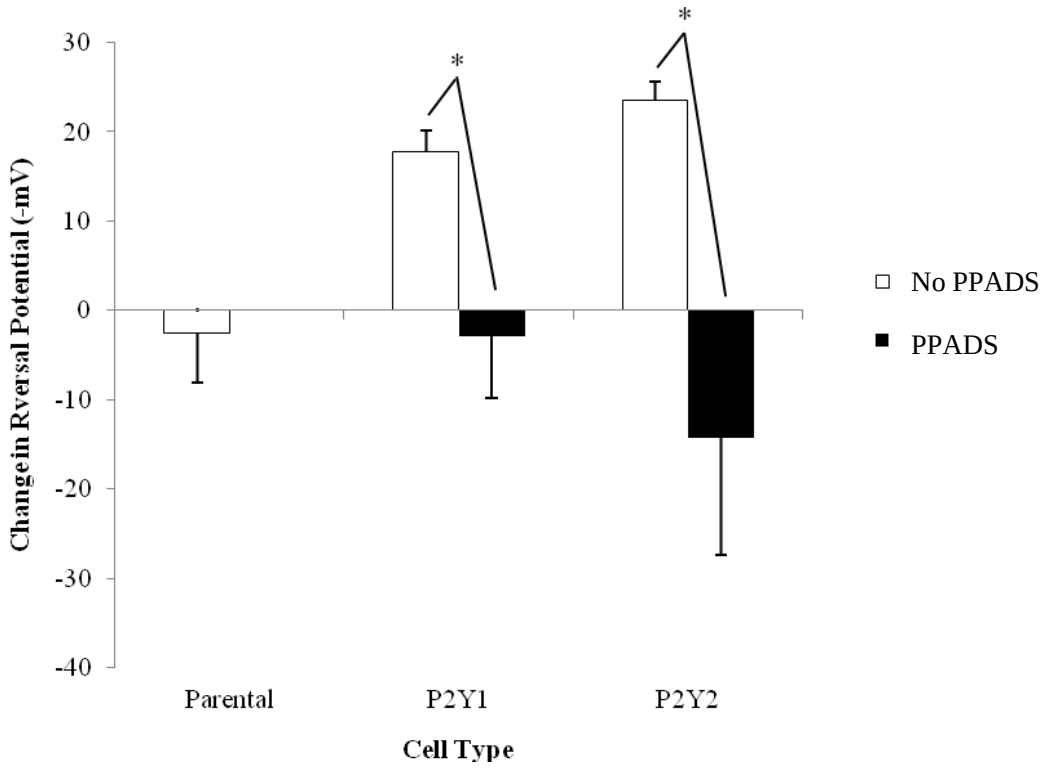

Figure 13 Reversal potentials for P2Y1 and P2Y2 receptor transfected cells do not depolarize when treated with 100 µM PPADS prior to hyposmotic exposure. A) Calculated whole cell conductance for P2Y1 (n=3) and P2Y2 (n=3) cells during perfusion with isosmotic PBS plus 10 mM TEA, isosmotic PBS plus 10 mM TEA and 100 µM PPADS and hyposmotic PBS plus 10 mM TEA and 100 µM PPADS. B) Calculated reversal potentials for P2Y1 (n=3) and P2Y2 (n=3) cells during perfusion with isosmotic PBS, isosmotic PBS plus 10 mM TEA, isosmotic PBS plus 10 mM TEA and 100 µM PPADS and hyposmotic PBS plus 10 mM TEA and 100 µM PPADS. C) Change in reversal potential for all three cell lines in response to hyposmotic exposure. White bars are responses to hyposmotic exposure without PPADS in bath solution. Black bars indicate that PPADS was applied prior to hyposmotic exposure. (* indicates $p < 0.05$)

0.0091 and 0.0071, respectively) the depolarization seen when these cells experience HOE without added drug (Figure 13C).

C. Current activated in hyposmotic CsCl solution is DCPIB-sensitive

The protocol for recording from cells in the CsCl solution was very similar to that of the PBS experiments, with the exceptions that 100 mM sucrose was a major osmolyte and the holding potential was 0 mV. In order to better isolate anion currents 1321N1 astrocytoma cells were recorded using bath and pipette solutions with 100 mM CsCl , replacing the NaCl and KCl used in PBS (for more information on CsCl solution contents see Materials and Methods). Since all major ions were distributed equally the across the cell membrane the reversal potential during whole cell recording was close to 0 mV. Thus the holding was also set to 0 mV in order to limit the amount of injected holding current.

Raw electrophysiological data for P2Y1, P2Y2 and Parental cells are shown in Figures 14, 15, and 16, respectively. P2Y1 and P2Y2 cells exhibit similar electrophysiological responses to HOE with an increase in current amplitude (Figures 14 and 15). Red lines in Figures 14E and 15E represent the difference between currents generated under isosmotic and hyposmotic conditions. These current voltage plots reverse just below and just above 0 mV for P2Y1 and P2Y2 cells, respectively. P2Y2 cells also expressed some degree of outward rectification (Figure 15E). Parental cells did not consistently demonstrate an increase in amplitude due to HOE (Figure 16).

The hyposmotically activated conductance in P2Y1 and P2Y2 cells was inhibited by bath application of 20 μM DCPIB, the specific blocker of $I_{Cl,swell}$ (Figure 17A).

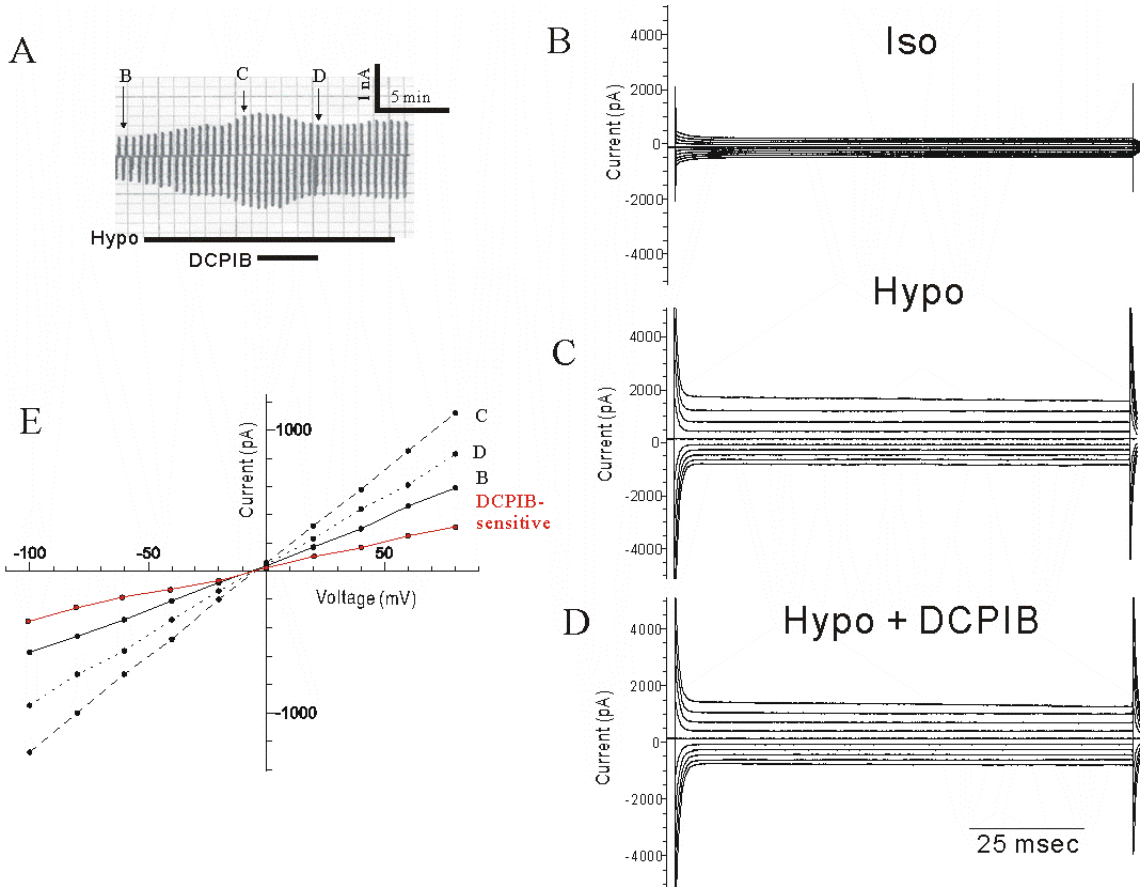

Figure 14 P2Y1 receptor transfected cells exhibit a hyposmotically activated chloride current that is inhibited by 20 µM DCPIB. A) Illustrated is a strip chart derived from data obtained from a P2Y1 cell initially bathed in isosmotic CsCl solution (300 mOsm). The cell was subsequently exposed to hyposmotic CsCl solution (200 mOsm) and then hyposmotic CsCl solution plus 20 µM DCPIB. B) Cell currents recorded while the cell was perfused with B) isosmotic CsCl, C) hyposmotic CsCl solution and D) hyposmotic CsCl solution plus 20 µM DCPIB. Location of current traces in the strip chart is similarly indicated. E) Current-voltage relationships for the three current traces in B) through D) are displayed in black. The red plot represents the difference in current elicited under hyposmotic and hyposmotic + DCPIB conditions.

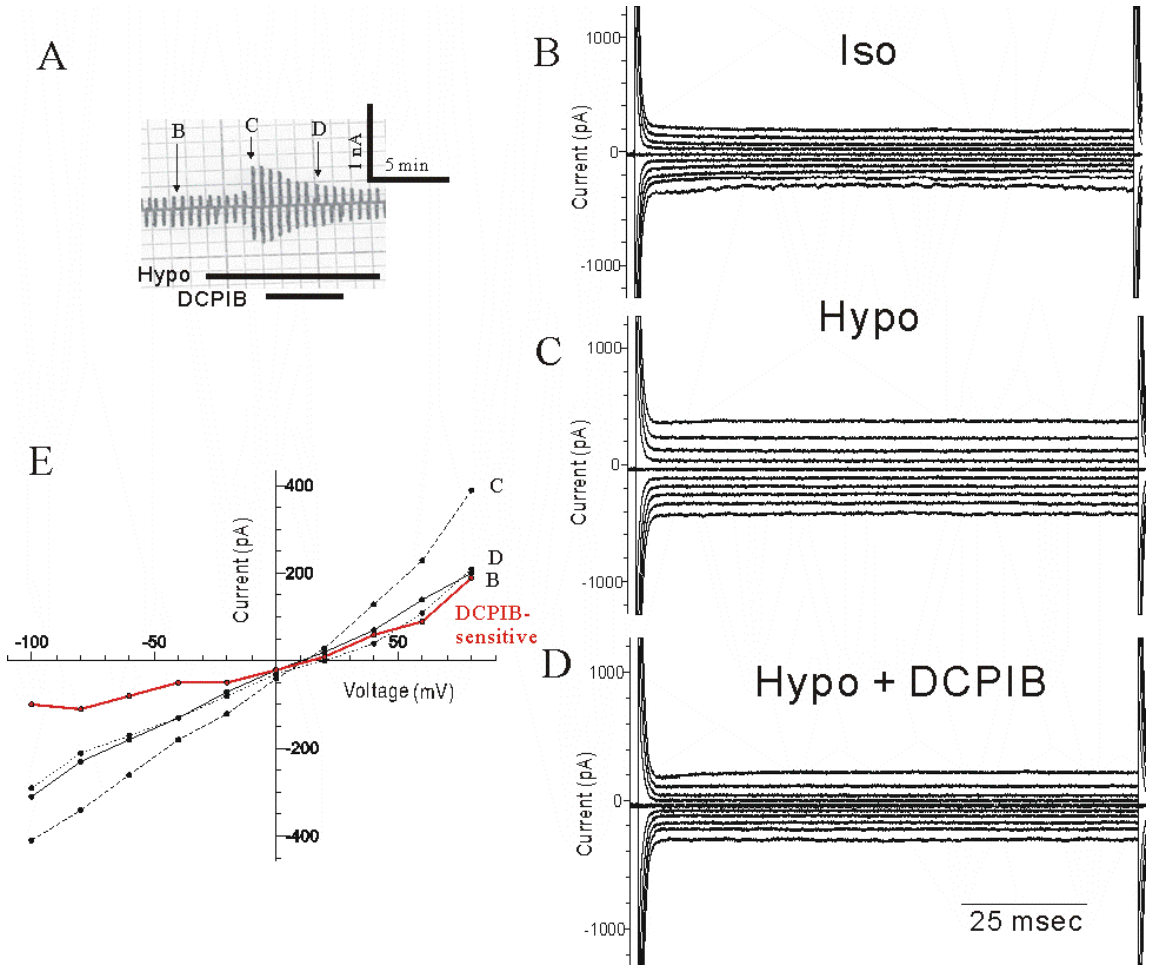

Figure 15 P2Y2 receptor transfected cells exhibit a hyposmotically activated chloride current that is inhibited by 20 µM DCPIB. A) Illustrated is a strip chart derived from data obtained from a P2Y2 cell initially bathed in isosmotic CsCl solution (300 mOsm). The cell was subsequently exposed to hyposmotic CsCl solution (200 mOsm) and then hyposmotic CsCl solution plus 20 µM DCPIB. B) Cell currents recorded while the cell was perfused with B) isosmotic CsCl, C) hyposmotic CsCl solution and D) hyposmotic CsCl solution plus 20 µM DCPIB. Location of current traces in the strip chart is similarly indicated. E) Current-voltage relationships for the three current traces in B) through D) are displayed in black. The red plot represents the difference in current elicited under hyposmotic and hyposmotic + DCPIB conditions.

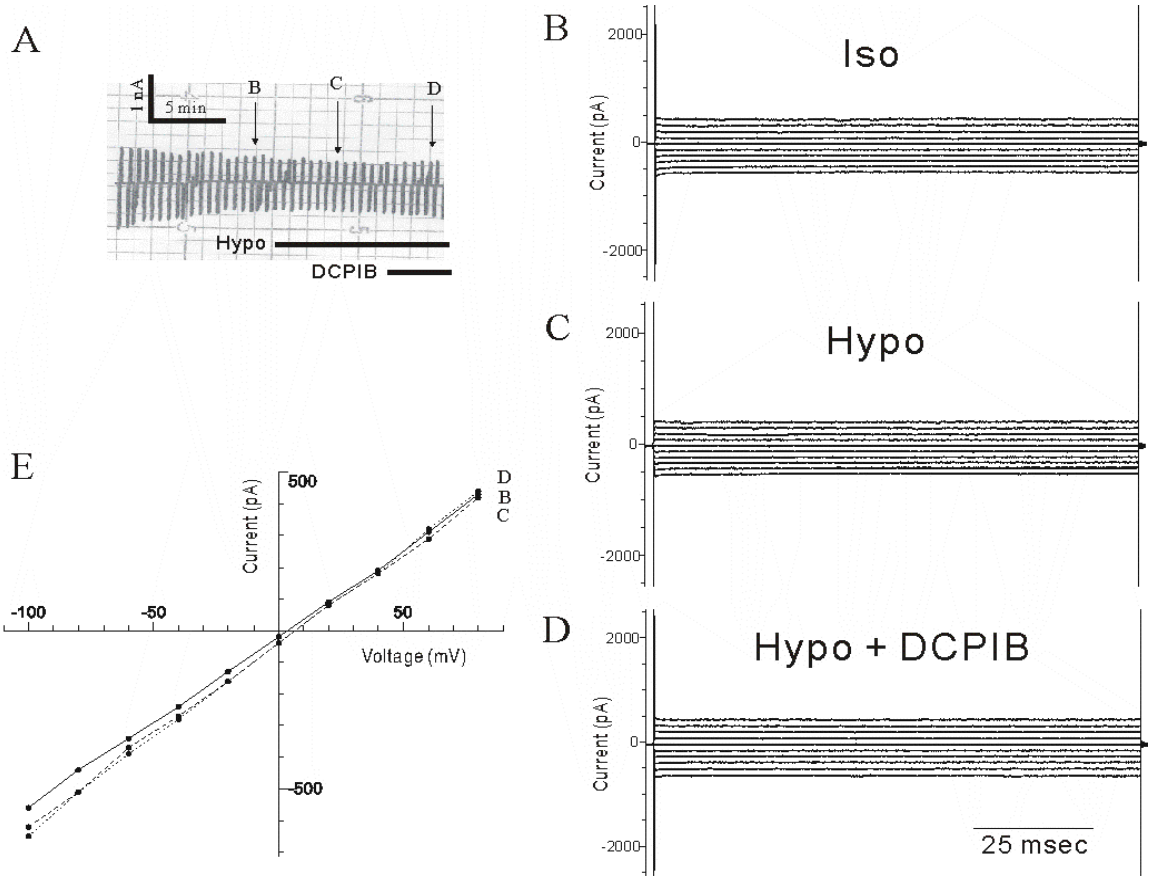

Figure 16 Flat Parental cells do not exhibit a hyposmotically activated chloride current that is inhibited by 20 µM DCPIB. A) Illustrated is a strip chart derived from data obtained from a flat Parental cell initially bathed in isosmotic CsCl solution (300 mOsm). The cell was subsequently exposed to hyposmotic CsCl solution (200 mOsm) and then hyposmotic CsCl solution plus 20 µM DCPIB. B) Cell currents recorded while the cell was perfused with B) isosmotic CsCl, C) hyposmotic CsCl solution and D) hyposmotic CsCl solution plus 20 µM DCPIB. Location of current traces in the strip chart is similarly indicated. E) Current-voltage relationships for the three current traces in B) through D).

A

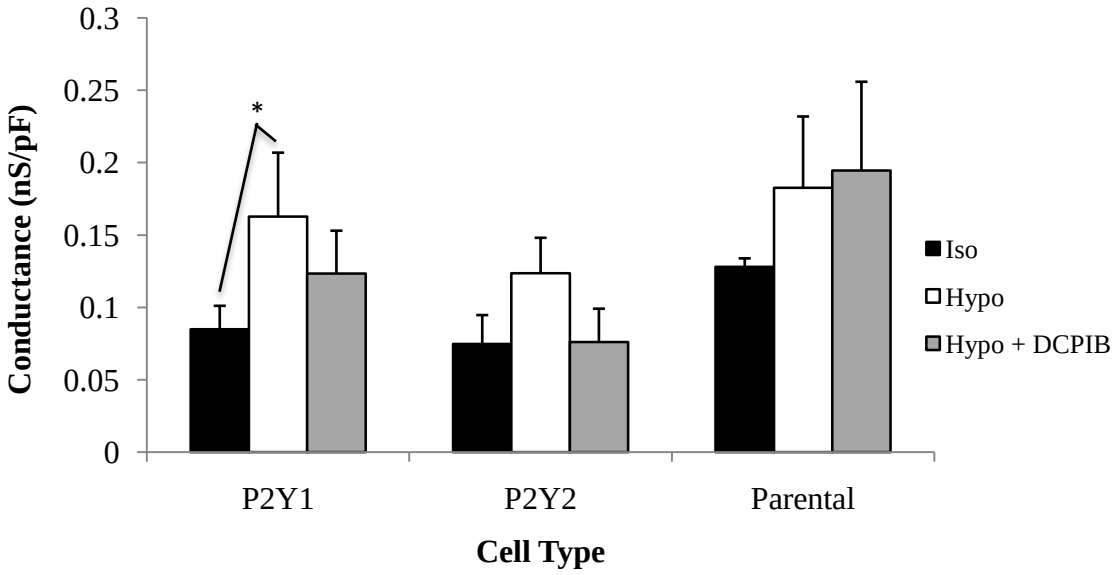

B

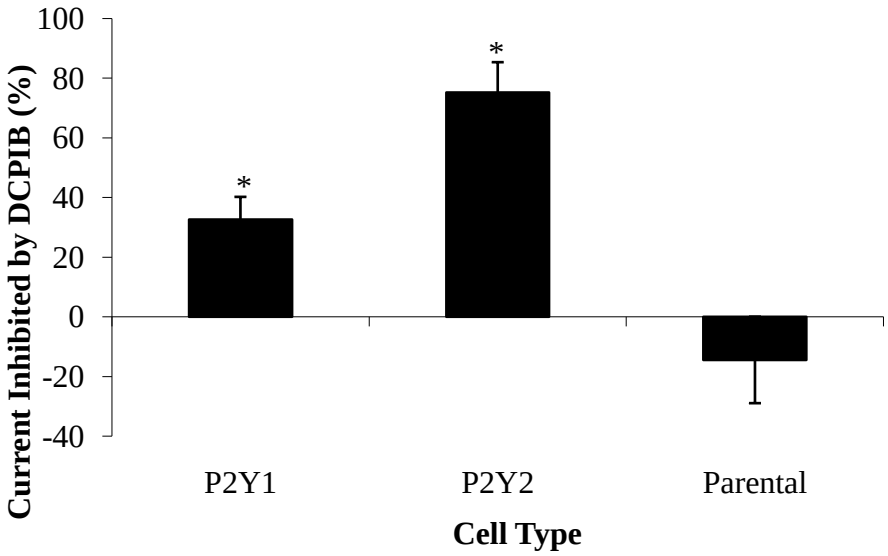

Figure 17 DCPIB inhibits hyposmoticly-activated chloride current in P2Y1 and P2Y2 receptor transfected cells but not in flat Parental cells. A) Calculated whole cell conductance for P2Y1 (n=4), P2Y2 (n=4) and Parental (n=2) cells during perfusion with isosmotic CsCl, hyposmotic CsCl and hyposmotic CsCl plus 20 µM DCPIB. B) Percent inhibition of hyposmotically activated current, measured at +80 mV, by 20 µM DCPIB in P2Y1 (n=4), P2Y2 (n=4) and Parental (n=2) cells. Cells chosen for these experiments were identified as morphologically "flat" visually by phase-contrast microscopy. Cells were then perfused in CsCl solution as described in the Materials and Methods section and subjected to hyposmotic exposure for 5-10 mins prior to addition of DCPIB. (* indicates $p < 0.05$)

Average whole cell normalized conductance for P2Y1 and P2Y2 cells increased from 0.0850 ± 0.0162 nS/pF and 0.0747 ± 0.0201 nS/pF to 0.1628 ± 0.0442 nS/pF and 0.1235 ± 0.0247 nS/pF, respectively. Subsequent application of DCPIB caused a decrease in conductance to 0.1233 ± 0.0298 nS/pF and 0.0760 ± 0.0232 nS/pF for P2Y1 and P2Y2 cells, respectively. The hyposmotically activated current, measured at +80 mV, was reduced by 32.6 ± 7.6% and 75.2 ± 10.1% for P2Y1 and P2Y2 cells, respectively (Figure 17B). Parental cells did not experience any decrease in conductance or current as a result of DCPIB application (Figure 17).

Initial experiments targeted cells that were morphologically flat (Figures 14-17). This choice made acquiring a stable voltage clamp recording difficult to obtain and in the case of Parental nearly impossible (note the n = 2 for flat Parental cells in Figure 17). Thus, an additional subset of morphologically rounder cells was chosen for analysis. Different results were obtained when recording from round compared with flat Parental .

Raw electrophysiological data for round P2Y1 and Parental cells are shown in Figures 18 and 19, respectively. Rounded P2Y1 and Parental cells exhibited similar electrophysiological responses to HOE with an increase in current amplitude. Red lines in Figures 18E and 19E represent the difference between currents generated under hyposmotic and hyposmotic plus DCPIB conditions for P2Y1 and Parental cells, respectively. These currents demonstrated outward rectification and reversal potentials just above 0 mV for both P2Y1 and Parental cells.

The hyposmotically activated conductance in round P2Y1 and Parental cells was inhibited by bath application of 20 μM DCPIB (Figure 20A). Average whole cell normalized conductance for round P2Y1 and Parental cells increased from 0.1330 ±

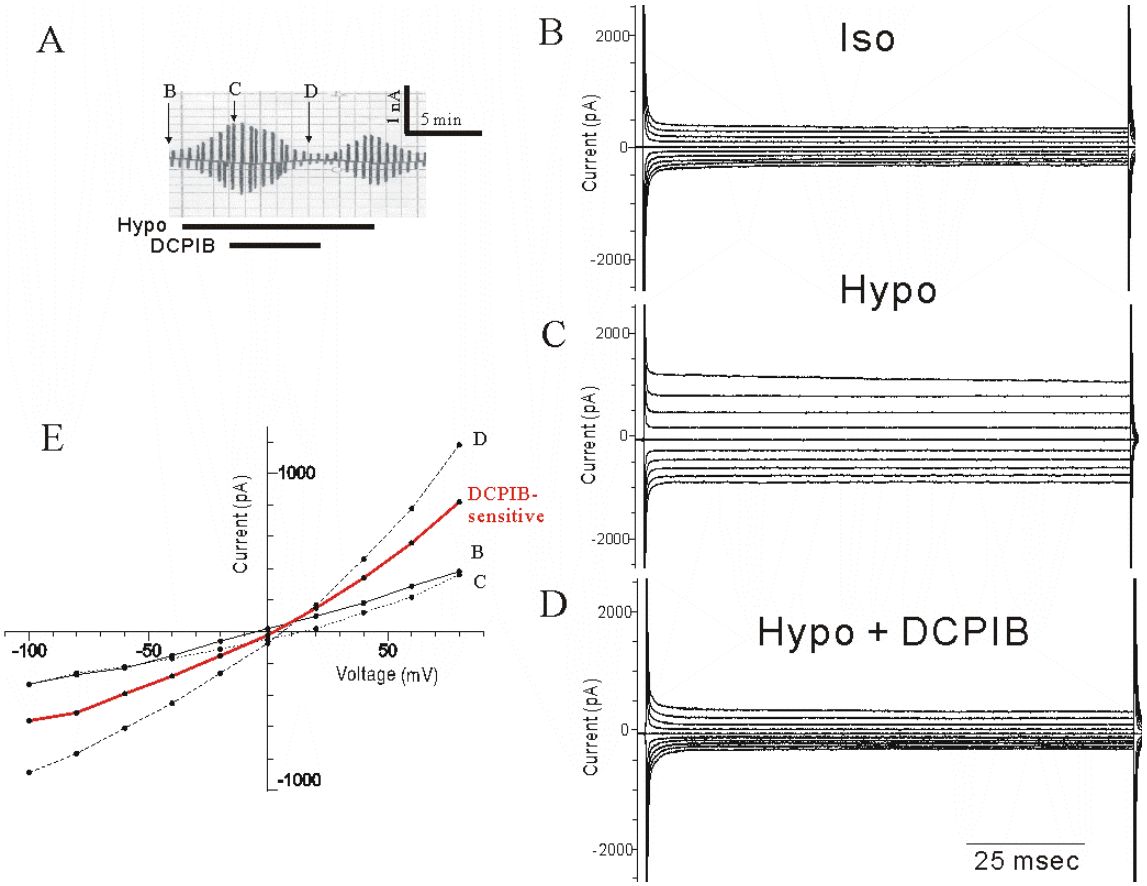

Figure 18 Rounded P2Y1 receptor transfected cells exhibit a hyposmotically activated chloride current that is inhibited by 20 µM DCPIB. A) Illustrated is a strip chart derived from data obtained from a P2Y1 cell initially bathed in isosmotic CsCl solution (300 mOsm). The cell was subsequently exposed to hyposmotic CsCl solution (200 mOsm) and then hyposmotic CsCl solution plus 20 µM DCPIB. B) Cell currents recorded while the cell was perfused with B) isosmotic CsCl, C) hyposmotic CsCl solution and D) hyposmotic CsCl solution plus 20 µM DCPIB. Location of current traces in the strip chart is similarly indicated. E) Current-voltage relationships for the three current traces in B) through D) are displayed in black. The red plot represents the difference in current between currents elicited under hyposmotic and hyposmotic + DCPIB conditions.

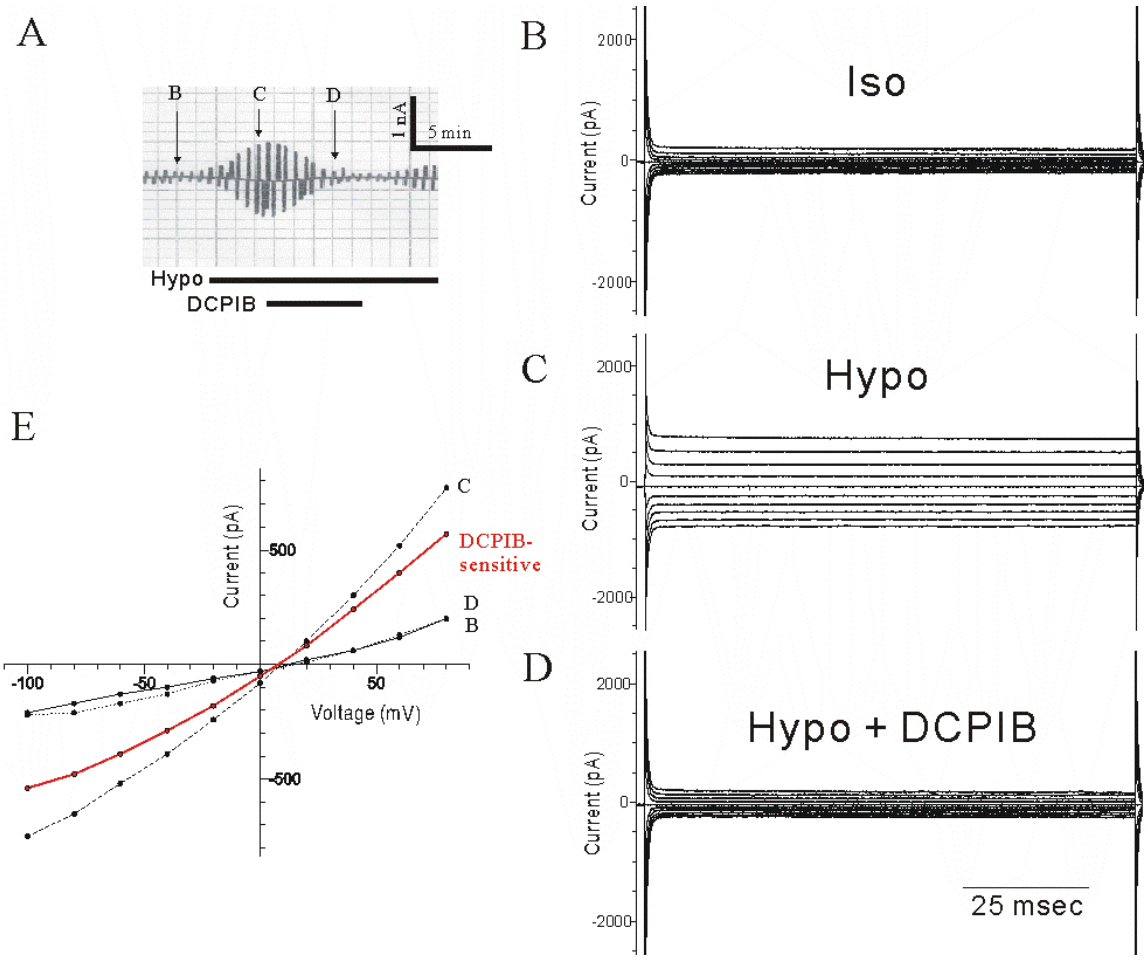

Figure 19 Rounded Parental cells exhibit a hyposmotically activated chloride current that is inhibited by 20 µM DCPIB. A) Illustrated is a strip chart derived from data obtained from a Parental cell initially bathed in isosmotic CsCl solution (300 mOsm). The cell was subsequently exposed to hyposmotic CsCl solution (200 mOsm) and then hyposmotic CsCl solution plus 20 µM DCPIB. B) Cell currents recorded while the cell was perfused with B) isosmotic CsCl, C) hyposmotic CsCl solution and D) hyposmotic CsCl solution plus 20 µM DCPIB. Location of current traces in the strip chart is similarly indicated. E) Current-voltage relationships for the three current traces in B) through D) are displayed in black. The red plot represents the difference in current between currents elicited under hyposmotic and hyposmotic + DCPIB conditions.

A

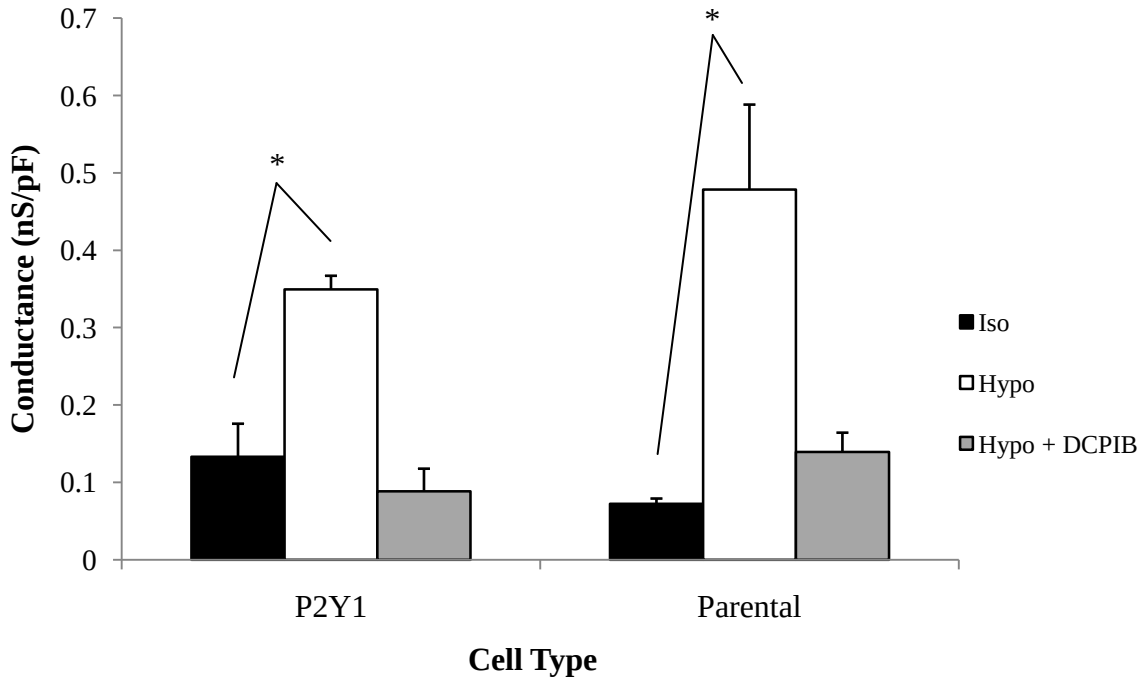

B

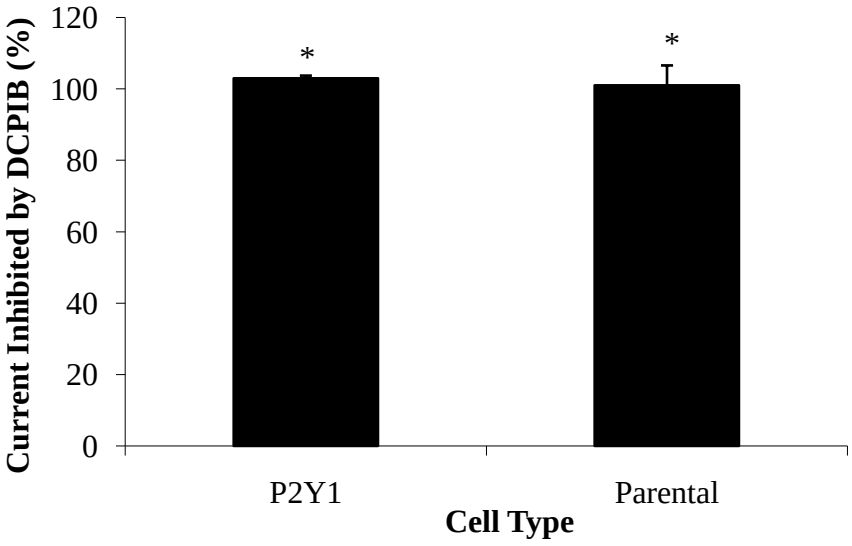

Figure 20 DCPIB inhibits hyposmotic-induced current in rounded P2Y1 and Parental cells in CsCl solution. A) Calculated whole cell conductance for P2Y1 (n=3) and Parental (n=4) cells during perfusion with isosmotic CsCl, hyposmotic CsCl and hyposmotic CsCl plus 20 µM DCPIB. B) Percent inhibition of hyposmotically activated current, measured at +80 mV, by 20 µM DCPIB in P2Y1 (n=3) and Parental (n=4) cells. Cells chosen for these experiments were identified as morphologically rounded. Cells were then perfused in CsCl solution as described in the Materials and Methods section and subjected to HOE for 5-10 min prior to addition of DCPIB. (* indicates $p < 0.05$)

0.0430 nS/pF and 0.0725 ± 0.0068 nS/pF to 0.3493 ± 0.0179 nS/pF and 0.4782 ± 0.1102 nS/pF, respectively. Subsequent application of DCPIB during HOE caused a decrease in conductance to 0.0883 ± 0.0296 nS/pF and 0.1393 ± 0.0251 nS/pF for round P2Y1 and Parental cells, respectively. The hyposmotically activated current, measured at +80 mV, was reduced by 103 ± 0.8% and 101 ± 5.6% for P2Y1 and Parental cells, respectively in the presence of DCPIB (Figure 20B).

D. Exogenous ATP activates a DCPIB-insensitive chloride conductance

The effect of exogenous 1 mM ATP was analyzed under CsCl conditions in the three cell types (Figures 21 – 24). Raw electrophysiological data showed an increase in current amplitude in both P2Y1 and P2Y2 cells after exposure to 1 mM ATP (Figures 21 and 22). This current exhibited inward rectification, a reversal potential near 0 mV and insensitivity to 20 μM DCPIB. Parental cells did not exhibit an increase in current amplitude when exposed to exogenous ATP (Figure 23). 1 mM ATP caused normalized whole-cell conductance increases from 0.1107 ± 0.0367 nS/pF to 0.1983 ± 0.0304 nS/pF in P2Y1 cells and 0.0680 ± 0.0246 nS/pF to 0.1130 ± 0.0551 nS/pF in P2Y2 cells, respectively, while Parental cells showed no increase (Figure 24). Initial experiments using micromolar concentrations of exogenous ATP showed no change in current. Also, P2Y1 cells (n=2) exposed to 500 μM ATP activated current of amplitude only 10% of the currents elicited by 1 mM ATP (Data not shown).

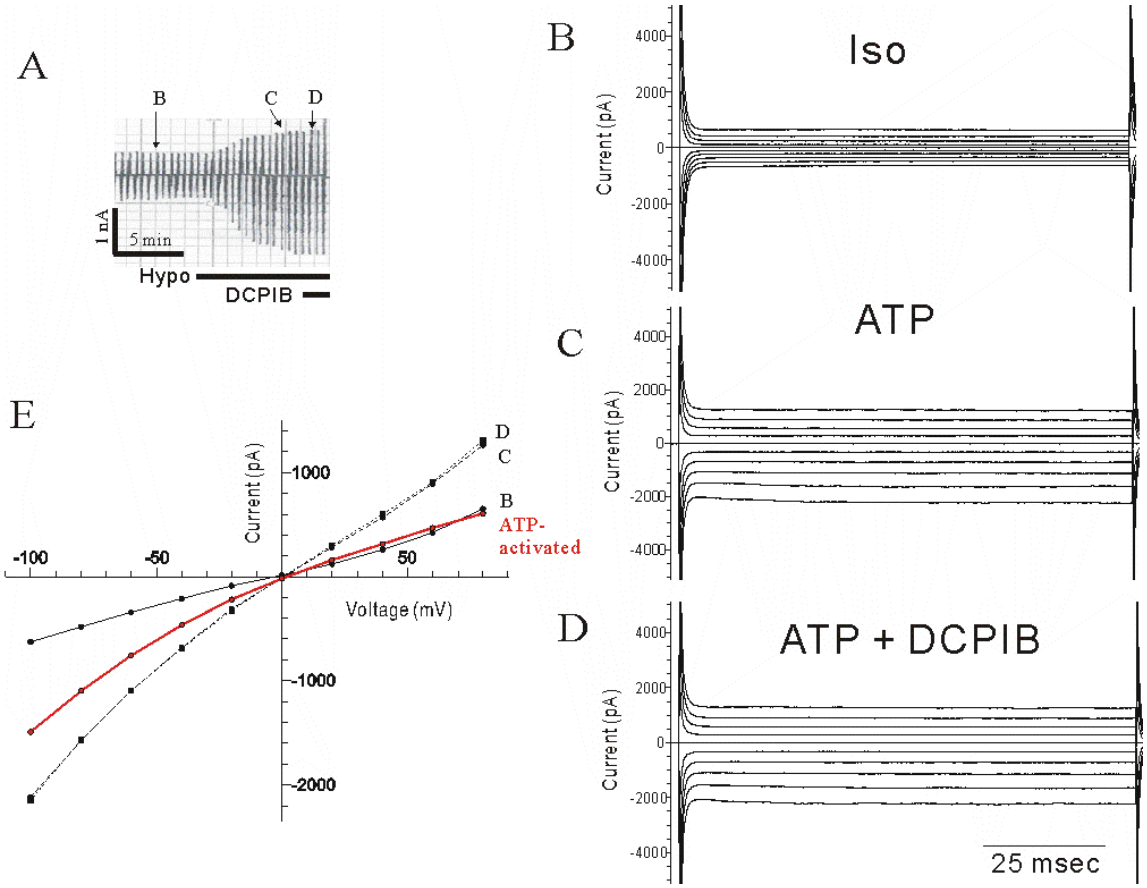

Figure 21 Exogenous ATP activates an inwardly rectified, DCPIB-insensitive chloride current in P2Y1 receptor transfected cells. A) Illustrated is a strip chart derived from data obtained from a P2Y1 cell initially bathed in isosmotic CsCl solution (300 mOsm). The cell was subsequently exposed to 1 mM ATP (200 mOsm) and then 1 mM plus 20 µM DCPIB. Cell currents recorded while the cell was perfused with B) isosmotic CsCl, C) 1 mM ATP in isosmotic CsCl and D) 1 mM ATP in isosmotic CsCl solution plus 20 µM DCPIB. Location of current traces in the strip chart is similarly indicated. C) Current-voltage relationships for the three current traces B) through D) are displayed in black. The red plot represents the difference in currents elicited in the presence and absence of ATP.

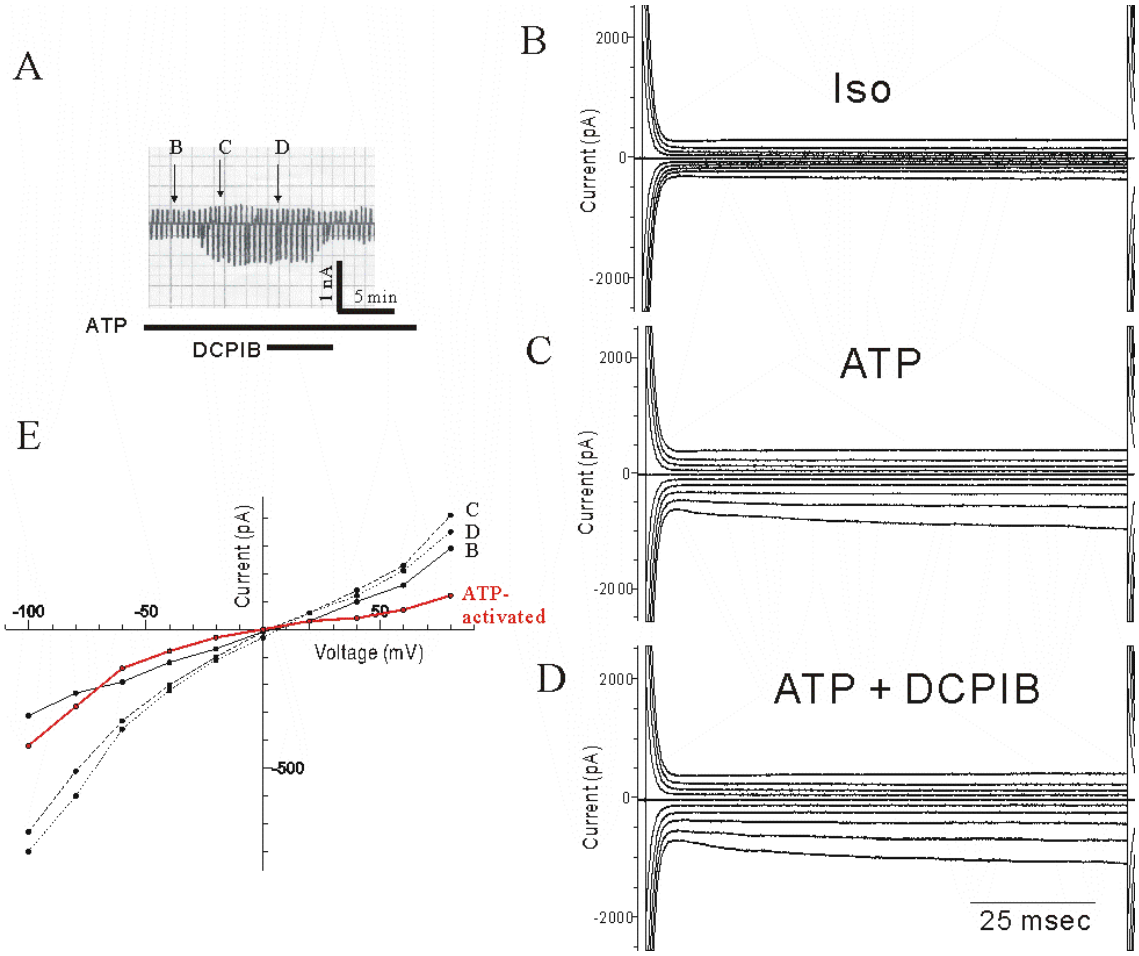

Figure 22 Exogenous ATP activates an inwardly rectified, DCPIB-insensitive chloride current in P2Y2 receptor transfected cells. A) Illustrated is a strip chart derived from data obtained from a P2Y2 cell initially bathed in isosmotic CsCl solution (300 mOsm). The cell was subsequently exposed to 1 mM ATP (200 mOsm) and then 1 mM plus 20 µM DCPIB. Cell currents recorded while the cell was perfused with B) isosmotic CsCl, C) 1 mM ATP in isosmotic CsCl and D) 1 mM ATP in isosmotic CsCl solution plus 20 µM DCPIB. Location of current traces in the strip chart is similarly indicated. C) Current-voltage relationships for the three current traces B) through D) are displayed in black. The red plot represents the difference in currents elicited in the presence and absence of ATP.

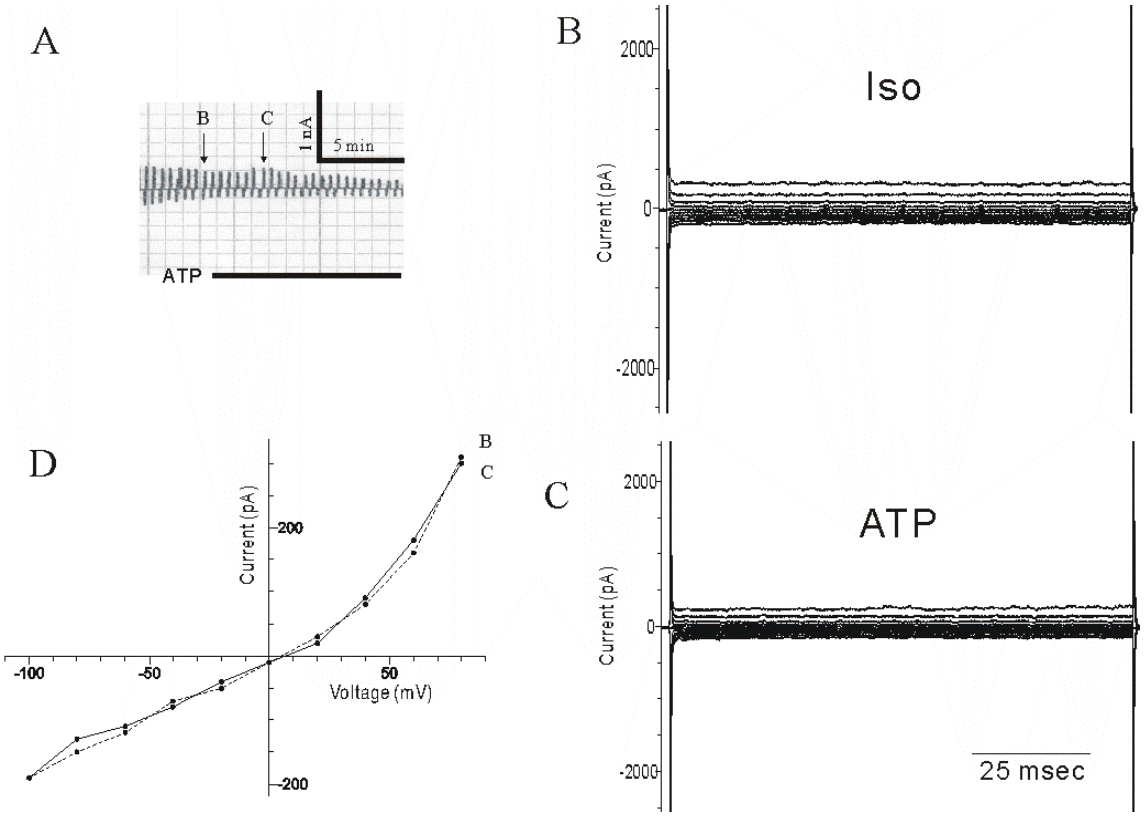

Figure 23 Exogenous ATP does not activate any chloride current in round Parental cells. A) Illustrated is a strip chart of a Parental cell that is initially bathed in isosmotic (300 mOsm) CsCl solution and is subsequently treated with 1 mM ATP. Cell currents recorded while the cell is perfused with B) isosmotic CsCl solution and C) isosmotic CsCl solution containing 1 mM ATP. Location of current traces in the strip chart is similarly indicated. D) Current-voltage relationships for current traces in B and C.

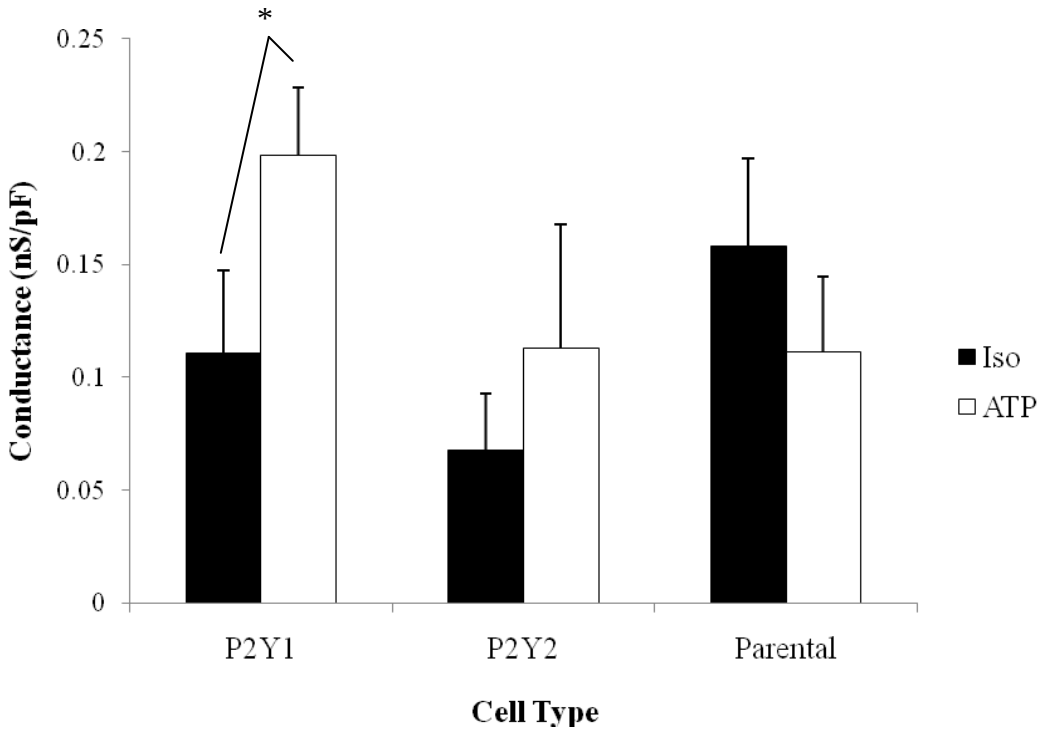

Figure 24 Exogenous ATP activates a chloride conductance in P2Y1 and P2Y2 receptor transfected cells, but not in Parental cells. A) Normalized conductance during perfusion of isosmotic CsCl solution (Iso) and isosmotic CsCl solution plus 1 mM ATP (ATP) in P2Y1 (n=3), P2Y2 (n=3) and Parental cells (n=3). Cells were then perfused in CsCl solution as described in the Materials and Methods section and subjected to 1 mM ATP for 5-10 min prior to addition of DCPIB. (* indicates $p < 0.05$)

E. Western Blotting

Western blotting confirms P2Y1 and P2Y2 receptor expression in P2Y1 and P2Y2 cells, but not in Parental cells. All cell lysates showed staining for Anti-β-actin protein in both western blots shown (Figures 25 and 26). P2Y1 receptor bands in the 90 kD range can be seen in both P2Y1 and P2Y2 cell lanes (Figure 25). P2Y2 receptor antibody generates similar results, with both P2Y1 and P2Y2 cells producing bands above 90 kD (Figure 26). These bands are in the same kD range as described by the antibody manufacturer (Alomone Labs) for human platelets. In an effort to inhibit cross-reactivity between the two subtypes P2Y1 and P2Y2 receptor antibodies were pre-incubated with P2Y2 and P2Y1 peptide antigen, respectively, prior to use, as described in the Materials and Methods section. Even under these circumstances bands were observed in P2Y2 cell lysates when incubated with P2Y1 receptor antibody (Figures 25) and in P2Y1 cell lysates when incubated with P2Y2 antibody (Figures 26).

F. Immunostaining

Initial experiments were performed under fixatives of 4, 2, 1 and 0.5% paraformaldehyde solution. Similar intensities of receptor staining were found in each for each fixing solution used (data not shown). Minimal fixation was desired, as the P2Y1 and P2Y2 receptor antibodies were derived from antigens in their native form, and thus 0.5% paraformaldehyde was used in subsequent studies.

All 1321N1 cell types were analyzed immunocytochemically for both P2Y1 and P2Y2 receptor expression. Staining P2Y1 cells with anti-P2Y1 antibody yielded positive

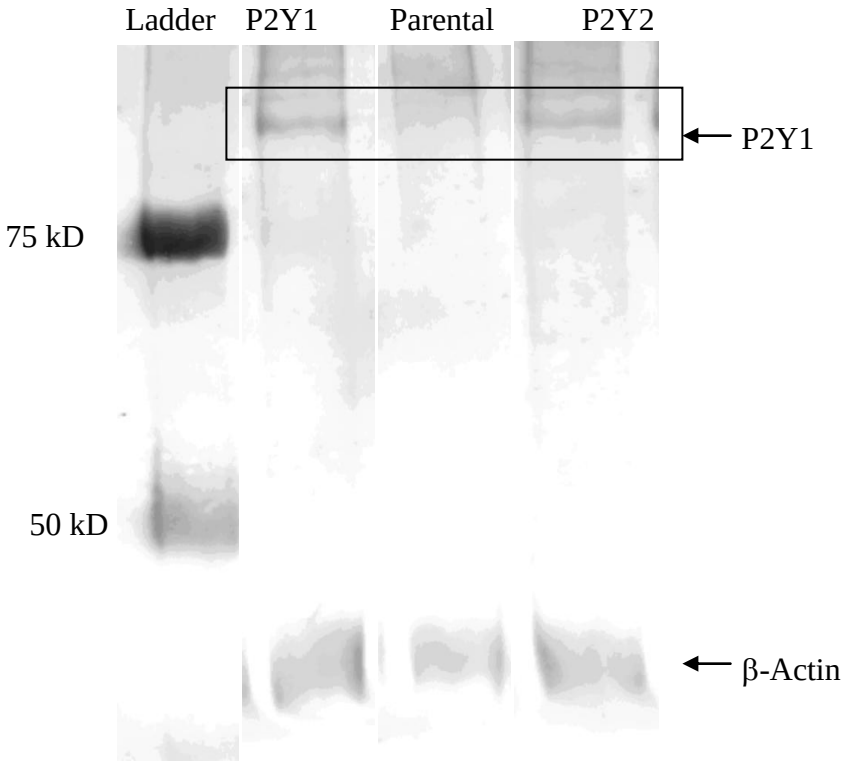

Figure 25 P2Y1 receptor expression in 1321N1 cell lines. Western blot probed with anti-P2Y1 and anti-β-Actin as the primary antibodies. The anti-P2Y1 antibody was incubated with P2Y2 peptide antigen prior to use as described in the Materials in Methods section. Anti-β-Actin was used as a positive control.

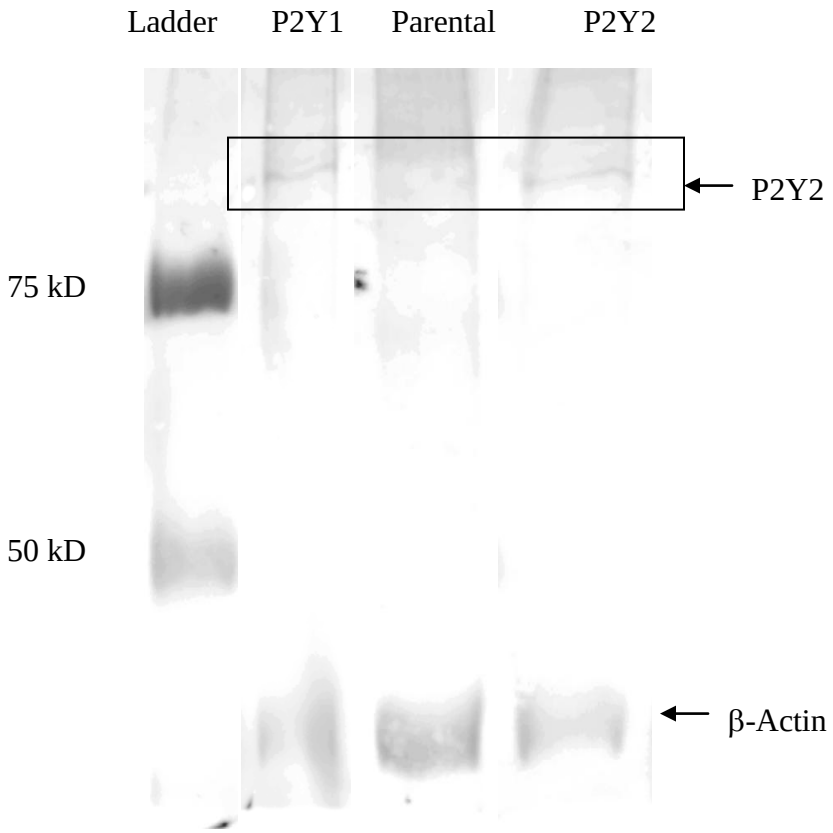

Figure 26 P2Y2 receptor expression in 1321N1 cell lines. Western blot probed with anti-P2Y2 and anti-β-Actin as the primary antibodies. The anti-P2Y2 antibody was incubated with P2Y1 control peptide prior to use as described in the Materials in Methods section. Anti-β-Actin was used as a positive control.

results (Figure 27A). However, anti-P2Y2 antibody also stained P2Y1 cells, albeit to a lesser degree (Figure 27D). Pre-incubation, with P2Y1 control antigen as described in the Materials and Methods, still yielded positive labeling with P2Y1 and P2Y2 receptor antibody (Figure 27B and 27E, respectively). The level of staining when P2Y2 control antigen was pre-incubated with P2Y2 receptor antibody was not visibly different than when P2Y2 receptor antibody was used alone (Figure 27F). When no primary antibody was used (the negative control) there was almost no staining of the P2Y1 cells (Figure 27C).

Similarly, P2Y2 cells were analyzed for both P2Y1 and P2Y2 receptor expression. P2Y2 cells exhibited staining when exposed to anti-P2Y2 (Figure 28A) and anti-P2Y1 receptor antibody (Figure 28D). Pre-incubation of either of these antibodies with P2Y2 control antigen did not decrease the level of staining (Figures 28B and E). Staining of P2Y2 cells with P2Y1 receptor antibody that was pre-incubated with P2Y1 control antigen did reduce staining to control levels (Figure 28F). When no primary antibody was used, the negative control, there was almost no staining of the P2Y2 cells (Figure 28C).

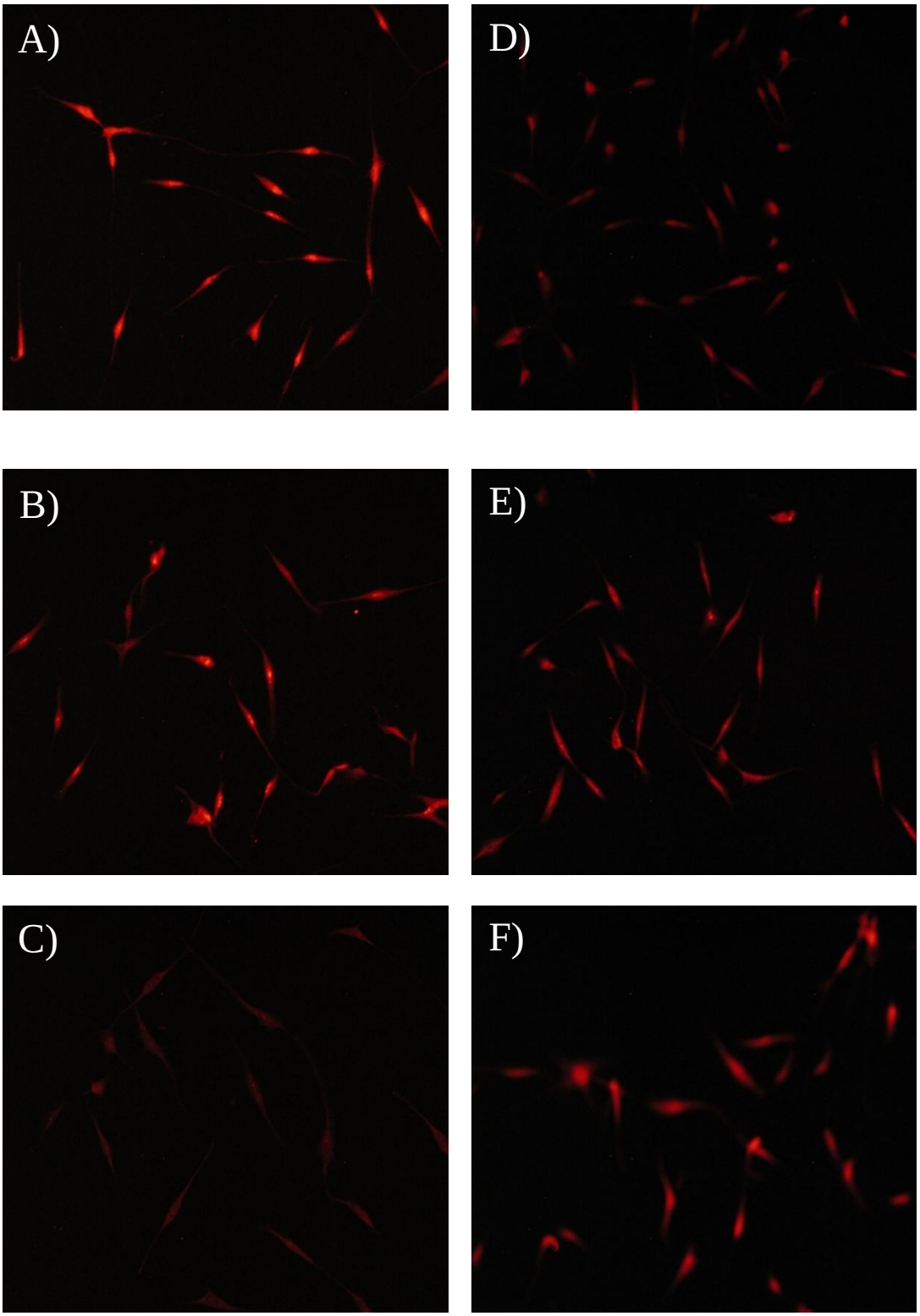

Figure 27 Immunostaining of P2Y1 cells. A) P2Y1 cells stained using P2Y1 antibody, B) P2Y1 antibody pre-absorbed with P2Y1 peptide antigen, C) no primary antibody, D) P2Y2 antibody, E) P2Y2 antibody pre-absorbed with P2Y1 peptide antigen, F) and P2Y2 antibody pre-absorbed with P2Y2 peptide antigen.

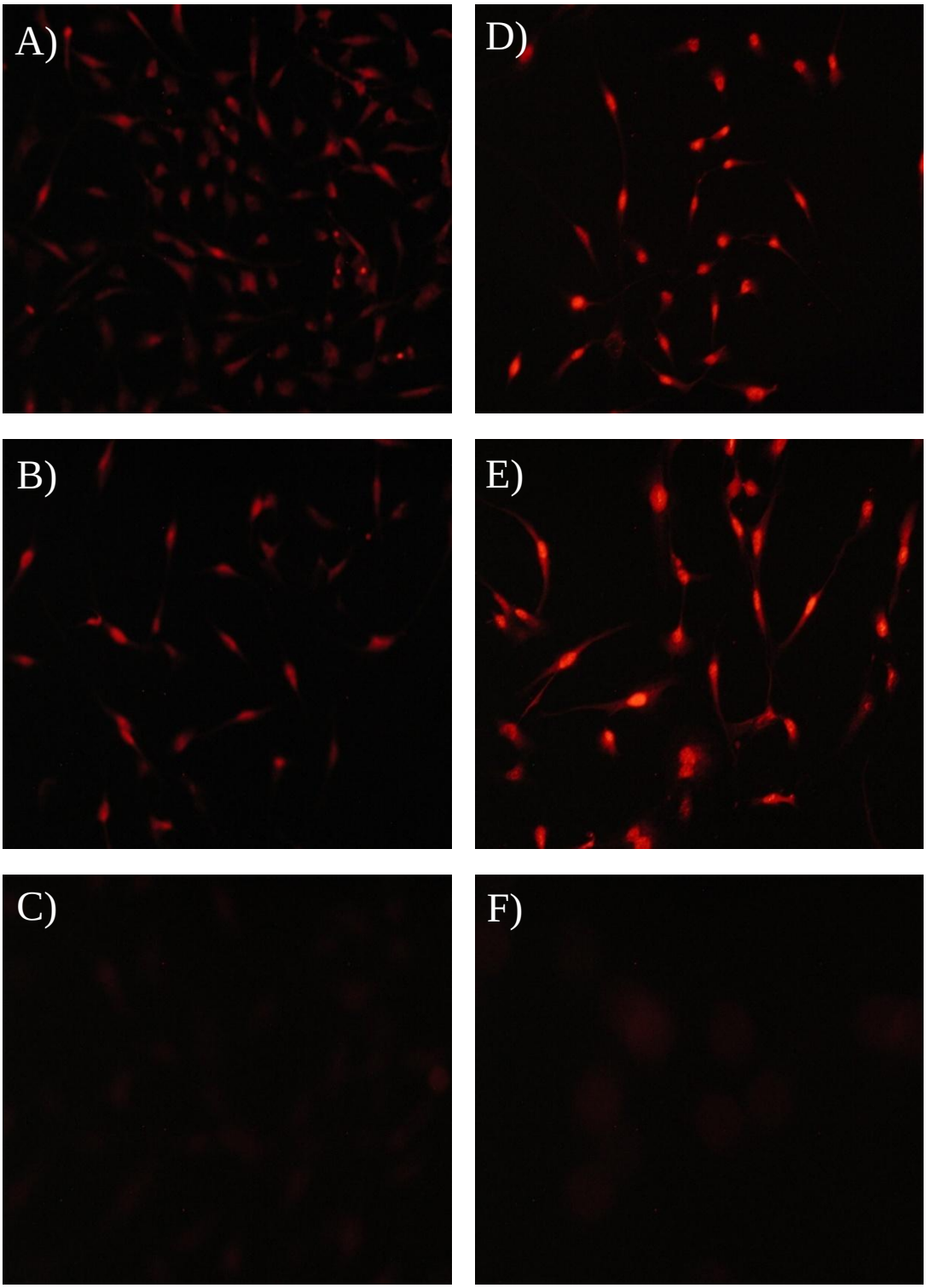

Figure 28 Immunostaining of P2Y2 cells. A) P2Y2 cells stained using P2Y2 antibody, B) P2Y2 antibody pre-absorbed with P2Y2 peptide antigen, C) no primary antibody, D) P2Y1 antibody, E) P2Y1 antibody pre-absorbed with P2Y2 peptide antigen, F) P2Y1 antibody pre-absorbed with P2Y1 peptide antigen.

V. Discussion

A. Results Summary and Conclusions

Initial recordings suggested cells perfused with PBS activated a chloride conductance in response to HOE. Presence of $I_{Cl,swell}$ was then confirmed in the CsCl experiments. Not only did the hyposmotically activated current demonstrate electrophysiological characteristics of $I_{Cl,swell}$, but it also was potently inhibited by DCPIB, a selective $I_{Cl,swell}$ blocker (Decher et al. 2001). Experiments on rounded cells perfused with CsCl solution demonstrated that P2Y receptor expression is not necessary for $I_{Cl,swell}$ activation. $I_{Cl,swell}$ was activated just as potently in round Parental cells as in the P2Y1 or P2Y2 cells. A chloride current was activated by extracellular ATP, however it did not demonstrate the electrophysiological characteristics typically ascribed to $I_{Cl,swell}$. Previous literature describes an ATP activated chloride current with a pharmacological profile similar to that of the P2Y1 receptor subtype (Darby et al. 2003). Our studies indicate that both P2Y1and P2Y2 receptors are capable of activating the ATP induced current. These results are based on the P2Y receptor expression reported from the suppliers, however the immunocytochemical and western data in this study are contradictory to those reports. It is clear that at least one of the receptor subtypes, P2Y1 or P2Y2, are responsible for the current activation, however, until receptor expression is confirmed, it is unclear whether P2Y1, P2Y2 or both receptors are responsible.

B. Electrophysiological Characteristics and TEA sensitivity of 1321N1 Human Astrocytoma Cells in Isosmotic PBS

Before analyzing the electrophysiology of the 1321N1 cells it is important to recognize the conditions under which they were studied. All studies were performed *in vitro*. Phosphate buffered saline (PBS) was used as an extracellular medium and I designed the pipette solution to closely resemble physiological intracellular conditions. All electrophysiological studies were performed using voltage clamp procedures. Such recordings do not give exact resting membrane potentials; however, comparisons between interpolated reversal potentials under different conditions can reveal changes in relative conductances for the ions present.

A negative membrane potential is considered a defining characteristic of astrocytes, as it is common to many astroglial sub-populations (Bordey & Sontheimer 2000), and is considered critical for the astrocyte function of potassium buffering (Kuffler & Nicholls 1966, Orkand, Nichols & Kuffler 1966). All 1321N1 astrocytoma cell subtypes; P2Y1, P2Y2 and Parental cells, had highly negative reversal potentials. While this is not indicative of resting membrane potential it does imply a high relative conductance for potassium which is true for most astrocytes. P2Y1 and P2Y2 cell types had more negative reversal potentials than that of the Parental cell line. An increase in potassium conductance across a membrane will cause membrane hyperpolarization, and perhaps P2Y receptor expression facilitates increased potassium conductance under basal conditions. Both P2Y1 and P2Y2 receptor activity leads to increases in intracellular calcium (Burnstock 2007), which could activate BK channels. Exogenous ATP activation

of BK channels has already been observed in other cell types (Hafting & Sand 2000, Hafting et al. 2006).

Whole cell conductance of 1321N1 cells also was similar to that of cultured rat astrocytes (Li, Liu & Olson 2002). Again the P2Y1 and PY2 cell types demonstrate similar results that differ from those of the Parental cells. Parental cells generally displayed higher whole cell conductance than the P2Y1 and P2Y2 cells.

Another defining electrophysiological characteristic of astroglial cells is the presence of outward-rectifying potassium currents that are inhibited by 4-AP and TEA (Bordey & Sontheimer 2000). Outward-rectifying currents were found consistently in the P2Y1 and P2Y2 cells and 10 mM TEA was able to inhibit the majority of this current at +80 mV. Parental cells did exhibit TEA-sensitive rectified currents, although not to the same extent as P2Y1 and P2Y2 cells. Again, BK channel activity in the 1321N1 cells could be tied to P2Y receptor function, and explain the lack of outward-rectifying current in the Parental cells. The concentration of TEA needed to inhibit 50% of the outward rectifying current was found to be 0.37 mM in P2Y1 cells, which is consistent with BK channel inhibition described in previous literature (Catacuzzeno, Pisconti, Harper, Petris & Franciolini 2000) as well as with other rectified K channels (Garcia-Diaz, Nagel & Essig 1983).

TEA was used in this study to block the basal rectified current and thus reveal other hyposmotically activated currents. While TEA effectively inhibits current measured at positive potentials it has little effect on the currents evoked at the more negative potentials near the reversal potential. The effect is that application of TEA did not have

significant effect on normalized conductance or reversal potentials in any cell line, and therefore it presumably did not inhibit any basal conductances.

C. Electrophysiological Response to Hyposmotic Exposure (HOE) in PBS

The goal of the present study was to analyze the role of P2Y receptors in hyposmotically activated currents; specifically $I_{Cl,swell}$. While recording cells perfused with PBS, this was done in two ways. First, three subtypes of the 1321N1 human astrocytoma cell line was used. As explained in Methods, one subtype expressed P2Y1 receptors, another P2Y1 and yet another lacked any P2Y receptor expression. By comparing cells transfected with either P2Y1 or P2Y2 receptors to the P2Y lacking phenotype, conclusions could be drawn as to their effect on hyposmotically activated currents. The second way was the use of PPADS, which is a broad spectrum nucleotide receptor blocker. PPADS is not specific for either of the subtypes used in this study, nor is it specific for P2Y receptors in general (Burnstock 2007). However, since it had no effect on Parental cells we can conclude that PPADS is specific for P2Y receptors in this study.

The response of P2Y1 and P2Y2 cells to HOE in PBS was significantly different than that of Parental cells. While all cell subtypes had increases in current amplitude and conductance, they differed in PPADS sensitivity and change in reversal potential. As stated above, Parental cells did not respond to PPADS. However, P2Y1 and P2Y2 cells showed significant inhibition of hyposmotic-induced current by PPADS. Also, the reversal potentials of P2Y1 and P2Y2 cells depolarize during HOE, while that of Parental

cells does not. In experiments where PPADS is present P2Y1 and P2Y2 cells respond to HOE by hyperpolarizing. This is similar to the response of Parental cells and thus, confirms P2Y receptor activity is responsible for the depolarization during HOE.

The depolarizing change in reversal potential seen in P2Y1 and P2Y2 cells during HOE could be interpreted as an increase in the conductance of chloride relative to that of potassium. In the PBS experiments E_K = -93.4 mV and E_{Cl} = -2.8 mV, thus an increase in potassium conductance would result in hyperpolarization and an increase in chloride conductance would produce depolarization. As discussed previously, a cell performing RVD would expel osmolytes and only potassium and chloride have electrochemical gradients directed out of the cell. If one was to assume that only potassium and chloride conductances change during HOE, then calculations of potassium and chloride relative conductance can be made using the Goldman-Hogkin-Katz equation. It would appear, based on reversal potential depolarization, that P2Y1 and P2Y2 cells experience an increase in the conductance of chloride relative to potassium during HOE from 0.0324 and 0.0374 to 0.0907 and 0.1730, respectively. Similar calculations for Parental cells result in a decrease in the conductance of chloride relative to potassium during HOE from 0.0829 to 0.0689.

D. Electrophysiological Response to HOE in CsCl Solution

To better isolate $I_{Cl,swell}$ in 1321N1 astrocytoma cells, equimolar concentrations of CsCl in the pipette and bath solutions was used. The $I_{Cl,swell}$-inhibiting drug DCPIB was also used in these CsCl experiments. Cesium was used in order to eliminate sodium and potassium conductance similar to other protocols (Decher et al. 2001, Abdullaev et al.

2006, Darby et al. 2003). Cesium is extremely impermeable to biological membranes and therefore chloride currents can be isolated (Diamond & Wright 1969). DCPIB was also used in these experiments as a selective $I_{Cl,swell}$ inhibitor (Abdullaev et al. 2006, Decher et al. 2001). For reasons described in the results, morphologically distinct populations of cells were subjected to CsCl experiments. Recordings were made from morphologically flat 1321N1 cells of all three subtypes and from morphologically round cells of the P2Y1 and Parental subtypes.

Hyposmotically activated $I_{Cl,swell}$ was identified in round P2Y1 and Parental cells, as well as flat P2Y1 and P2Y2 cells, but not in flat Parental cells. The hyposmotically activated current exhibited all characteristics that define $I_{Cl,swell}$. In all cases DCPIB was an effective inhibitor of the hyposmotically activated current and this DCPIB-sensitive current displayed slight outward-rectification in all cell types. Time inactivation at positive membrane potentials was present in all subtypes expressing the current. The inactivation was less pronounced than in the PBS studies, however the holding potential of 0 mV, instead of -70 mV, could have affected the channel kinetics. While prominent time inactivation for $I_{Cl,swell}$ is seen at a holding potential of -80 mV (Shuba et al. 2004) it is much less pronounced when the holding potential is -50 mV (Decher et al. 2001) and -40 mV (Chiang, Luk & Wang 2004).

Morphologically flat Parental cells do not exhibit $I_{Cl,swell}$, while round Parental cells do. The reason seems to be associated with the morphology of the Parental cells. The vast majority of 1321N1 cells of all subtypes are flat. Rounded cells appear much less often and appear to be either losing adhesion to the glass coverslip or are preparing to divide. One reason for $I_{Cl,swell}$ not presenting in flat Parental cells could be differential

expression of membrane proteins during the cell cycle. A study in mouse liver cells also only identified $I_{Cl,swell}$ in rounded cells (Wondergem et al. 2001). In this study round cells accounted for only 10% of the cell population, but were almost always found to be mitotic. Conversely, flat cells were consistently found to be not mitotic. $I_{Cl,swell}$ may not be activated in flat Parental cells simply because it is not inserted into the membrane.

E. Exogenous ATP Activates a Chloride Current

Experiments involving exogenous ATP in isosmotic medium were performed to determine whether P2Y receptors are sufficient to activate $I_{Cl,swell}$ in 1321N1 cells. It is important to note that during these experiments round Parental cells were targeted, in order to be sure that channel expression was present. The concentration of ATP used in these experiments was 1 mM, which is well above the normal range for P2Y activation (Bours et al. 2006). Typical EC_{50}s for P2Y1 are P2Y2 are around 21 μM and 1 μM, respectively (May, Weigl, Karel & Hohenegger 2006, Meshki, Tuluc, Bredetean, Ding & Kunapuli 2003). A high concentration was used for two reasons. First, micromolar concentrations of ATP, similar to those that activate P2Y receptors, were not successful in activating any current. This could be attributed to ATP concentrations in the bulk media being different from those in the pericellular space (Joseph et al. 2003), due to multiple factors including ecto-ATPases that metabolize the ATP as it diffuses to the membrane. Second, even when 1 mM ATP was applied to the bath solution during Parental cell experiments there was no response. This indicates that the exogenous ATP is acting on the P2Y1 and P2Y2 receptors of the corresponding cells, and not some other

pathway. Current was also evoked in P2Y1 cells when a concentration of 500 μM ATP was used, although to a much lesser degree than when 1 mM ATP was used.

Without HOE, exogenous ATP still can activate a chloride conductance via P2Y receptor activation. Previous literature showed ADP is a more potent agonist than ATP for activation of chloride current in rat astrocytes, and suggests the P2Y1 receptor subtype as its mediator (Darby 2003). Currents are activated in both P2Y1 and P2Y2 cells when exposed to exogenous ATP in CsCl solution, however the currents display characteristics dissimilar to that of $I_{Cl,swell}$. The ATP activated current lacks inactivation at depolarizing potentials and, more importantly, displays inward rectification. These characteristics were consistent in all P2Y1 and P2Y2 cells studied and indicate ATP activates a different current than $I_{Cl,swell}$. The ATP-induced current has a similar current-voltage relationship to that of ClC-2 (Duann et al. 2000). Although ClC-2 has been shown to be dependent on intracellular ATP, no evidence exists for its activation by extracellular ATP (Roman et al. 2001). Another chloride current, aptly termed $I_{Cl,ATP}$ responds to ATP, but does not demonstrate inward rectification (Yamamoto-Mizuma, Wang & Joseph 2004).

F. P2Y Receptor Expression in P2Y1, P2Y2 and Parental Cell Subtypes

Great effort was made to identify P2Y receptor expression in the three 1321N1 cell subtypes. Both western blotting and immunostaining were employed using polyclonal antibodies for P2Y1 and P2Y2 receptors. Commercially purchased antibodies were raised in rabbit from peptide antigens from the third intracellular loop, between transmembrane domains 5 and 6, of their respective receptors. Because antibodies for

P2Y1 and P2Y2 receptors were polyclonal and raised from similar domains there was a fear of cross-reactivity. To account for this, P2Y receptor antibodies were pre-incubated with the peptide antigen of the other P2Y receptor. This method was used in both western blotting and in immunostaining.

Western and immunoblotting could not distinguish P2Y1 from P2Y2 receptor expression, however it did clearly show that Parental cells do not express either P2Y1 or P2Y2 receptors. In western blots, Parental cell lysates demonstrated bands for β-Actin but not for either P2Y1 or P2Y2 receptors. Parental cells were consistently negative when immunostained with either primary antibody. These results validate that the electrophysiological difference between the receptor and the Parental subtypes can be attributed to the P2Y receptor expression.

Western blots were positive for both receptor proteins in P2Y1 and P2Y2 cells. This was in spite of the fact that each antibody was pre-incubated with peptide antigen from the other receptor as described above. Immunostaining also revealed both P2Y1 and P2Y2 receptor expression in P2Y1 and P2Y2 cells. P2Y1 and P2Y2 cells that were not incubated with primary antibody demonstrated significantly less staining. Both of these facts indicate that the antibodies in question were staining for the intended receptors. However, pre-incubation of P2Y1 antibody with P2Y1 antigen and P2Y2 antibody with P2Y2 antigen during immunostaining did not significantly modify labeling of the receptors in both cell types. This implies that the control antigens were ineffective in absorbing the active antibodies and cross-reactivity could still be a problem. Further experimentation involving calcium mobilization in response to specific agonists should

be performed in order to clarify if P2Y1 and P2Y2 receptor expression is functional in the corresponding cell types.

G. The Role of P2Y Nucleotide Receptors in $I_{Cl,swell}$ Activation

Previous literature has made the claim that exogenous ATP plays a role in $I_{Cl,swell}$ activation via P2Y receptors, although the exact nature of this role has been debated. One set of studies argues that exogenous ATP is not necessary for $I_{Cl,swell}$ activity, but potentiates the response when applied in addition to HOE (Mongin & Kimelberg 2003). These studies measured radiolabeled aspartate concentrations in perfusate from cells during HOE exposure in the presence and absence of ATP. Aspartate is known to be permeable to VRAC, the channel thought to be responsible for $I_{Cl,swell}$. Micromolar amounts of ATP were able to greatly increase aspartate release from cells during HOE, however exogenous ATP in the absence of HOE was unable to initiate aspartate release. Another study reported that exogenous ATP, released during cell swelling, is required for $I_{Cl,swell}$ activation (Darby et al. 2003). These experiments employed voltage clamp techniques to record chloride current from cultured rat astrocytes in a fashion similar to the present study. The hyposmotically activated chloride current was inhibited by apyrase, as well as a number of nucleotide receptor blockers. Also, application of exogenous ATP in the millimolar range activated a chloride current. However, neither apyrase nor the P2Y receptor blockers were able to block the entire hyposmotic current. Neither study managed to directly answer the question of whether nucleotide signaling alone is sufficient to activate $I_{Cl,swell}$.

The goal of this study was to determine if P2Y signaling is necessary and sufficient for $I_{Cl,swell}$ activation. When exposed to hyposmotic medium round Parental cells activate $I_{Cl,swell}$, demonstrating that P2Y receptor expression is not necessary. The lack of $I_{Cl,swell}$ during HOE in flat Parental cells could demonstrate lack of expression of VRACs in the membrane, or that flat cells have a different cytoskeleton architecture that prevents significant swelling. It should also be pointed out that Parental cells in the PBS studies were also morphologically flat, which could explain why an increase in chloride conductance was not seen.

H. Unanswered Questions and Future Directions

As MacVicar and colleagues stated (in reply to Mongin & Kimelberg 2003), chloride channel activation is a complex phenomenon in astrocytes, and our findings are no different. Round Parental cells can clearly activate $I_{Cl,swell}$ during HOE. Why are flat P2Y1 and P2Y2 cells able to activate $I_{Cl,swell}$ during HOE and flat Parental cells are not? There may be multiple mechanisms for gating or membrane insertion of VRAC. Perhaps elevated intracellular calcium gates VRAC activation. P2Y receptor activation is able to gate VRAC by such a mechanism, as was seen in the flat P2Y1 and P2Y2 cells. Gating could also be accomplished by another mechanism related to the cell cycle (Wondergem et al. 2001). Whether the round Parental cells are in a different stage of the cell cycle than their flat counterparts is speculation at this point, however it would explain why round Parental cells are able to activate VRAC and flat Parental are not. Another question is whether exogenous ATP is activating $I_{Cl,swell}$ or another population of chloride channels? The present voltage clamp experiments depicts the ATP activated current as having a

different electrophysiological profile than that of $I_{Cl,swell}$. This suggests that the current activated by 1 mM exogenous ATP is probably mediated by a channel other than VRAC. It has been shown that many chloride channels are activated during HOE (Zhang & Jacob 1997). Considering ATP has been shown to reach P2Y activating concentrations in the pericellular space of astrocytes during HOE (Okada et al. 2006) it is not surprising that a portion of the chloride current evoked during HOE is sensitive to nucleotide blockers (Darby et al. 2003).

Future studies are needed to determine how P2Y receptors are involved in gating $I_{Cl,swell}$ and what channel mediates the ATP-activated current. Studies in CsCl using PPADS and other nucleotide receptor pathway antagonists could answer the question of how P2Y receptors affect gating or membrane insertion of $I_{Cl,swell}$. Electrophysiological and pharmacological characterization of the ATP-activated channel could lead to its identification. Finally, to reach beyond academic questions and into medical applications, *in vivo* research is needed to identify if $I_{Cl,swell}$ plays a role in the physiological response to brain edema. If this role is better understood, then activity of $I_{Cl,swell}$ could be modified in order to prevent neural injury during stroke and other brain traumas.

References

Abbracchio, M.P., Burnstock, G., Boeynaems, J.M., Barnard, E.A., Boyer, J.L., Kennedy, C., Knight, G.E., Fumagalli, M., Gachet, C., Jacobson, K.A., & Weisman, G.A. (2006). International Union of Pharmacology LVIII: update on the P2Y G protein-coupled nucleotide receptors: from molecular mechanisms and pathophysiology to therapy. *Pharmacol Rev*, 58, 281-341.

Abdullaev, I.F, Rudkouskaya, A., Schools, G.P., Kimelberg, H.K., & Mongin, A.A. (2006). Pharmacological comparison of swelling-activated excitatory amino acid release and Cl- currents in cultured rat astrocytes. *J Physiol*, 572.3, 677-689.

Agre, P., Brown, D., & Nielson, S. (1995). Aquaporin water channels: unanswered questions and unresolved controversies. *Curr Opin Cell Biol*, 7, 472-483.

Ahn, M., Camden, J.M., Schrader, A.M., Redman, R.S., & Turner, J.T. (2000) Reversible regulation of P2Y(2) nucleotide receptor expression in the duct-ligated rat submandibular gland. *Am J Physiol Cell Physiol* 270, C286-C294.

Alomone Labs. Protocols. 20 December 2007. <www.alomone.com>

Andrews, M.A., Maughan, D.W., Nosek, T.M., & Godt, R.E. (1991). Ion-specific and general ionic effects on contraction of skinned fast-twitch skeletal muscle from the rabbit. *J Gen Physiol*, 98, 1105-1125.

Askenasy N, Navon G. (1997) Continuous monitoring of intracellular volumes in isolated rat hearts during normothermic perfusion and ischemia. *J Magn Reson*, 124(1), 42-50.

Bagchi, S., Liao, Z., Gonzalez, F.A., Chorna, N.E., Seye, C.I., Weisman, G.A., & Erb, L. (2005). The P2Y2 nucleotide receptor interacts with alphav integrins to activate Go and induce cell migration. *J Biol Chem*, 280, 39050-7.

Bardoni, R., Goldstein, P.A., Lee, C.J., Gu, J.G., & MacDermott, A.B. (1997). ATP P2X receptors mediate fast synaptic transmission in the dorsal horn of the rat spinal cord. *J Neurosci*, 17, 5297-304.

Barhanin, J., Lesage, F., Guillemare, E., Fink, M., Lazdunski, M., & Romey, G. (1996). K(V)LQT1 and lsK (minK) proteins associate to form the I(Ks) cardiac potassium current. *Nature*, 384, 78-80.

Barron, K.D., Dentinger, M.P., Kimelberg, H.K., Nelson, L.R., Bourke, R.S., Keegan, S., Mankes, R., & Cragoe, E.J. Jr. (1988). Ultrasonic features of a brain injury model in cat. I. Vascular and neuroglial changes and the prevention of astroglial swelling by a fluorenyl (aryloxy) alkanoic acid derivative. *Acta Neuropathol (Berl)*, 75, 295-307.

Beck, FX, Dorge, A, & Thurau, K. (1988). Cellular osmoregulation in renal medulla. *Renal Physiol Biochem,* 11, 174-186.

Bell, P.D., Lapointe, J.Y., Sabirov, R., Hayashi, S., Peti-Peterdi, J., Manabe, K., Kovacs, G., & Okada, Y. (2003). Macula densa cell signaling involves ATP release through a maxi anion channel. *Proc Natl Acad Sci USA,* 100, 4322-4327.

Bender, A.S., Schousboe, A., Reichelt, W., & Norenberg, M.D. (1998). Ionic mechanisms in glutamate-induced astrocyte swelling: role of K+ influx. *J Neurosci Res,* 52, 307-321.

Boese, S.H., Wehner, F., & Kinne, R.K.H. (1996). Taurine permeation through swelling-activated anion conductance in rat IMCD cells in primary culture. *Am J Physiol* 271, F498-F507.

Bordey, A. & Sontheimer, H. (2000). Ion channel expression by astrocytes in situ: comparison of different CNS regions. *Glia,* 30, 27-38.

Bours, M.J.L., Swennen, E.L.R., Virgilio, F.D., Cronstein, B.N., & Dagnelie, P.C. (2006). Adenosine 5'-triphosphate and adenosine as endogenous signaling molecules in immunity and inflammation. *Pharmacol Ther,* 112, 358–404

Braun, S., and H. Schulman. (1996) Distinct voltage-dependent gating behaviors of a swelling-activated chloride current in human epithelial cells. *J Physiol (Camb),* 495, 743-753.

Buchthal, F., Engbaek, L., Sten-Knudsen, O., & Thomasen, E. (1947). Application of adenosinetriphosphate and related compounds to the spinal cord of the cat. *J Physiol,* 106, 3P-4P.

Burg, M.B. (1995). Molecular basis of osmotic regulation. *Am J Physiol,* 268, F983-F996.

Burg, M.B. (1996). Coordinate regulation of organic osmolytes in renal cells. *Kidney Int,* 49, 1684-1685.

Burnstock, G. (1972). Nucleotide Nerves. *Pharm Rev,* 24, 510-81.

Burnstock, G. (2004). Introduction: P2 Receptors. *Curr Top Med Chem,* 4, 793-803.

Burnstock, G. (2008). Unresolved issues and controversies in nucleotide signaling. *J Physiol,* 586, 3307-3312.

Burnstock, G., Campbell, G., Satchell, D., & Smythe, A. (1970) Evidence that adenosine triphosphate or a related nucleotide is the transmitter substance released by non-adrenergic inhibitory nerves in the gut. *Br J Pharmacol,* 40(4), 668-88.

Busch, A.E, Varnum, M., Adelman, J.P., & North, R.A. (1992). Hypotonic solution increases the slowly activating potassium current IsK expressed in xenopus oocytes. *Biochem Biophys Res Commun,* 184, 804-10.

Catacuzzeno, L., Pisconti, D.A., Harper, A.A., Petris, A., & Franciolini, F. (2000). Characterization of the large-conductance Ca-activated K channel in myocytes of rat saphenous artery. *Pflugers Arch,* 441, 208-18.

Chiang, C-E., Luk, H-N., & Wang, T-M. (2004). Swelling-activated chloride current is activated in guinea pig cardiomyocytes from edotoxic shock. *Cardiovascular Research*, 62, 96-104.

Chorna, N.E., Santiogo-Perez, L.I., Erb, L., Seye, C.I., Neary, J.T., Sun, G.Y., Weisman, G.A., & Gonzalez, F.A. (2004) P2Y2 receptors activate neuroprotective mechanisms in astrocytic cells. *J Neurochem,* 91, 119-132.

Christenson, O. & Hoffman, E.K. (1992). Cell swelling activates K+ and Cl- channels as well as nonselective, stretch-activated cation channels in Ehrlich ascites tumor cells. *J Membr Biol,* 129, 12-36.

Cockayne, D.A., Hamilton, S.G., Zhu, Q.M., Dunn, P.M., Zhong, Y., Novakovic, S., Malmberg, A.B., Cain, G., Berson, A., Kassotakis, L., Hedley, L., Lachnit, W.G., Burnstock, G., McMahon, S.B., & Ford, A.P. (2000). Urinary bladder hyporeflexia and reduced pain-related behaviour in P2X3-deficient mice. *Nature*, 407, 1011-5.

Cossins, A.R. (1991) A sense of cell size. *Nature,* 352, 667–668.

Coulombe, A. & Coraboeuf, E. (1992) Large-conductance chloride channels of new-born rat cardiac myocytes are activated by hypotonic media. *Pflugers Arch* 422, 143-150.

Darby, M., Kuzmiski, J.B., Panenka, W., Feighan, D., & MacVicar, B.A. (2003) ATP released from astrocytes during swelling activates chloride channels. *J Neurophysiol,* 89, 1870-1877.

Decher, N, Lang, H.J, Nilius, B., Brüggemann, A., Busch, A.E., & Steinmeyer, K. (2001). DCPIB is a novel selective blocker of I(Cl,swell) and prevents swelling-induced shortening of guinea-pig atrial action potential duration. *Br J Pharmacol,* 134, 1467-79.

Deutsch, C. & Chen, L.Q. (1993). Heterologous expression of specific K+ channels in T lymphocytes: functional consequences for volume regulation. *Proc Natl Acad Sci USA,* 90, 10036-40.

Dezaki, K., Tsumura, T., Maeno, E., & Okada, Y. (2000) Receptor-mediated facilitation of cell volume regulation by swelling-induced ATP release in human epithelial cells. *Japanese J Physiol*, 50, 235-241.

De Smet, P., Oike, M., Droogmans, G., Van Driessche, W., & Nilius, B. (1994) Responses of endothelial cells to hypotonic solutions: lack of regulatory volume decrease. *Pflugers Arch,* 428(1), 94-6.

Diamond, J.M. & Wright, E.M. (1969). Biological Membranes: The physical basis of ion and nonelectrolyte selectivity. *Ann Rev Physiol,* 31, 581-646.

Dong, Y. & Benveniste, E.N. (2001) Immune function of astrocytes. *Glia,* 36, 180-190.

Drury, A.N. & Szent-Györgyi, A. (1929). The physiological activity of adenine compounds with especial reference to their action upon the mammalian heart. *J Physiol,* 68, 213-37.

Duan, D., Ye, L., Britton, F., Horowitz, B., & Hume, J.R. (2000) A novel anionic inward rectifier in native cardiac myocytes. *Circ Res,* 86: E63-E71.

Dube, L., Parent, L., & Sauve, R. (1990) Hypotonic shock activates a maxi K+ channel in primary cultured proximal tubule cells. *Am J Physiol,* 259, F348-F356.

Dubyak, G.P. & El-Moatassum, C. (1993). Signal transduction via P2-nucleotide receptors for extracellular ATP and other nucleotides. *Am J Physiol,* 265, C577-606.

Dunham, P.B., Klimczak, J., & Logue, P.J. (1993). Swelling activation of K−Cl cotransport in LK sheep erythrocytes: a three state process. *J Gen Physiol,* 101, 733–766.

Dutta, A.K, Okada, Y., & Sabirov, R.Z..(2002). Regulation of an ATP-conductive large-conductance anion channel and swelling induced ATP release by arachidonic acid. *J Physiol (London)* 542, 803-816.

Echevarria, M., Windhager, E.E., Tate, S.S., & Frindt, G. (1994). Cloning and expression of AQP3, a water channel from the medullary collecting duct of rat kidney. *Proc Natl Acad Sci USA,* 91, 10997-11001.

Erb, L., Liao, Z., Seye, C.I., & Weisman, G.A. (2006). P2 receptors: intracellular signaling. *Eur J Physiol,* 452, 552-62.

Ernest, N.J., Weaver, A.K., Van Duyn, L.B., & Sontheimer, H.W. (2005). Relative contribution of chloride channels and transporters to regulatory volume decrease in human glioma cells. *Am J Physiol Cell Physiol,* 288, C1451-C1460.

Falke, L.C. & Misler, S. (1989). Activity of ion channels during volume regulation by clonal N1E115 neuroblastoma cells. *Proc Natl Acad Sci USA,* 86, 3919-3923.

Filipovic, D., & Sackin, H. (1991). A calcium-permeable stretch-activated cation channel in renal proximal tubule. *Am J Physiol,* 262, F119-F129.

Fredholm, B.B., Ijzerman, A.P., Jacobson, K.A., Klotz, K-N., & Linden, J. (2001). International Union of Pharmacology. XXV. Nomenclature and Classification of Adenosine Receptors. *Pharm Rev,* 53, 537-52.

Furlong, T.J., Moriyama, T., & Spring, K.R. (1991). Activation of osmolytes efflux from cultured renal papillary epithelial cells. *J Membr Biol,* 123, 269-277.

Fushimi, K., Uchida, S., Hara, Y., Hirata, Y., Marumo, F., & Sasaki, S. (1993). Cloning and expression of apical membrane water channel of rat kidney collecting tubule. *Nature,* 361, 549-552.

Galindo, A., Krnjevic, K., & Schwartz, S. (1967). Micro-iontophoretic studies on neurons in the cuneate nucleus. *J Phsyiol,* 192, 359-77.

García-Díaz, J.F., Nagel, W., & Essig, A. (1983). Voltage-dependent K conductance at the apical membrane of Necturus gallbladder. *Biophys J,* 43, 269–278.

Goldstein, L., Davis-Amara, E.M., & Musch, M.W. (1996). Organic osmolytes channels: transport characteristics and regulation. *Kidney Int,* 49, 1690-1694.

Gillespie, J.H. (1934). The biological significance of the linkages in adenosine triphosphoric acid. *J Physiol,* 80, 345-359.

Greenway, H. & Osmond, C.B.. (1972) Salt responses of enzymes from species differing in salt tolerance. *Plant Physiol,* 49, 256-259.

Greger, R. (1985). Ion transport mechanisms in thick ascending limb of Henle's loop of mammalian nephron. *Physiol Rev,* 65, 760-797.

Grunder, S., Thiemann, A., Pusch, M., & Jentsch, T.J. (1992). Regions involved in the opening of ClC-2 chloride channel by voltage and cell volume. *Nature,* 360, 759-762.

Grunewald, R.W., & Kinne, R.K.H. (1989). Intracellular sorbitol content in isolated rat inner medullary collecting duct cells. Regulation by extracellular osmolarity. *Pflugers Arch* 414, 178-184.

Guharay, F., & Sachs, F. (1984). Stretch-activated single ion channel currents in tissue-cultured embryonic chick skeletal muscle. *J Physiol (Lond)*, 352, 685-701.

Hafting, T., Haug, T.M., Ellefsen, S., & Sand, O. (2006). Hypotonic stress activates BK channels in clonal kidney cells via nucleotide receptors, presumably of the P2Y1 subtype. *Acta Physiol (Oxford)*, 188(1), 21-31.

Hafting, T. & Sand, O. (2000). Nucleotide activation of BK channels in clonal kidney cells (Vero cells). *Acta Physiol Scand*, 170, 99-109.

Hagberg, A., Qu, H., Saether, O., Unsgard, G., Haraldseth, O., & Sonnewald, U. (2001). Differences in neurotrasmitter synthesis and intermediary metabolism between glutamatergic and GABA-ergic neurons during 4 hours of middle cerebral artery occlusion in the rat: The role of astrocytes in neuronal survival. *J Cereb Blood Flow Metab*, 21, 1451-1463.

Hall, J.A., Kirk, J., Potts, J.R., Rae, C., & Kirk, K. (1996). Anion channel blockers inhibit swelling-activated anion, cation, and nonelectrolyte transport in HeLa cells. *Am J Physiol*, 488, 359-369.

Haydon, P.G. (2000). Neuroglial networks: neurons and glia talk to each other. *Curr Biol*, 10, R712-R714.

Hazama, A., Shimizu, T., Ando-Akatsuka, Y., Hayashi, S., Tanaka, S., Maeno, E., & Okada, Y. (1999). Swelling-induced, CFTR-independent ATP release from a human epithelial cell line. Lack of correlation with volume-sensitive Cl- channels. *J Gen Physiol*, 114, 525-533.

Hazama, A., Fan, H., Abdullaev, I., Maeno, E., Tanaka, S., Ando-Akatsuka, Y., & Okada, Y. (2000). Swelling-activated, cystic fibrosis transmembrane conductance regulator-aumented ATP release and Cl- condcutances in C127 cells. *J Physiol (London)*, 523, 1-11.

Hertz, L. & Zielke, H.R. (2004). Astrocytic control of glutamatergic activity: astrocytes as stars of the show. *Trends Neurosci*, *12*, 735-43.

Hill, A.E. (1994). Osmotic flow in membrane pores of molecular size. *J Membr Biol*, 137, 197-203.

Hirsch, J.R, & Schlatter, E. (1997). Ca2+-dependent K+ channels in the cortical collecting duct of rat. *Wien Klin Wochenschr* 109, 485-488.

Hisadome, K., Koyama, T., Kimura, C., Droogmans, G., Ito, Y., & Oike, M. (2002). Volume-regulated anion channels sere as an auto/paracrine nucleotide release pathway in aortic endothelial cells. *J Gen Physiol*, 119, 511-520.

Hoffmann, E.K., Lambert, I.H., & Simonsen, L.O. (1988). Mechanisms in volume regulation in Ehrlich ascites tumor cells. *Renal Physiol Biochem,* 11, 221-247.

Hoffman, E.K., & Mills, J.W. (1999). Membrane events involved in volume regulation. *Curr Top Membr,* 48, 123-196.

Hume, J.R., Duan, D., Collier, M.L., Yamazaki, J., & Horowitz, B. (2000). Anion transport in heart. *Physiol Rev,* 80, 31-81.

Inoue, K., Schuichi, K., & Tsuda, M. (2007). The role of nucleotides in the neuron-glia communication responsible for the brain functions. *J Neurochem,* 102, 1447-1458.

Iwasa, K., Tasaki, I., & Gibbons, R.C. (1980). Swelling of nerve fibers associated with action potentials. *Science,* 210, 338-339.

Jackson, P.S., & Strange, K. (1993). Volume-sensitive anion channels mediate swelling-activated inositol and tourine efflux. *Am J Physiol,* 265, C1489-C1500.

Jackson, P.S., & Strange, K. (1995). Single-channel properties of a volume-sensitive anion conductance. *J Gen Physiol,* 105, 643-660.

Jacobsen, B.S. (1983). Interaction of the plasma membrane with the cytoskeleton: an overview. *Tissue Cell,* 15, 829-852.

Jennings, M.J. (1999) Volume-senseitive K^+/Cl^- cotransport in rabbit erythrocytes. Analysis of the rate-limiting activation and inactivation events. *J Gen Physiol,* 114, 743–757.

Jennings, M.L. & Schultz, R.K. (1991) Okadaic acid inhibition of KCl cotransport. Evidence that protein dephosphorylation is necessary for activation of transport by either cell swelling or *N*-ethylmaleimide. *J Gen Physiol,* 97, 799–817.

Jalonen, T. (1993). Single-channel characteristics of the large-conductance anion channel in rat cortical astrocytes in primary culature. *Glia,* 9, 227-237.

Jenson, B.S., Stroback, D., Olesen, S.P., & Christophersen, P. (2001). The Ca2+-activated K+ channel of intermediate conductance: a molecular target for novel treatments? *Curr Drug Targets,* 2, 401-422.

Jentsch, T.J. (1996). Chloride channels: A molecular perspective. *Curr Opin Neurobiol,* 6, 303-310.

Jentsch, T.J., Friedrich, T., Schriever, A., & Yamada, H. (1999). The CLC chloride channel family. *Pflugers Arch,* 437, 783-795.

John, G.R., Lee, S.C., & Brosnan, C.F. (2003). Cytokines: Powerful regulators of glial cell activation. *Neuroscientist,* 9, 10-22.

Joseph, S.M., Buchakjian, M.R., & Dubyak, G.R. (2003). Colocalization or ATP release sites and ecto-ATPase activity at the extracellular surface of human astrocytes. *J Biol Chem,* 278, 23331-23342.

Junankar, P.R. & Kirk, K. (2000). Organic osmolytes channels: a comparative view. *Cell Physiol Biochem,* 10, 355-360.

Kaji, D. M. & Tsukitani, Y. (1991) Role of protein phosphatase in activation of KCl cotransport in human erythrocytes. *Am J Physiol,* 260, C176-C180.

Kang, J., Kang, N., Lovatt, D., Torres, A., Zhao, Z., Lin, J., & Nedergaard, M. (2008). Connexin 43 hemichannels are permeable to ATP. *J Neurosci,* 28, 4702-11.

Kawahara, K., Ogawa, A., & Suzuki, M. (1991). Hyposmotic activation of Ca-activated K channels in cultured rabbit kidney proximal tubule cells. *Am J Physiol,* 260: F27-F33.

Khakh, B.S., & Henderson, G. (1998). ATP receptor-mediated enhancement of fast excitatory neurotransmitter release in the brain. *Mol Pharmacol,* 54, 372-8.

Khanna, R., Chang, M.C., Joiner, W.J., Kaczmarek, L.K., & Schlichter, L.C. (1999). hSK4/hIK1, a calmodulin-binding KCa channel in human T lymphocytes. Roles inproliferation and volume regulation. *J Biol Chem,* 274(21), 14838-49.

Kielan, T. & Drew, P.D. (2005). Cytokines of the nervous system. In: Inflammatory disorders of the nervous system (Minagar A, Alexander JS, eds). Human Press, Totowa, NJ.

Kimelberg, H.K., Feustel, P.J., Jin, Y., Paquette, J., Boulos, A., & Keller, R.W., Tranmer BI. (2000). Acute treatment with tamoxifen reduces ischemic damage following middle cerebral artery occlusion. *NeuroReport,* 11, 2675-2679.

Kimelberg, H.K. (2004). The problem of astrocyte identity. *Neurochem Int,* 45, 191-202.

Kinne, R.K.H., Czekay, R.P., Grunewald, J.M., Mooren, F.C., & Kinne-Saffran, E. (1993). Hypotonicity-evoked release of organic osmolytes from distal renal cells: systems, signals, and sidedness. *Renal Physiol Biochem,* 16, 66-78.

Knowles, J.R. (1980). Enzyme-catalyzed phosphoryl transfer reactions. *Annu Rev Biochem,* 49, 877-919.

Koyama, Y., Baba, A., & Iwata, H. (1991). L-Glutamate-induced swelling of cultured astrocytes is dependent on extracellular Ca2+. *Neurosci let,* 122, 210-212.

Kregenow, F.M. (1977). Transport in avian red blood cells. In: Transport Processes in Red Cells (Ellory JC and Lew VL eds). Academic Press, London, pp. 383-465.

Kuffler, S.W. & Nicholls, J.G. (1966). The physiology of neuroglial cells. *Ergeb Physiol*, 57, 1-90.

Kuperman, A.S., Okamoto, M., Beyer, A.M., & Volpert, W.A. (1964). Procaine action: antagonism by adensosine triphophate and other nucleotides. *Science,* 144: 1222-1223.

Lang, F., Busch, G.L., Ritter, M., Volkl, H., Waldegger, S., Gulbins, E. & Hausinger, D. (1998). Functional significance of cell volume regulatory mechanisms. *Physiol Rev*, 78, 247-306.

Lang, F., Messner, G., Wang, W., & Oberleithner, H. (1983). Interaction of intracellular electrolytes and tubular transport. *Klin. Wochenschr,* 61, 1029-1037.

Lauf, P.K. & Adragna, N.C. (2000). K-Cl cotransport: properties and molecular mechanism. *Cell Physiol Biochem,* 10, 341-354.

Lauf, P.K., Zhang, J., Gagnon, K.B., Delpire, E., Fyffe, R.E., & Adragna, N.C. (2001). K-Cl cotransport: immunohistochemical and ion flux studies in human embryonic kidney (HEK293) cells transfected with full-length and C-terminal-domain-truncated KCC1 cDNAs. *Cell Physiol Biochem,* 11, 143-160.

Leaf, A. (1956). On the mechanisms of fluid exchange of tissues in vitro. *Biochem J,* 62, 241-248.

Leis, J., Bekar, L., & Walz, W. (2005). Potassium homeostasis in the ischemic brain. *Glia,* 50, 407-416.

Levitan, I., and S. Garber. (1995) Voltage-dependent inactivation of volume-regulated Cl − current in human T84 colonic and B-cell myeloma cell lines. *Pflügers Archiv,* 431, 297-299.

Li, G., Liu, Y., & Olson, J.E. (2002). Calcium/calmodulin-modulated chloride and taurine conductances in cultured rat astrocytes. *Brain Res,* 925(1), 1-8.

Ling, B.N., Webster, C.L., & Eaton, D.C. (1992). Eicosanoids modulate apical Ca2+-dependent K+ channels in cultured rabbit principal cells. *Am J Physiol,* 263, F116-F126.

Lucke, B. & McCutcheon, M. (1932). The living cell as an osmotic system and its permeability to water. *Physiol Rev,* 12, 68-139.

MacKnight, A.D.C. (1988). Principles of cell volume regulation. *Renal Physiol Biochem,* 11, 114-141.

MacKnight, A.D.C. & Leaf, A. (1977). Regulation of cellular volume. *Physiol Rev,* 57, 510-573.

Markiewicz, I., Lukomska, B. (2006). The role of astrocytes in the physiology and pathology of the central nervous system. *Acta Neurobiol Exp,* 66, 343-358.

May, C., Weigl, L., Karel, A., & Hohenegger, M. (2006). Extracellular ATP activates ERK1/ERK2 via a metabotropic P2Y1 receptor in a Ca2+ independent manner in differentiated human skeletal muscle cells. *Biochem Pharmacol,* 71, 1497-509.

McCarty, N.A. & O'Neil, R.G. (1991). Calcium-dependant control of volume regulation in renal proximal tubule cells: I. swelling activated release. *J Membr Biol,* 123, 149-160.

Meiniel, A. (2007). The secretory ependymal cells of the subcommissural organ: which role in hydrocephalus. *J Biochem Cel Biol,* 39, 463-8.

Mercado, A., Song, L.Y., Vazquez, N., Mount, D.B., & Gamba, G. (2000). Functional comparison of the K-Cl cotransporters KCC1 and KCC4. *J Biol Chem* 275, 30326-30334.

Meshki, J., Tuluc, F., Bredetean, O., Ding, Z., & Kunapuli, S.P. (2004). Molecular mechanism of nucleotide-induced primary granule release in human neutrophils: role for the P2Y2 receptor. *Am J Physiol Cell Physiol,* 286, C264-71.

Mills, J.W. (1987). The cell cytoskeleton: possible role in volume control. *Curr Top Membr Transp,* 30, 75-101.

Mongin, A.A. & Kimelberg, H.K. (2003). Is autocrine ATP release required for activation of volume-sensitive chloride channels? *J Neurophysiol,* 90, 2791-2793.

Mongin, A.A., & Kimelberg, H.K. (2005). Astrocytic swelling in neuropathology. In: Kettenmann H.O. & Ransom B.R., (eds.) *Neuroglia*. New York: Oxford University Press.

Morán, J., Maar, T.E., & Pasantes-Morales, H. Impaired cell volume regulation in taurine deficient cultured astrocytes. *Neurochem Res*, 19: 415-20, 1994.

Mount, D.B., Mercado, A., Song, L., Xu, J., George, A.L. Jr., Delphire, E., & Gampa, G. (1999). Cloning and characterization of KCC3 and KCC4, new members of the cation-chloride cotransporter gene family. *J Biol Chem,* 274, 16355-16362.

Ndubaku, U. & de Bellard, M.E. (2008). Glial cells: old cells with new twists. *Acta Histochemica,* 110, 182-195.

Niemeyer, M.I., Cid, L.P., & Sepúlveda, F.V. (2001). K+ conductance activated during regulatory volume decrease. The channels in Ehrlich cells and their possible molecular counterpart. *Comp Biochem Physiol A Mol Integr Physiol*, 130, 565-75.

Nilius, B. & Droogmans, G. (2001). Ion channels and their functional role in vascular endothelium. *Physiol Rev,* 81, 1415-1459.

Nilius, B., Voets, T., Prenen, J., Barth, H., Aktories, K., Kaibuchi, K., Droogmans, G., & Eggermont, J. (1999). Role of Rho and Rho kinase in the activation of volume-regulated anion channels in bovine endothelial cells. *J Physiol,* 516, 67-74.

North, R.A. (2002). Molecular physiology of P2X receptors. *Physiol Rev,* 82, 1023-67.

Noulin, J.F., Brochiero, E., Lapointe, J.Y., Laprade, R. (1999). Two types of K+ channels at the basolateral membrane of proximal tubule: inhibitory effect of taurine. *Am J Physiol,* 277, F290-F297.

Okada, S.F., Nicholas, R.A., Kreda, S.M., Lazarowski, E.R., & Boucher, R.C. (2006). Physiological regulation of ATP release at the apical surface of human airway epithelia. *J Biol Chem,* 281, 22992-23002.

Okada Y, Oiki S, Hazama A, & Morishima S. (1998). Criteria for the molecular identification of the volume-sensitive outwardly rectifying Cl- channel. *J Gen Physiol,* 112, 365-367.

Olsen, M.L., Campbell, S.L., & Sontheimer, H. (2007). Differential distribution of Kir4.1 in spinal cord astrocytes suggests regional differences in K+ homeostasis. *J Neurophysiol,* 98, 786-793.

Olson J.E. (1999). Osmolyte contents of cultured astrocytes grown in hyposmotic medium. *Biochim Biophys Acta,* 1453, 175-179.

Olson, J.E. & Li, G-Z. (1997). Increased potassium, chloride, and taurine conductances in astrocytes during hypoosmotic swelling. *Glia,* 20, 254-261.

Orkand, R.K., Nicholls, J.G., & Kuffler, S.W. (1966). Effect of nerve impulses on the membrane potential of glial cells in the central nervous system of amphibia. *J Neurophysiol,* 29, 788-806.

Orlando, G.S., Tobey, N.A., Wang, P., Abdulnour-Nakhoul, S., & Orlando, R. C. (2002) Regulatory volume decrease in human esophageal epithelial cells. *Am J Physiol,* 283, G932-G937.

Payne JA. (1997). Functional characterization of the neuronal-specific K-Cl cotransporter: implications for [K+]o regulation. *Am J Physiol,* 273, C1516-1525.

Perry, P. B. & O'Neill, W. C. (1993) Swelling-activated K fluxes in vascular endothelial cells: volume regulation via K−Cl cotransport and K channel. *Am J Physiol,* 265, C763-C769.

Race, J.E., Makhlouf, F.N., Logue, P.J., Wilson, F.H., Dunham, P.B., & Holtzman, E.J. (1999). Molecular cloning and functional characterization of KCC3 a new K-Cl cotransporter. *Am J Physiol,* 277, C1210-1219.

Roman, R.M., Smith, R.L., Feranchak, A.P., Clayton, G.H., Doctor, R.B., & Fitz, J.G. (2001). ClC-2 chloride channels contribute to HTC cell volume homeostasis. *Am J Physiol*, 280, G344-53.

Roman, R.M., Wang, Y., Lidofsky, S.D., Feranchak, A.P., Lomri, N., Scharschmidt, B.F., & Fritz, J.G. (1997). Hepatocellular ATP-binding cassette protein expression enhances ATP release and autocrine regulation of cell volume. *J Biol Chem*, 272, 21970-21976.

Roman, R.M., Feranchak, A.P., Salter, K.D., Wang, Y., & Fritz, J.G. (1999). Endogenous ATP release regulates Cl- secretion in cultured human and rat biliary epithelial cells. *Am J Physiol*, 276, G1391-1400.

Roy, G. & Malo, C. (1992). Activation of amino acid diffusion by a volume increase in cultured kidney (MDCK) cells. *J Membr Biol,* 130, 83-90.

Ruhfus, B., Bauernschmitt, H.G., & Kinne, R.K.H. (1998). Properties of a polarized primary culture from rat renal inner medullary collecting duct (IMCD) cells. *In Vitro Cell Dev Biol Anim,* 34, 227-231.

Sabirov, R.Z., Dutta, A.K. & Okada, Y. (2001). Volume-dependent ATP-conductive large-conductance anion channel as a pathway for swelling induced ATP release. *J Gen Physiol,* 118, 251-266.

Sachs, J.R. & Martin, D.W. (1993). The role of ATP in swelling-stimulated K−Cl cotransport in human red cell ghosts: phosphorylation-dephosphorylation events are not in the signal transduction pathway. *J Gen Physiol,* 102, 551–573.

Sanchez, O.R, Pasantes-Morales, H., Lazaro, A., & Cereijido, M. (1991). Osmolarity-sensitive release of free amino acids from cultured kidney cells (MDCK). *J Membr Biol,* 121, 1-9.

Schafer, R., Sedehizade, F., Welte, T., & Reiser, G. (2003). ATP- and UTP-activated P2Y receptors differently regulate proliferation of human lung epithelial tumor cells. *Am J Physiol*, 285, L376-85.

Schipke, C.G. & Kettenman, H. (2004). Astrocyte response to neuronal activity. *Glia*, 47, 226-232.

Schlatter, E. (1993). Regulation of ion channels in the cortical collecting duct. *Renal Physiol Biochem* 16, 21-36.

Schwiebert, E.K., Egan, M.E., Hwang, T.H., Fulmer, S.B., Allen, S.S., Curtting, G.R., & Guggino, W.B. (1995). CFTR regulates outwardly rectrifying chloride channels through an autocrine mechanism involving ATP. *Cell*, 81, 1063-1073.

Schwiebert, E.M. & Zsembery, A. (2003). Extracellular ATP as a signaling molecule for epithelial cells. *Biochim Biophys Acta*, 1615, 7-32.

Shen, M.R., Chou, C.Y., & Ellory, J.C. (2000) Volume-sensitive KCl cotransport associated with human cervical carcinogenesis. *Pflügers Arch*, 440, 751–760.

Shuba, L.M., Missan, S., Zhabyeyev, P., Linsdell, P., & McDonald, T.F. (2004). Selective block of swelling-activated Cl^- channels over cAMP-dependent Cl^- channels in ventricular myocytes. *European J Pharmacology*, 491, 111-120.

Somjen, G.G. (1988). Nervenkitt: notes on the history of the concept of neuroglia. *Glia*, 1, 2-9.

Somjen, G.G. (2002). Ion regulation in the brain: implications for pathophysiology. *Neuroscientist*, 8, 254-267.

Somjen, G.G. (2004). Ions in the brain: normal function, seizures, and stroke. New York: Oxford University Press. pp. 63-73.

Stefan, C., Jansen, S., & Bollen, M. (2005). NPP-type ectophosphodiesterases: unity in diversity. *Trends Biochem Sci*, 30, 542-550.

Stoner, L.C. & Morley, G.E. (1995). Effect of basolateral or apical hypo-osmolarity on apical maxi K channels of everted rat collecting tubule. *Am J Physiol*, 268, F569-F580.

Stout, C.E., Costantin, J.L., Naus, C.G., & Charls, A.C. (2002). Intercellular calcium signaling in astrocytes via ATP release through connexin hemichannels. *J Biol Chem*, 277, 10482-10488.

Strange, K. (1993). Molecular identity of the outwardly rectifying, swelling-activated anion channel: Time to reevaluate pICln. *J Gen Physiol,* 111, 617-622.

Su, W., Shmukler, B.E., Chernova, M.N., Stuart-Tilley, A.K., De Franceschi, L., Brugnara, C., & Alper, S.L. (1999). Mouse K-Cl cotransporter KCC1: cloning, mapping, pathological expression, and functional regulation. *Am J Physiol,* 277, C899-912.

Sykova, E. & Chvatal, A. (2000). Glial cells and volume transmission in the CNS. *Neurochem Int,* 36, 397-409.

Thiemann, A., Grunder, S., Pusch, M., & Jentsch, T.J. (1992). A chloride channel widely expressed in epithelial and non-epithelial cells. *Nature,* 356, 57-60.

Thorn, J.A. & Jarvis, S.M. (1996). Adenosine Transporters. *Gen Pharmacol,* 27, 613-20.

Thornhill, W.B., & Laris, P.C. (1984). KCl loss and cell shrinkage in the Ehrilich ascites tumour cell induced by hypotonic media, 2-deoxyglucose and propanolol. *Biochem Biophys Acta,* 773, 207–218.

Topilko, P. (2007). Boundary cap cells - a nest of neural stem cells in the peripheral nervous system. *Bull Acad Natl Med,* 7, 1383-92.

Tu, M.T., Luo, S.F., Wang, C.C., Chien, C.S., Chiu, C., Lin, C.C., & Yang, C.M. (2000). P2Y(2) receptor-mediated proliferation of C(6) glioma cells via activation of Ras/Raf/MEK/MAPK pathway. *Br J Pharmacol,* 129,1481-9.

Van Harreveld, A. (1972). The extracellular space in the vertebrate central nervous system. In: Bourne, G.H. (ed.) *The structure and function of nervous tissue*. New York: Academic Press.

Vergara, C., Latorre, R., Marrion, N.V., & Adelman, J.P. (1998). Calcium-activated potassium channels. *Curr Opin Neurobiol,* 8(3), 321-9.

Villegas, S.N., Poletta, F.A., & Carri, N.G. (2003). Glia: a reassessment based on novel data on the developing and mature central nervous system. *Cell Biol Int, 27,* 599-609.

Wang, J., Morishima, S., & Okada, Y. (2003). IK channels are involved in the regulatory volume decrease in human epithelial cells. *Japanese J Physiol,* 284, C77-84.

Wang, Y., Roman, R., Lidofsky, S.D., & Fritz, J.G. (1996). Autocrine signaling through ATP release represents a novel mechanism for cell volume regulation. *Proc Natl Acad Sci USA,* 93, 12020-12025.

Wehner, F., Olsen, H., Tinel, H., Kinne-Saffran, D., & Kinne RKH. (2003). Cell volume regulation: osmolytes, osmolytes transport, and signal transduction. *Rev Physiol Biochem Pharmacol,* 148, 1-80, 2003.

Wondergem, R., Gong, W., Monen, S.H., Dooley, S.N., Gonce, J.L., Conner, T.D., Houser, M., Ecay, T.W., & Ferslew, K.E. (2001). Blocking swelling-activated chloride current inhibits mouse liver cell proliferation. *J Physiol,* 532, 661-72.

Yamamoto-Mizuma, S., Wang, G-X., & Joseph, R. (2004). P2Y nucleotide receptor regulation of CFTR chloride channels in mouse cardiac myocytes. *J Physiol*, 556: 727-737.

Yancey, P.H., Clark, M.E., Hand, S.C., Bowlus, R.D., & Somero, G.N. (1982). Living with water stress: evolution of osmolytes systems. *Science,* 217, 1214-1222.

Yegutkin, G.G. (2008). Nucleotide- and nucleoside-converting ectoenzymes: Important odulators of nucleotide signaling cascade. *Biochim Biophys Acta,* 1783, 673-694.

Zhang, J.J. & Jacob, T.J. (1997). Three different Cl- channels in the bovine ciliary epithelium activated by hypotonic stress. *J Physiol (Lond),* 499, 379-389.

Zimmermann, H. (1992). 5'-nucleotidase: molecular structure and functional aspects. *Biochem J,* 285, 345-65.

Zimmermann, H. (1996). Biochemistry, localization and functional roles of ecto-nucleotidases in the nervous system. *Prog Neurobiol,* 49, 589-618.